INFORMATION TO USERS

This manuscript has been reproduced from the microfilm master. UMI films the text directly from the original or copy submitted. Thus, some thesis and dissertation copies are in typewriter face, while others may be from any type of computer printer.

The quality of this reproduction is dependent upon the quality of the copy submitted. Broken or indistinct print, colored or poor quality illustrations and photographs, print bleedthrough, substandard margins, and improper alignment can adversely affect reproduction.

In the unlikely event that the author did not send UMI a complete manuscript and there are missing pages, these will be noted. Also, if unauthorized copyright material had to be removed, a note will indicate the deletion.

Oversize materials (e.g., maps, drawings, charts) are reproduced by sectioning the original, beginning at the upper left-hand corner and continuing from left to right in equal sections with small overlaps.

Photographs included in the original manuscript have been reproduced xerographically in this copy. Higher quality 6" x 9" black and white photographic prints are available for any photographs or illustrations appearing in this copy for an additional charge. Contact UMI directly to order.

ProQuest Information and Learning
300 North Zeeb Road, Ann Arbor, MI 48106-1346 USA
800-521-0600

MODIFICATION OF OPIOID PEPTIDES TO ENHANCE PERMEABILITY INTO THE BRAIN

by

Ken A. Witt

A Dissertation Submitted to the Faculty of the
COMMITTEE OF PHARMACOLOGY AND TOXICOLOGY (GRADUATE)

In Partial Fulfillment of the Requirements
For the Degree of

DOCTOR OF PHILOSOPHY

In the Graduate College

THE UNIVERSITY OF ARIZONA

2001

UMI Number: 3023485

Bell & Howell Information and Learning Company
300 North Zeeb Road
P.O. Box 1346
Ann Arbor, MI 48106-1346

THE UNIVERSITY OF ARIZONA ®
GRADUATE COLLEGE

As members of the Final Examination Committee, we certify that we have read the dissertation prepared by KEN A WITT

entitled MODIFICATION OF OPIOID PEPTIDES TO ENHANCE PERMEABILITY INTO THE BRAIN

and recommend that it be accepted as fulfilling the dissertation requirement for the Degree of DOCTOR OF PHILOSOPHY

Thomas P. Davis	7-6-01 Date
Edward French	7-6-01 Date
Robert Dorr	7-6-01 Date
Henry Yamamura	7-6-01 Date
	Date

Final approval and acceptance of this dissertation is contingent upon the candidate's submission of the final copy of the dissertation to the Graduate College.

I hereby certify that I have read this dissertation prepared under my direction and recommend that it be accepted as fulfilling the dissertation requirement.

Dissertation Director Thomas P. Davis — 7-6-01 Date

STATEMENT BY AUTHOR

This dissertation has been submitted in partial fulfillment of requirements for an advanced degree at The University of Arizona and is deposited in the University Library to be made available to borrowers under rules of the Library.

Brief quotations from this dissertation are allowable without special permission, provided that accurate acknowledgment of source is made. Requests for permission for extended quotation from or reproduction of this manuscript in whole or in part may be granted by the copyright holder.

SIGNED: 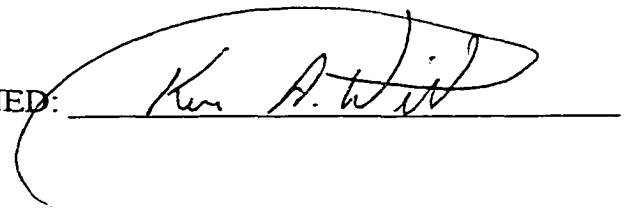

Acknowledgements

I would first like to thank my advisor Dr. Thomas P. Davis for his support and encouragement throughout my graduate studies. He is an excellent role model and has greatly influenced my scientific understanding and problem solving abilities. I would also like to thank the members of my committee, namely Dr. Henry Yamamura, Dr. Edward French, Dr. Robert Dorr, and Dr. William Stamer for their pharmacological expertise and assistance with my research.

I have also been extremely fortunate to work with many people in the Davis lab. Dr. Richard Egleton has been instrumental in my education and more than any other individual provided me with the understanding of the blood-brain barrier and delivery mechanisms, as well as providing the methodological comprehension to help me accurately and effectively complete my studies (with a great deal of patience). I would also like to thank Dr. Jason Huber, who has also contributed to my education and has been a continual collaborator on each of my research projects. Dr. Thomas Abbruscato and Terry Gillespie provided assistance with the analytical portions of my dissertation. Cheryl Slate and Hongbing Wei, who performed the receptor binding studies on my respective projects.

I would also like to thank the other members of the lab that I have worked with over the years: Dr. Karen Mark, Dr. Rachel Brown, Sharon Hom, Vincent Hau, Brian Hawkins, and of course Chris Campos.

I would especially like to thank my family for their support. My brothers John and Todd for not killing me as a child, when I likely deserved it (*most of the time however I was completely innocent, ask mom*). My mom (a.k.a. Carol) and my dad (a.k.a. Jim) who have provided me with love and support throughout my life, and without whom none of this would be possible (*and for not letting my brothers kill me when I may have deserved it*).

Lastly, I would like to thank my beautiful nog, Karin, who puts up with me and brings out the very best in myself.

Dedication

This work is dedicated to my beloved nog, Karin, and my parents Carol and Jim without whom none of this would have been possible.

TABLE OF CONTENTS

TABLE OF CONTENTS Continued

TABLE OF CONTENTS Continued

LIST OF FIGURES

LIST OF TABLES

ABSTRACT

Uptake and distribution of peptides into the central nervous system (CNS) is limited by a number of factors, central to which is the blood-brain barrier (BBB). Peripheral influences: blood-flow, protein binding in blood, clearance, and metabolism, also greatly affect the ability of peptide drugs to enter the CNS. Nevertheless, the BBB is frequently the rate-limiting factor in peptide drug permeation into the brain. The use of chemical modification, or pharmacological manipulation of the BBB, can improve CNS uptake of peptide drugs. In this examination, methods of peptide distribution, lipophilicity, protein binding, stability, receptor binding, clearance, and BBB permeation were used to assess the affects of various strategies on the delivery a model opioid peptide, DPDPE. DPDPE is a well characterized δ-opioid peptide analogue of met-enkephalin. Characterization of DPDPE uptake at the BBB was assessed both *in vitro,* using primary culture bovine brain microvessel endothelial cells, and *in situ,* using brain perfusion analysis in the rat.

The first aspect of this examination was aimed at assessing lipophilicity and stereoselectivity via tri-methylating DPDPE, thereby enhancing lipophilicity and creating four distinctive diastereoisomer configurations. Each diastereoisomer was assessed for protein interaction, lipophilicity, BBB permeation (*in vitro & in situ*), receptor-binding affinity, metabolic stability and end analgesic effect. Significant variation was shown between the parent form and methylated diastereoisomers, as well as significant variation between each respective diastereoisomer in relation to analgesia and BBB penetration.

The second aspect of the examination was aimed at PEGylating [conjugation of a poly(ethylene glycol) to a drug] DPDPE, with focus on BBB permeability characterization. Pharmacokinetic and pharmacodynamic properties were also assessed. PEGylation resulted in significantly decreased clearance, with increased drug half-life, resulting in enhanced analgesia. Penetration at the BBB was decreased, due to the conjugated compound enhanced hydropholicity, however the PEGylation of DPDPE did reduce efflux out of the brain by reducing DPDPE affinity for P-glycoprotein.

Chapter 1. Introduction

Morphology and Biochemistry of Blood-Brain and Blood-CSF Barriers

History of the Blood-Brain Barrier.

The brain functions within a well-controlled environment separate from the milieu of the periphery. The mechanisms that control the unique environment of the brain are collectively referred to as the "blood-brain barrier". Paul Ehrlich (1885, 1906) and Edwin Goldman (1909, 1913) observed that water soluble dyes injected into the peripheral circulation did not stain the brain or color the cerebrospinal fluid (CSF), however the choroid plexus showed heavy staining. Additional experiments showed that the same dyes injected into the subarachnoid space colored the brain and CSF, but not the peripheral tissues. Lewandowsky, while studying potassium ferrocyannide penetration into the brain (1900), was the first to coin the term blood-brain barrier and called it "bluthirnschranke". The observations drawn from the dye studies brought about the concept of a barrier between blood and brain, as well as between blood and CSF.

Later investigators employed basic dyes that were highly lipid soluble and able to transverse the BBB (Friedemann, 1942), showing that the brain was stained by direct transport of the dyes across the cerebral microvasculature. Broman (1941) observed that there were two barrier systems in the brain, the blood-CSF barrier at the choroid plexus and the blood-brain barrier (BBB) at the cerebral microvasculature. Furthermore, Broman (1941) argued that the barrier function of the BBB was via the capillary endothelial cells and not the astrocytic end feet. The debate as to whether the astrocytic

end feet or the capillary endothelium comprise the BBB was layed to rest by electron microscopic cytochemical studies performed in the late 1960s by Reese and Karnovsky (1967), and later by Brightman and colleagues (1970). Horseradish peroxidase (MW 39,800) was used to visualize the BBB (Reese and Karnovsky, 1967). Systemic injections of horseradish peroxidase failed to reach brain extracellular fluid, whereas intracerebroventricular injection into the CSF stained the brain extracellular fluid. Horseradish peroxidase diffused past the astrocytic end feet and basement membrane, and stopped at the tight junctions of the cerebral endothelial cells. These experiments substantiated the argument that tight junctions between cerebral endothelial cells comprise the BBB, restricting the free movement of substances from blood and interstitial fluid.

Later, dialogue concerning the uniqueness of the BBB tight junctions and physiology, relating to capillary networks of peripheral organs were addressed by and elegant study performed by Stewart and Wiley (1981). In these experiments, embryonic quail brain was transplanted to embryonic chick gut. Although the quail brain was vascularized by chick gut vessels, the transplanted microvessels maintained physiological characteristics of the BBB and excluded dyes, such as trypan blue. Conversely, embryonic quail gut transplanted to embryonic chick brain was vascularized by vessels of chick brain origin, yet these microvessels were leaky to trypan blue and did not maintain BBB characteristics. These experiments support the belief that the physiological characteristics of the BBB arise from the expression of a distinctive set of genes within the capillary endothelium or possibly cofactors from the surrounding tissue.

Pericyte, Astrocyte and Basal Lamina Association with the BBB

The periendothelial accessory structures of the BBB include pericytes, astrocytes, and a basal membrane. The endothelial cells of the BBB are distributed along the length of the vessel and completely encircles the lumen. A thin basement membrane (i.e. basal lamina) supports the ablumenal surface of the endothelium. The basal lamina surrounds the endothelial cells and pericytes; the region between which is known as the Virchow-Robin space. Astrocytes are adjacent to the endothelial cell, with astrocytic end feet sharing the basal lamina (*Figure 1.2.1 & 1.2.2*).

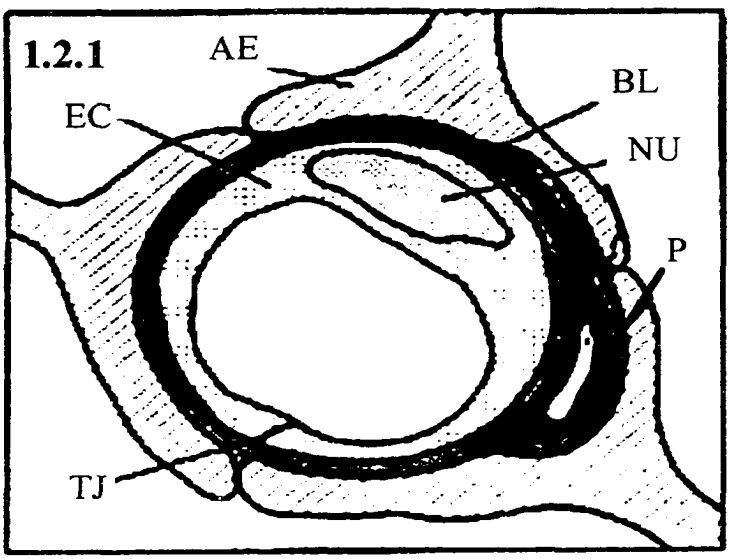

Figure 1.2.1 A representative cross-section of a cerebral capillary of the BBB. Shown are the astrocytic end feet (AE), basal lamina (BL), endothelial cell (EC), nucleus (NU), pericyte (P), and tight junction (TJ).

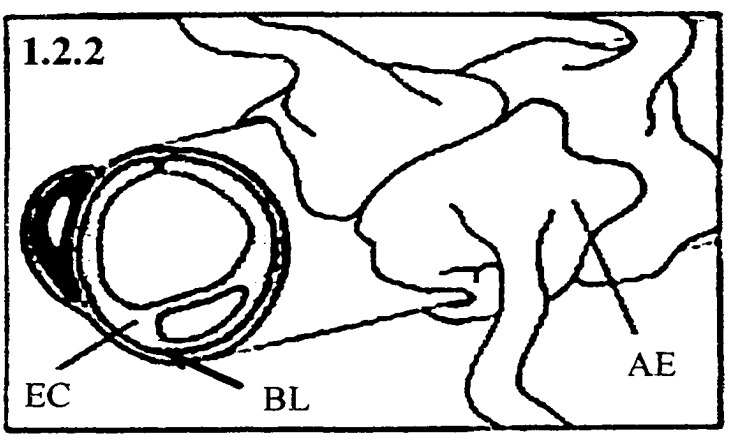

Figure 1.2.2 A representative cross / longitudinal-section of a cerebral capillary of the BBB. Shown are the astrocytic end feet (AE), basal lamina (BL), and endothelial cell (EC).

The association of pericytes to blood vessels has been suggested to regulate endothelial cell proliferation, survival, migration, differentiation, and vascular branching (Hellstrom et al., 2001). Pericytes in the periphery are flat, undifferentiated, contractile connective tissue cells, which develop around capillary walls. Microvascular pericytes have shown to lack the α-actin isoform, typical of contractile cells (Nehls and Drenckhahn, 1991), thus these cells may not be involved in capillary contraction. Pericytes have a close physical association with the endothelium. Gap junction communication between pericyte and endothelial cells, as well as at endothelial-endothelial junctions, has been shown *in vitro* (Larson et al., 1987). Pericytes send out cellular projections, which penetrate the basal lamina and cover approximately 20-30% of the microvascular circumference (Frank et al., 1987). Pericytes are thought to contribute to endothelial cell proliferation, via selective inhibition of endothelial cell growth (Antonelli-Orlidge et al., 1989). Lack of pericytes has lead to endothelial hyperplasia and abnormal vascular morphogenesis in the brain (Hellstrom et al., 2001). Research indicates that pericytes of the BBB might be derived from microglia, since these pericytes demonstrate the capacity to phagocytize exogenous protein form the central nervous system (Coomber and Stewart, 1985). Additionally, there is some evidence that pericytes are able to mimic astrocyte ability to induct BBB "tightness" (Minakawa et al., 1991).

Astrocytes are glial cells which envelop > 99% of the BBB endothelium. Intercellular adhesion between astrocytes in the blood-brain barrier has been observed in the form of gap junctions and adheren junctions (Brightman and Reese, 1969; Shivers et al., 1988). There is significant body of evidence, *in vitro* and *in vivo*, to indicate that

astrocyte interaction with the cerebral endothelium help determine BBB function, morphology (i.e. tightness), and protein expression (Beck et al., 1984; Arthur et al., 1987; Cancilla et al., 1983). Astrocytes serve as scaffolds, guiding neurons to their proper place during development and direct vessels of the BBB. The association of astrocytes to the cerebral microvasculature is underlined by the association of neurons to astrocytes. The ~20 nm gap between adjacent astrocytes, which is readily diffusible by horseradish peroxidase (Brightman and Reese, 1969), indicates that they most likely do not contribute to the physical barrier of the BBB.

Between brain capillaries, astrocytes, and pericytes is the basal lamina, which consists of laminin, fibronectin, tenascin, collagens, and proteoglycan (Timpl and Brown, 1996). The basal lamina provides mechanical support for cell attachment, serves as a substratum for cell migration, separates adjacent tissue, and can act as a barrier to the passage of macromolecules. Cell adhesion to the basal lamina involves the integrins (Hynes, 1992). Integrins are transmembrane receptors that bridge the cytoskeletal elements of a cell to the extracellular matrix and are heterodimers of α and β subunits.

Neuronal involvement in BBB formation remains unclear. *In vivo* and *in vitro* studies support the hypothesis of a neural induction of the cerebral microvasculature, indicating a specific role of neurons and / or astrocytes in BBB formation (Wolburg, 1995; Bauer and Bauer, 2000). Coculture experiments using cerebral capillary endothelial cells and neurons (as well as neuronal plasma membranes) have shown dose-dependent increases in γ-glutamyl transpeptidase activity, higher than seen with

cocultured glial cells (Tontsch and Bauer, 1991), indicating an inductive effect of neurons.

Cell Membranes

The function of the membranes is complex and multifaceted, and can be divided into eight general categories. *First*, membranes compartmentalize, providing continuous, relatively unbroken sheets. *Second*, membranes prevent unrestricted exchange of molecules, providing a selectively permeable barrier. *Third*, membranes contain the machinery for the physical transport of substances from one side of the membrane to the other. *Fourth*, the membrane is involved in response of the cell to external stimuli, via signal transduction. *Fifth*, membranes allow cells to recognize one another, to adhere, and to exchange materials in an intracellular interaction. *Sixth*, membranes provide a means to organize cellular biochemical activities, through an extensive framework or scaffolding within which components can be arranged for effective interaction. *Seventh*, membranes maintain cell polarity. *Eighth*, membranes are involved in the process of energy transduction (i.e. conversion of one type of energy to another), such as the transfer of chemical energy from carbohydrates and fats to ATP.

Hugh Davson and James Danielli first proposed that the plasma membrane was composed of a lipid bilayer that was lined on both its inner and outer surface by a layer of globular proteins. Furthermore, they stated that the lipid bilayer was penetrated by protein-lined pores, providing entry for ions and solutes to enter and exit the cell (Davson and Danielli, 1943). Later Singer and Nicolson proposed the "fluid-mosaic model "

(1972), in which proteins occur as a "mosaic" of discontinuous particles that penetrate the lipid sheet and that these membranes are dynamic structures with mobile components capable of engaging in numerous types of interactions.

Cell membranes consist of phospholipids, proteins, and cholesterols, with carbohydrates on the outer surface. A lipid bilayer has been determined to be ~60 Å thick. The combined acyl chains of the lipid bilayer span a width of ~30 Å, with the head groups adding another ~15 Å on both the interior and exterior surface (Karp, 1999).

Membranes contain a diverse population of lipids, all of which are amphipathic. These membranes contain a phosphate group usually built on a glycerol backbone (i.e. phosphoglycerides). Membrane glycerides contain two hydroxyl groups of glycerol, esterified to fatty acids, and the third group esterified to a phosphate group. The phosphate group is commonly linked to either a choline (i.e. phosphatidylcholine), serine (i.e. phosphotidylserine), ethanolamine (phosphatidylethanolamine), or inositol (phosphotidylinositol). These small groups are hydrophilic and, with the associated charged phosphate group, form a highly water-soluble domain (i.e. head group). The two fatty acyl chains are long, unbranched, and contain hydrophobic hydrocarbons. Sphingolipids are derivatives of sphingosine, an amino alcohol, which contains a long hydrocarbon chain. The sphingosine is linked to a fatty acid via its amino group, resulting in the sphingolipid. Another component of the lipid membrane is the sterol cholesterol, which is smaller than other lipids and less amphipathic (Devaux, 1991; Gennis, 1989).

Cholesterol molecules are oriented with their hydrophilic hydroxyl group at the membrane surface and their hydrophobic tail embedded in the lipid bilayer. Cholesterol contains rings, which are rigid and flat, that thereby reduce the free movement of the fatty acid tails of the phospholipids.

The carbohydrate membrane content ranges between 2 to 10 percent by weight. Greater than 90 % of the carbohydrates are covalently linked to proteins (i.e. glycoproteins), the remaining carbohydrates are linked to lipids (i.e. glycolipids). Glycoprotein carbohydrates are short, branched oligosaccharides, with generally less than 15 sugars per chain (Karp, 1999). The thin layer of glycoprotein and oligosaccharides (i.e. glycocalyx) of the outer surface of the cell membrane mediate interactions of cell adhesion and forms antigens involved in recognition of "self".

Membrane proteins are diverse and arranged in the membrane in specific orientations and locations, and are asymmetrically situated. These proteins are involved in numerous functions including ion and nutrient transport, cell adhesion, cell recognition, and intercellular interactions. The three classes of proteins are integral, peripheral, and lipid-anchored. Integral proteins pass through the lipid bilayer, with domains in both the extracellular and cytoplasmic sides of the membrane. Peripheral proteins are located outside the bilayer on the cytoplasmic surface, with noncovalent bonding to the membrane. Lipid-anchored proteins are located outside the bilayer, exterior or cytoplasmic surfaces, and covalently linked to a lipid molecule within the membrane (Unwin and Henderson, 1984).

Anatomy and Physiology of the Cerebral Capillary Endothelia

The surface area of the brain microvasculature is ~ 100 $cm^2 \cdot g^{-1}$ tissue, with the capillary volume and endothelial cell volume constituting approximately 1% and 0.1% of the tissue volume, respectively (Pardridge et al., 1990). The mean intercapillary distance in the human brain is ~ 40μm (Duvernoy et al., 1983). This short distance allows for near instantaneous solute equilibration throughout the brain interstitial space for small molecules, once the BBB has been overcome. The microvasculature of the central nervous system (CNS) can be differentiated from the peripheral tissue endothelia in that it possess uniquely distinguishing characteristics:

(1) Cerebral capillary endothelial cells contain *tight junctions*, which seal cell-to-cell contacts between adjacent endothelial cells forming a continuous blood vessel. The tight junctions between BBB endothelial cells leads to high endothelial electrical resistance, in the range of 1500-2000 $\Omega \cdot cm^2$ (pial vessels), as compared to 3-33 $\Omega \cdot cm^2$ in other tissues (Crone and Christensen 1981; Butt et al., 1990). The electrical resistance across *in vivo* cerebral microvessel endothelial cells, of non-pial origin, has been estimated to be as high as 8000 $\Omega \cdot cm^2$ (Smith and Rapoport, 1986). The net result of this elevated resistance is low paracellular permeability.

The intercellular clefts are around 200 Å wide, which would allow ready diffusion of tissue solutes, therefore it is clear that these clefts are constricted. The study of junctional complexes reducing diffusion across cellular sheets was initial investigated by Farquhar and Palade (1963). The complex is classified as *macula* and *zonula adhaerens* and *zonula occludens*. The adherens junction is around 200 Å, while the area composing

the zonula occludens (i.e. tight junction) is essentially completely occluded. The junctional complex forms interconnected, intramembrane strands arranged as a series of multiple barriers (Schneebergter and Karnovsky, 1976).

Figure 1.1 depicts the current theoretical understanding of a cerebral capillary junction at the *molecular level.* An integral tight junctional membrane component is *occludin,* a 65 KDa protein brings opposing cell leaflets into contact. *Claudins* comprise a multigene family and to date there are 20 claudin isomers, which form dimers that bind homotypically to claudins on adjacent endothelial cells to form the primary seal of the tight junction (Furuse et al., 1999). *Zonula occludens (ZO-1/2/3)* are cytoplasmic proteins that interact with occludin and serve to as recognition proteins for tight junctional placement, and support structure for signal transduction proteins (Haskins, et al., 1998). ZOs belong to the MAGUK family of proteins (membrane associated guanylate kinase-like proteins) and have a number of binding sites for cytoskeletal proteins, signal transduction molecules, and kinases. *AF6* is a Ras effector molecule associated with ZO-1 (Joh et al., 1997). *7H6* antigen is a phosphoprotein found at tight junctions impermeable to ions and macromolecules (Satoh et al., 1996). *Junctional adhesion molecules (JAM)* are localized at the tight junction and are a member of the immunoglobulin superfamily (IgSF). Additionally, tight junctions are shown to microdomains on the cell membrane rich in cholesterol, which contain caveolin-1 (Nusrat et al., 2000).

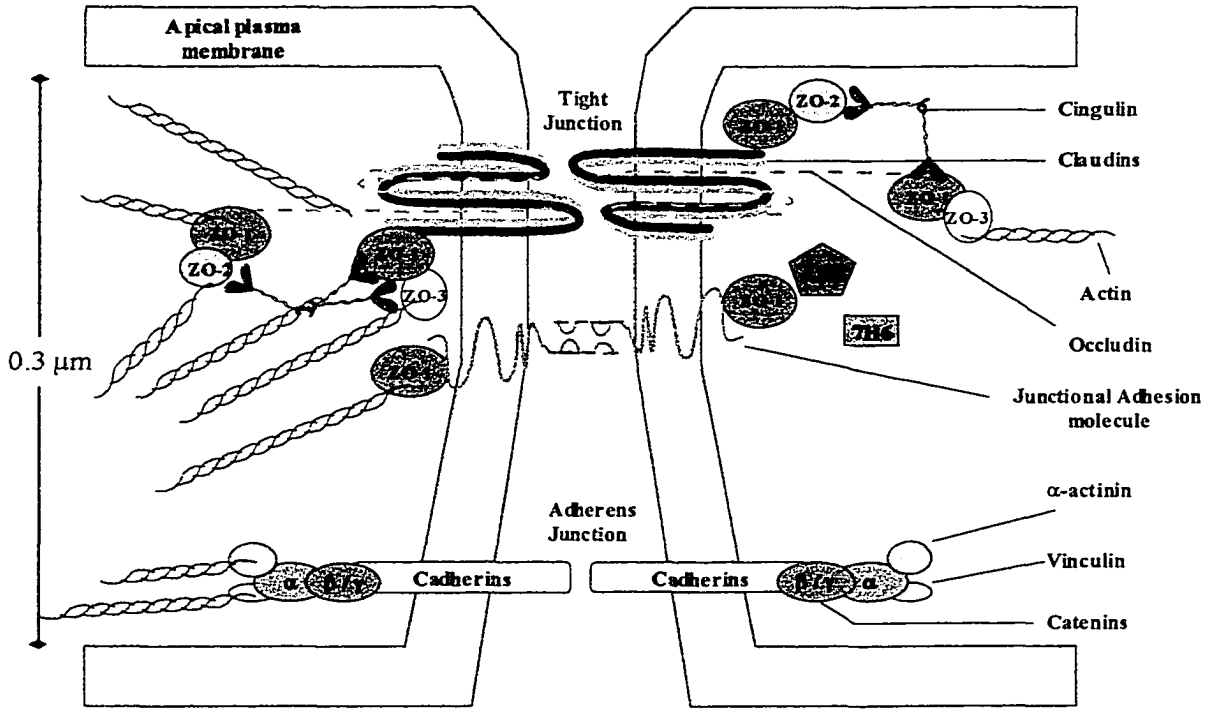

Figure 1.1 Proposed interactions of the major tight junctional cytoskeletal and adhesion junction proteins present at the BBB (adapted from Huber et al., 2001)

(2) The cytoplasm of the *endothelial cell is of uniform thickness*, with *very few pinocytotic vesicles* (hollowed out portion of cell membrane filled with fluid, forming a vacuole which allows for nutrient transport), and lack fenestrations (i.e. openings). Therefore, transit across the BBB involves translocation through (i) the capillary endothelium, (ii) the internal cytoplasmic domain, (iii) and then through the ablumenal membrane and pericyte and / or basal lamina. Three principle types of transendothelial transport have been postulated. These include vesicular channels (Simionescu et al., 1975), fusion-fission (Clough and Michel, 1981), and transcytosis (Palade, 1960).

(3) There is a *greater number and volume of mitochondria* in BBB endothelial cells compared to peripheral endothelia in rat (Oledndorf et al., 1977). This increase in mitochondria, and increased energy potential, is thought to be required for active transport of nutrients to the brain from the blood. Oldendorf and Brown (1975) estimated that 5-6 times more mitochondria per capillary cross-section exist in rat cerebral capillaries than in rat skeletal muscle capillaries. These finding suggest that the enhanced cerebral capillary work capacity may be related to energy-dependent transcapillary transport.

(4) There is also an *enzymatic barrier* at the cerebral endothelia, capable of metabolizing drug and nutrients (Minn et al., 1991; Brownlees et al., 1993; Brownson et al., 1994). These enzymes are principally directed at metabolizing neuroactive blood-borne solutes. Enzymes such as γ-glutamyl transpeptidase (γ-GTP), alkaline phosphatase, and aromatic acid decarboxylase are in elevated concentration in cerebral microvessels, yet often in low concentration or absent in non-neuronal capillaries. A partial list of enzymes, and functions, involved in drug metabolism at the BBB is given in *table-1.1*

(5) Coomber and Stewart (1985) performed a comparative morphometric analysis of cerebral vs. muscle capillary endothelial cells and found a *decrease in the wall thickness of brain capillaries of approximately 39%.* Additionally, the number of pinocytotic vesicles of the muscle capillaries was seven times greater than those associated with the cerebral capillaries. They postulated that the decrease in wall thickness of the cerebral capillaries could be a modulation to the restrictive permeability

of the BBB, allowing nutrients a shortened transport time to cross through the membrane and cytoplasm, and enter the brain parenchyma.

(6) A *polarity exists between the lumenal and ablumenal membrane surfaces* of the endothelial cells. The concept of the functional polarity of the BBB emerged from quantitative biochemical studies (Betz and Goldstein, 1978). The enzymes γ-GTP and alkaline phosphatase are shown to be present at the lumenal endothelium, whereas Na^+-K^+-ATPase and the sodium dependent (A-system) neutral amino acid transporter are associated with the ablumenal portion of the endothelium (Betz et al., 1980). The glucose receptor GLUT-1 was shown, through use of immunogold labeling and electron microscopy, to have 3:1 ratio of distribution, ablumenal to lumenal at the BBB (Farrell and Pardridge, 1991). Na^+-K^+-ATPase is enriched at the ablumenal surface (Betz et al., 1980). Additionally, the P-glycoprotein (P-gp) drug efflux transporter is presently thought to exist at the lumenal membrane surface, although arguments that P-gp is actually associated with the astrocytes which enfold the endothelial cells (Pardridge, 1997) is presently being debated. Structural, pharmacological and biochemical evidence for lumenal and ablumenal polarization of receptors, enzymes, and channels at the cerebral endothelia (Vorbrodt, 1993) establishes the BBB to be a working non-stagnant membrane unequivocally evolved to maintain brain homeostasis.

Enzyme	Functions observed	Reference
Dopa-decarboxylase	Convert L-Dopa to dopamine	Bertler et al., 1966
Monoamine oxidase-B	Inactivates catecholamines (5-HT)	Minn et al., 1991
Pseudocholinesterase	Deacetylates heroin to morphine	Gerhart et al., 1987
Cytochrome P450	O-Demethylates codeine to morphine	Chen et al., 1990; Perrin et al., 1990
UDP-Glucuronosyltransferase	Metabolizes 1-naphthol	Ghersi-Egea et al., 1994
Epoxide hydrolase	Reacts with epoxides (Benzo[a]pyre 4,5-oxide)	Ghersi-Egea et al., 1989; 1994
Renin	Angiotensinogen to Angiotensin I	Kowaloff et al., 1980
Dipeptidyl dipeptidase	Enkephalin metabolism	Brecher et al., 1978; Benuck et al., 1981
ACE	Enkephalin, angiotensin I, neurotensin, and bradykinin metabolism	Brecher et al., 1978 Brownson et al., 1994
Aminopeptidase A	Metabolism of angiotensin	Bausback et al., 1988
Aminopeptidase M (N)	Opioid degradation (N-terminal Tyr)	Solhonne et al., 1987 Brownson et al., 1994
Glutamyl aminopeptidase	Convert angiotensin II to angiotensin III	Song et al., 1993
Enkephalinase * (neutral Endopeptidase 24.11)	*Enkephalin, Endothelin, and bradyknin* degradation	Vijayaraghavan et al., 1990; Brownson et al., 1994
Endopeptidase * (Endopeptidase 24.15)	Dynorphin, neurotensin, bradykinin, angiotensin II, and LHRH degradation	Molineaux et al., 1990; Pardridge, 1991
γ-Glutamyltranspeptidase * ‡	Convert leukotriene C4 to leukotriene D4	Black et al., 1994
Alkaline phosphatase ‡	purine and pyrimidine metabolism	Johnson and Anderson, 1996

Table-1.1 Drug degrading enzymes of the BBB, with partial list of enzymatic functions. * Indicates enzymes known to high in choroid plexus (Bourne et al., 1989; Ghersi-Egea et al., 1994). ‡ Indicates established BBB markers. ACE : angiotensin converting enzyme, LHRH : luteinizing hormone releasing hormone

Transport at the BBB

There are four basic mechanisms by which solute molecules move across membranes. First is *simple diffusion*, which proceeds from low to high concentrations. Second is *facilitated diffusion*, a form of carrier-mediated endocytosis, in which solute molecules bind to specific membrane protein carriers, also from low to high concentration. Third is *simple diffusion through an aqueous channel*, formed within the membrane. Fourth is *active transport through a protein carrier* with a specific binding site that undergoes a change in affinity. Active transport requires ATP hydrolysis and conducts movement against the concentration gradient. Movement between cells is referred to as *paracellular diffusion* (Karp, 1999). The BBB has a number of highly selective mechanisms for transport of nutrients into the brain (*Figure 1.3*).

Diffusion of substances into the brain can be divided into paracellular (i.e. between cells) and transcellular (i.e. across cells) diffusion, both of which are non-saturable and non-competitive. Paracellular diffusion does not occur to any great extent at the BBB, due to the "tight junctions". In the case of transcellular diffusion, the general rule is the higher the lipophilicity of a substance, the greater the diffusion into the brain (Pardridge, 1998). If two substances, identical on all other fronts, vary in molecular weight, the smaller substance will penetrate more rapidly; consequently small inorganic molecules (i.e. O_2, CO_2, NO, and H_2O) are highly permeable. Additionally, hydrogen bond reduction of a compound will enhance its membrane permeability. Removal or masking of a hydrogen bonding donor group from a compound will effectively decrease the transfer energy from water into the cell membrane (Burton *et al.*, 1996).

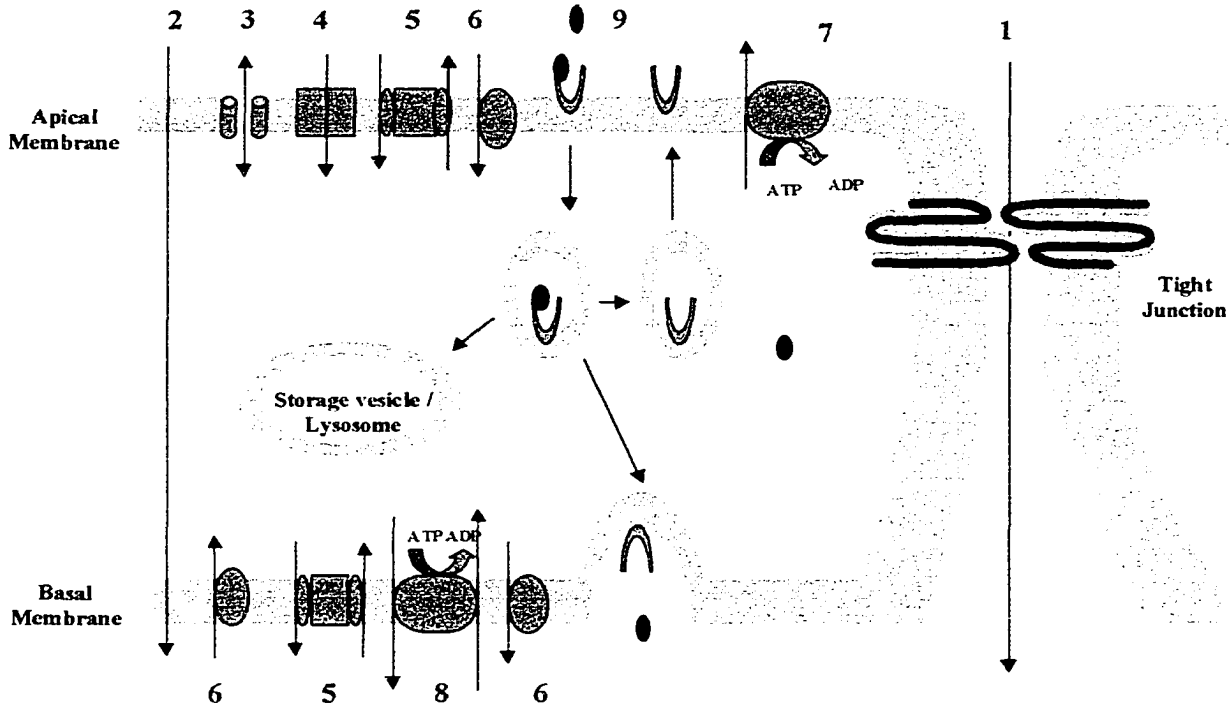

Figure 1.3 Transport mechanisms at the BBB. **1** = *paracellular diffusion* (sucrose), **2** = *transcellular diffusion* (ethanol), **3** = *ion channel* (K+ gated), **4** = *ion-symport channel* (Na+/K+/Cl- cotransporter), **5** = *ion-antiport channel* (Na+/H+ exchange), **6** = *facilitated diffusion* (Glucose via GLUT-1), **7** = *active efflux pump* (P-glycoprotein), **8** = *active-antiport transport* (Na+/K+ ATPase), **9** = *receptor mediated endocytosis* (transferrin & insulin)

Simple diffusion is a spontaneous process depending on random movement of solutes. The free-energy change of a solute diffusing across a membrane is directly dependent on the magnitude of the concentration gradient. If the solute is a non-charged species (i.e. nonelectrolyte), the movement across the membrane is described by the following equation:

$$\Delta G = (R) \times (T) \times (\ln \times [Ci]/[Co])$$

where ΔG is the Gibbs free-energy change (i.e the change during a process in the energy available to do work), R is the gas constant (1.987 cal/mol · °K), T is the absolute temperature (in degrees Kalvin), and [Ci]/[Co] is the ratio of the concentration of solute on the inside (I) and outside (o) of the membrane.

If the solute is a charged species (i.e electrolyte), the charge difference between compartments must be considered. The net movement of a solute with the same charge as the membrane is thermodynamically unfavorable, due to mutual repulsion of ions. The greater potential difference or voltage (i.e. charge) between compartments, the greater the difference in free energy. Therefore, for an electrolyte to diffuse between compartments two gradients must be considered: a chemical gradient, determined by differences in concentration, and an electric potential gradient, determined by difference in charge. Free-energy change for diffusion of an electrolyte across a membrane is:

$$\Delta G = [(R) \times (T) \times (\ln \times [Ci]/[Co])] + [(z) \times (F) \times (\Delta Em)]$$

where z is the charge of the solute, F is Faraday's constant (23.06 kcal/V·equivalent), and ΔEm is potential difference between compartments (Stein, 1967; Karp, 1999).

Another important aspect of diffusion is that the time required for a molecule to diffuse between two points is the *square* of the distance separating the two points. Albert Einstein's examination of theoretical aspects of diffusion (Einstein, 1905) resulted in the development known as the "Einstein relationship", which relates the time of diffusion to the distance traveled (i.e. the average molecular displacement; ΔX):

$$(\Delta X)^2 = 2 \times \text{Distance}$$

In the case of facilitated diffusion (a form of carrier-mediated endocytosis) there is a binding of a solute to a transporter on one side of the membrane that triggers a conformational change in the protein; this results in a carrying through of the substance to the other side of the membrane, from high to low concentration. Facilitated diffusion is passive (i.e. energy independent) and contributes to transport at the BBB of substances such as monocarboxyates, hexoses amines, amino acids, nucleoside, glutathione, small peptide, etc. (Tsuji and Tamai, 1999).

Carrier-mediated transport can also be divided into a number of different mechanisms dependent on energy and / or co-transport of another substance. Co-transport may be in the same direction (symport) or in the opposite direction (antiport). This process proceeds from a region of high concentration to a region of low concentration.

Endocytosis can be segregated into bulk-phase, also known as fluid phase, endocytosis and mediated endocytosis (receptor and absorptive mediated). Bulk-phase endocytosis (pinocytosis) is the nonspecific uptake of extracellular fluids and occurs at a constitutive level within the cell via mechanisms, which are independent of ligand binding (Simionescu et al., 1987). Bulk-phase endocytosis is temperature and energy dependent, non-competitive, and non-saturable. Bulk-phase endocytosis occurs to a very limited degree in the endothelial cells of the cerebral microvasculature (Pardridge, 1995).

Receptor-mediated endocytosis (RME) provides a means for selective uptake of macromolecules. Cells have receptors for the uptake of many different types of ligands, including hormones, growth factors, enzymes, and plasma proteins. RME occurs at the brain for substances, such as transferrin (Fishman et al., 1987), insulin (Duffy and Pardridge, 1987), leptin (Banks et al., 1996), and IGF-I & IGF-II (Duffy et al., 1988), and is a highly specific type of energy dependent transport. Substances that enter a cell by means of RME become bound to receptors that collect in specialized areas of the plasma membrane known as coated pits. The coated pits contain the electron dense clathrin protein, and other proteins (Moore et al., 1987). When bound to ligand these pits invaginate into the cytoplasm and then pinch free of the plasma membrane to form coated vesicles. The clathrin vesicle coat is rapidly removed to form smooth-coated endosomes that form a compartment of uncoupling receptor and ligand (CURL) (Stahl and Schwartz, 1986). The endosomal membrane contains proton ATPases that result in acidification of the endosome interior, and dissociation of the ligand from the receptor within the CURL.

Absorptive-mediated transport (AME) is triggered by an electrostatic interaction between a positively charged substance, usually a charge moiety of a peptide, the negatively charge plasma membrane surface (i.e. glycocalyx) (Gonatas et al., 1984). AME has a lower affinity and higher capacity than receptor-mediated endocytosis. The development of many new drug delivery technologies focuses on AME (Pardridge, 1999).

Another significant transport mechanism at the BBB is carrier-mediated efflux. This mechanism is involved in extruding drugs from the brain and is a major obstacle for

many pharmacological agents, with the ABC (ATP binding cassette) transporter P-glycoprotein being the principle efflux mechanism of these agents (Cordon-Cardo et al., 1989). There also exists efflux transporters for organic anions, via multidrug resistance associated protein (MRP) (Kusuhara et al., 1998), and anionic and cationic cyclic peptide (Tsuji, 2000). Additionally, the peptide transport system (PTS)-1 shows efflux transport of synthetic opioid peptide Tyr-MIF-1 (Banks et al., 1993).

Transport of Substances into the Brain

The ability of a particular substance to cross the BBB and enter the brain is dependent upon several factors (*Figure 1.4*). Factors at the BBB include concentration between compartments, size of molecule (i.e molecular weight), flexibility and conformation of molecule, amino acid composition, lipophilicity, cellular enzymatic stability, cellular sequestration, affinity for efflux mechanisms (i.e. P-glycoprotein), hydrogen bonding potential (i.e. charge), affinity for carrier mechanisms, and effects of existing pathological conditions. Peripheral factors include systemic enzymatic stability, plasma protein binding affinity, cerebral blood flow, uptake into other tissues, clearance rate, and effects of existing pathological conditions.

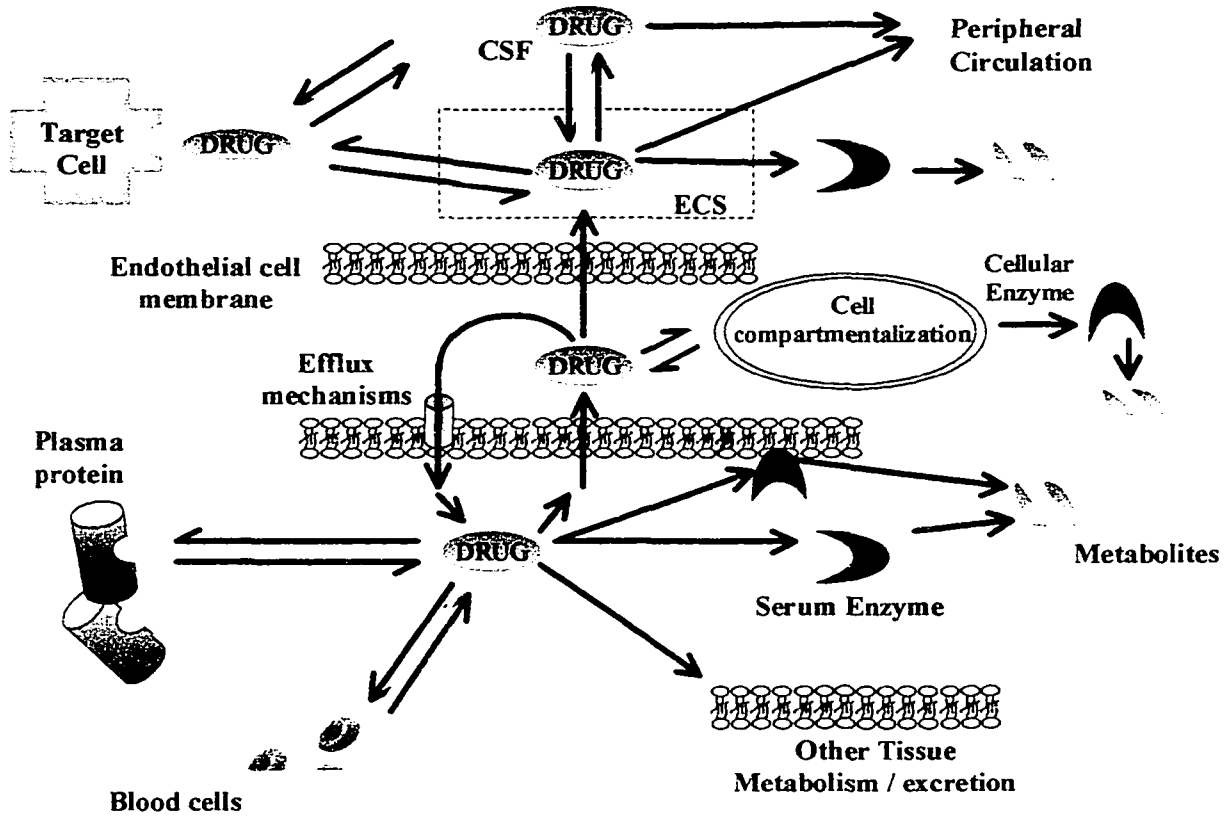

Figure 1.4 Potential factors which alter drug uptake into the brain

Anatomy and Physiology of Blood-CSF Barrier

While the largest interface between blood and brain is the BBB, this is also smaller less direct interface between blood and cerebrospinal fluid (CSF). Goldmann first demonstrated the existence of the blood-CSF barrier in 1913. Through the use of dyes with different properties it was found that the blood-CSF barrier was selectively permeable, rather than absolute (Bradbury, 1979).

The *choroid plexus* and the *arachnoid membrane* act together at the barriers between the blood and CSF. On the external surface of the brain the ependymal cells fold over onto themselves to form a double layered structure, which lies between the dura and pia, this is called the arachnoid membrane. Within the double layer is the subarachnoid space, which participates in CSF drainage. Passage of substances from the blood through the arachnoid membrane is prevented by tight junctions (Nabeshima et al., 1975). The arachnoid membrane is generally impermeable to hydrophilic substances, and its role is forming the Blood-CSF barrier is largely passive.

The choroid plexus forms the CSF and actively regulates the concentration of molecules in the CSF. The choroid plexus consist of highly vascularized, "cauliflower-like" masses of pia mater tissue that dip into pockets formed by ependymal cells. The preponderance of choroid plexus is distributed throughout the fourth ventricle near the base of the brain and in the lateral ventricles inside the right and left cerebral hemispheres. The cells of the choroidal epithelium are modified and have epithelial characteristics. These ependymal cells have microvilli on the CSF side, basolateral interdigitations, and abundant mitochondria (Segal, 1999). The ependymal cells, which line the ventricles, form a continuous sheet around the choroid plexus. While the capillaries of the choroid plexus are fenestrated, non-continuous and have gaps between the capillary endothelial cells allowing the free-movement of small molecules, the adjacent choroidal epithelial cells form tight junctions preventing most macromolecules from effectively passing into the CSF from the blood (Brightman, 1968). However, these epithelial-like cells have shown a low resistance as compared the cerebral endothelial

cells, approximately 200 $\Omega \cdot cm^2$, between blood and CSF (Saito and Wright, 1983); *Figure 1.5.*

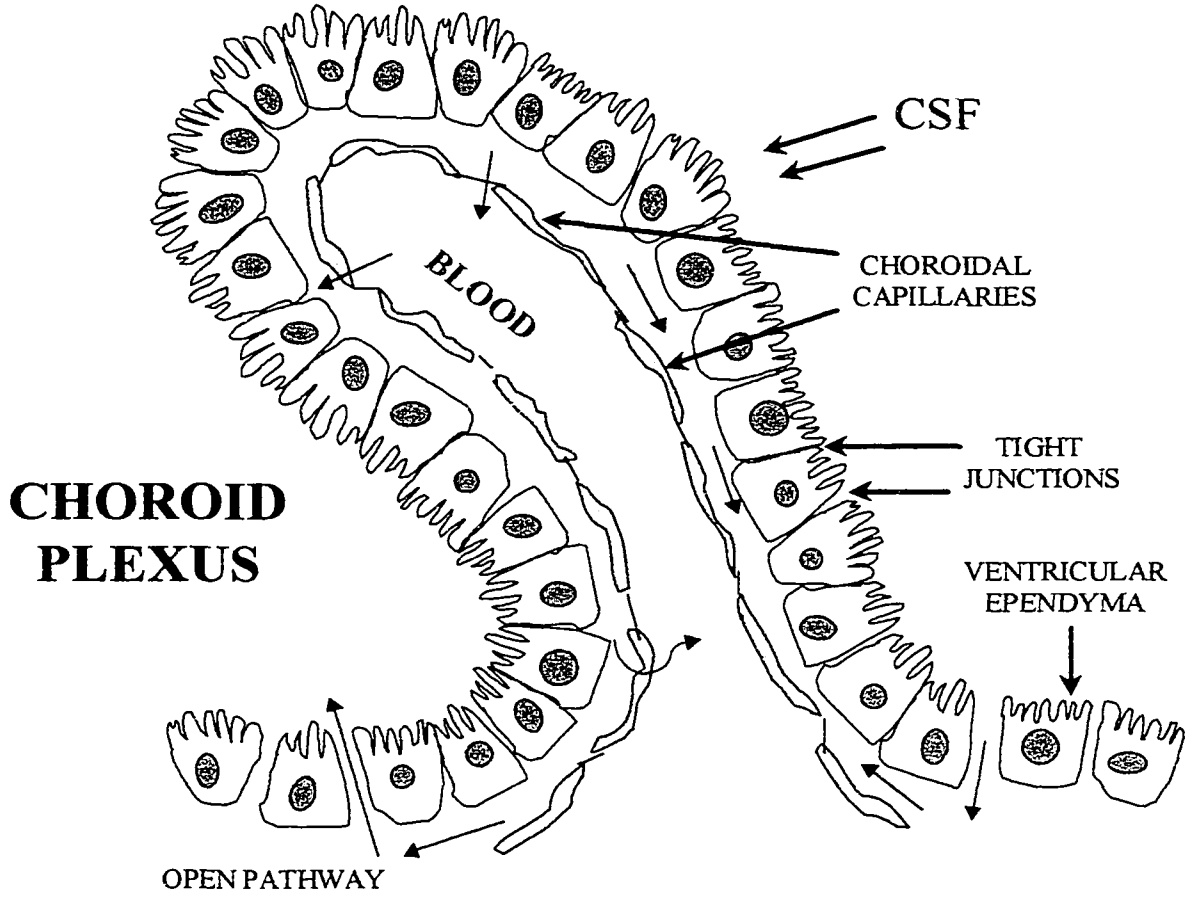

Figure 1.5 The choroid plexus, composed of CSF producing choroidal capillaries and ventricular ependyma. The choroid plexus is composed of fenestrated capillaries and an epithelial (ependymal) covering, which reverts from "tight" to moderately "open" at the base (Begley et al., 1996).

Cerebral-Spinal Fluid

The cerebrospinal fluid (CSF) is located within the ventricles, spinal canal, and subarachnoid spaces. The principle source of CSF are the choroid plexi of the lateral, third and fourth ventricles (*Figure 1.6*), and the volume varies between 10-20% of brain weight (Bradbury, 1979). The volume of CSF in humans is 140-150 ml, only 30-40 ml actually in the ventricular system, with a production rate of 21 ml/hr. The turnover rate of total CSF is species dependent and varies between approximately 1 hr for rat and 5 hr for human (Davson and Segal, 1996). The majority of the CSF is in the subarachnoid space, where the arachnoid membranes bridge the sulci of the brain, in the basal cisterns and around the spinal cord. CSF moves within the ventricles and subarachnoid spaces under the influence of hydrostatic pressure generated by it production. CSF cushions the brain, regulates brain extracellular fluid, allows for distribution of neuroactive substances, and is the "sink" that collects the waste products produced by the brain.

Concentration of most molecules is greater in the brain than in the CSF, creating a physiological gradient between the two compartments. The continuous flow of CSF through the ventricular system and out over the surface of the brain provides a "sink" that reduces the steady-state concentration of a molecule penetrating into the brain and CSF (Davson et al., 1961). This "sink" effect is greater the slower a molecule moves, which makes it particularly important for lipid-insoluble molecules of large molecular radius (Davson and Segal, 1996). Few drugs gain entry into the brain via CSF uptake due to the bulk flow movement. However, azidothymidine (AZT) enters the brain through rapid distribution into the CSF and subsequent transport at the CSF-barrier via a thymidine

transporter (i.e. pyrimidine nucleoside carrier) (Wu et al., 1992), such a transport is not present at the BBB (Cornford and Oldendorf, 1975).

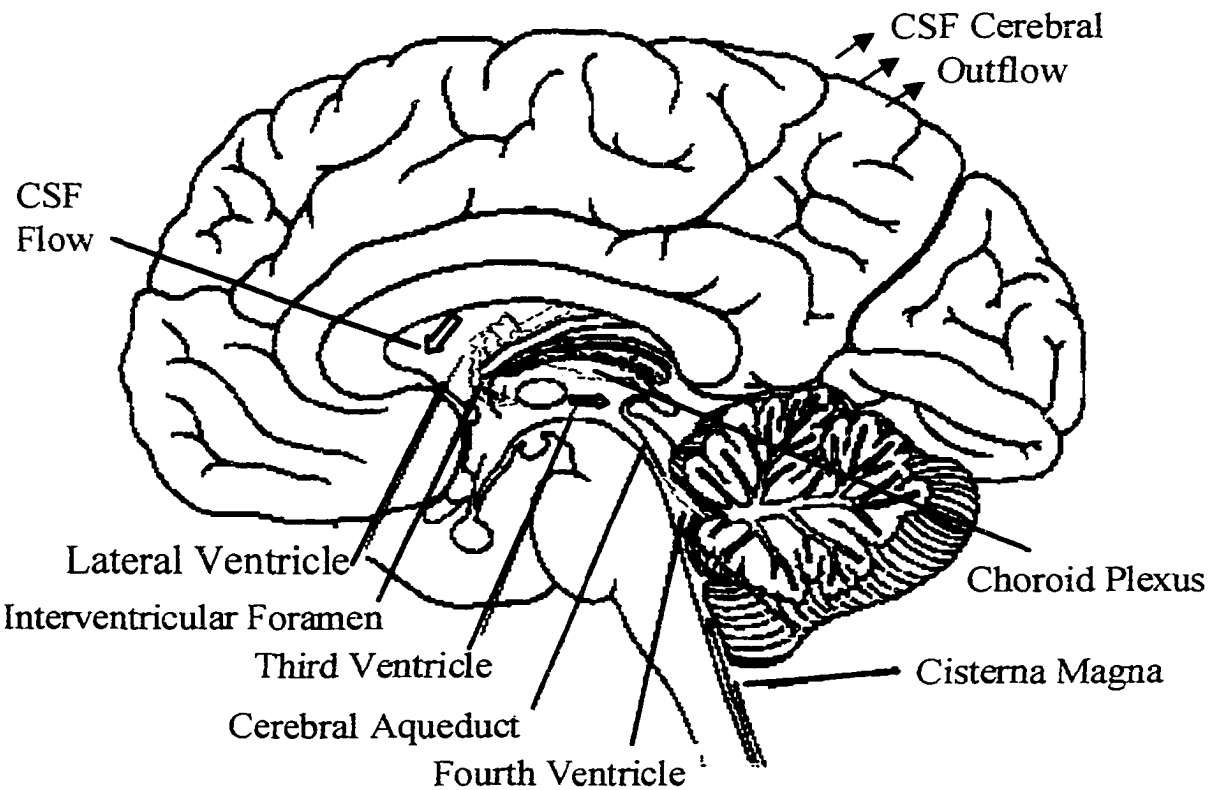

Figure 1.6 Cross-section through the brain. Shown is the creation of CSF at the choroid plexus in the lateral, third and fourth ventricle. CSF flows from ventricles (arrows), under hydrostatic pressure, eventually leaving the Brain via the subarachnoid villa into the venous blood.

Circumventricular Organs

At several locations around the ventricles are the circumventricular organs (CVO's), which have permeable fenestrated capillaries, with exception to the subcommisural organ. The surface area of the BBB is approximately 5000-fold greater than that of the CVO's (Crone, 1971). The circumventricular organs are midline structures bordering the 3rd and 4th ventricles. These barrier-deficient areas are recognized as important sites for communicating with the CSF and between the brain and peripheral organs via blood-borne products. CVO's include the pineal gland, median eminence, neurohypophysis, subfornical organ, area postrema, subcommissural organ, organum vasculosum of the lamina terminalis, and the choroid plexus. The intermediate and neural lobes of the pituitary are sometimes included (Davson and Segal, 1996).

Blood Supply to the Brain

The brain is highly metabolically active, yet has no effective way to store oxygen or glucose. It depends on a large and stable blood supply. The brain is approximately 2% of body weight, but uses ~15% of cardiac output and accounts for 25 % of oxygen consumption. Autoregulation of cerebral blood supply maintains a consistent flow of blood to the brain. However, local flow-rates vary, dependent upon which part of the brain is active at any given time. The major branches of the arterial blood supply to the brain are shown in *figure 1.7*.

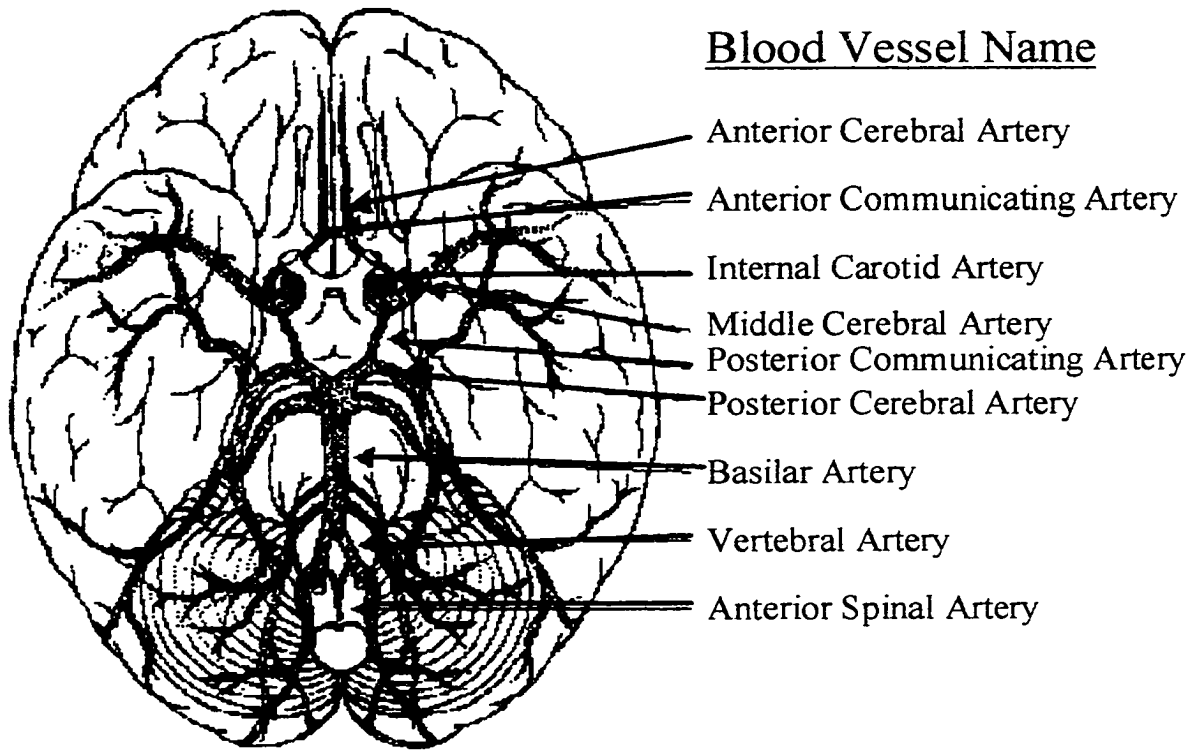

Figure 1.7 Ventral horizontal section of brain, showing blood supply via major blood vessels

Methods for the Examination Drug Transport through the BBB

The BBB is the major regulator of the internal environment of the CNS. The BBB is complex structure, consisting of multiple barrier elements, rendering limitations to any technique used to measure its activity. There are many techniques currently employed to examine BBB permeability characteristics. These techniques can be divided into two primary categories dependent on whether the method uses whole animal (*in vivo*) or cultured techniques (*in vitro*).

Carotid Artery Single-Injection Method

The carotid artery single-injection method for quantifying BBB transport was developed by Oldendorf (1970), and is also known as the BUI (brain uptake index) method. This method is an extension of the "indicator dilution technique" first applied by Crone (1963). This method measures a bolus injection (~200μl) of a buffered Ringer's solution (or serum or other vehicle) containing a [^{3}H]-labeled test compound or reference compound and [^{14}C]-labeled reference or test compound into the common carotid artery of an animal. The bolus passes through the brain within ~2s after injection, and the animal is decapitated 5-15s post injection. The 5-15 second time period between injection and decapitation allows for complete clearance of compound from cerebral blood vessels, with minimal efflux of test compound from brain (Pardridge and Fierer, 1985). The BUI is determined from the [^{3}H]/[^{14}C] ratio in the brain divided by the same ratio in the injected solution. This determines the amount of test compound lost to brain tissue after a single pass through the brain. This method can be used to estimate BBB

transport characteristics of both carrier-mediated and plasma protein mediated transport. This method has the added advantage of a short experimental time, however this short time period of measurement will also allow for greater error in quantification. Additionally, drugs that are slowly transported into the brain will have even greater error in measurement, due to small uptake volumes, thus this technique is not suited for study of peptide transport.

Intravenous Bolus Injection

This technique employs the cannulation of a femoral vein or artery and injection of a radiolabeled test compound (Ohno et al., 1978). Animals are sacrificed and arterial blood is collected, to measure against brain concentration. The radioactivity per gram of brain divided by radioactivity per μl of plasma is used to determine the brain volume of distribution, and can be used to determine a BBB permeability. This technique does not require access to the carotid artery and is relatively sensitive, however compounds which undergo rapid metabolism in the blood (i.e. peptides) can be difficult to accurately assess and may prevent accurate calculation. Additionally, drug transport kinetics at the BBB can not be determined with this method.

Brain Perfusion Technique

Brain perfusion via the carotid arteries is a highly effective technique for assessing the uptake of peptides and BBB transport kinetics over longer experimental time points (5-20min). This technique has been used extensively in rat (Takasota et al.,

1984) as well as guinea pig (Zlokovic et al., 1986), and has numerous applications. Carotid artery infusion involves cannulating an anesthetized animal at both common carotid arteries, with sectioned jugular veins to allow open-ended outflow. A perfusion of a radiolabeled compound, in a physiologically balanced Ringer's solution, through the carotid arteries proceeds at a constant flow-rate, approximating the animals cerebral blood flow. This technique also allows for CSF sampling to assess transport across the blood-CSF barrier. At a set time the perfused animal is decapitated and the amount of radiolabeled drug entering the brain is determined, expressed as a ratio dpm/gram of brain to dpm/μl of perfusate.

Brain perfusion assessment of compound uptake is more sensitive than brain uptake index, due to extended experimental time. This technique also eliminates metabolism by blood components, which may otherwise breakdown the compound of study. This technique must use chromatography of brain extracts to assess peptide metabolism by brain or vasculature. Additionally, the capillary depletion technique (Triguero et al., 1990) must be used differentiate transcytosis from nonspecific binding to brain vasculature.

Intra-Cerebral Microdialysis

The intra-cerebral microdialysis method involves the stereotactic placement of a probe into the brain, which contains a semi-permeable membrane at the tip with a molecular weight cut-off between 5 and 50 KDa (De Lange et al., 1998). This technique involves a solution of artificial CSF perfused at a slow rate through the probe, allowing

molecules of low molecular weight to diffuse into the membrane from the brain extracellular fluid. A drug introduced to the systemic circulation of an animal will appear in the out-flowing perfusate if it is able to penetrate the BBB. The principle advantage of this technique is that it can potentially provide simultaneous information regarding the free concentrations of drug in brain interstitial fluid, cerebrospinal fluid, and plasma (Begley, 1999). There are two principle problems with this technique. First, the dialysis membrane itself presents a diffusional barrier to substances in the respective fluids. Second, this technique is invasive and inserting a probe into the brain does cause local tissue damage, which may effect the BBB in the region of the probe.

Autoradiography

The transcytosis of compounds through the BBB may be demonstrated with autoradiography (Duffy and Pardridge, 1987). This analysis is best described as an *in vivo* morphologic method. In this analysis a radiolabeled compound or plasma protein is infused into the carotid artery for 10min, followed by decapitation and rapid snap-freezing. The brain tissue is cut on a cryostat and thaw-mounted to eliminate artifactual diffusion of radiolabeled compounds (Sar and Stumpf, 1983). This technique allows for differentiation of transcytosis from binding or endocytosis to the vasculature. Additionally, it is a highly sensitive and quantifiable method (Pardridge, 1991). The principle disadvantage to this method is the long exposure time and the use of HPLC to assess metabolism in brain and blood extracts.

Peroxidase Histochemstry

This analysis is also best described as an *in vivo* morphological method. Peroxidase histochemistry has been used to study the transcytosis of wheat germ agglutinin-peroxidase conjugate through the BBB (Broadwell et al., 1988). This methodology imposes the same provisions as autoradiography or perfusion approaches in assessing metabolism. This method is much faster than audioradiography and can be used in conjunction with electron microscopy. The principle disadvantage of this method is its relatively low sensitivity, disallowing it for assessment of peptide transport examination.

Positron Emission Tomography

Alterations in BBB permeability can be measured in humans with quantitative positron emission tomography (PET) scans, using tracers such as ^{82}Rb and ^{68}Ga-EDTA (Iannoti, 1992). This is a non-invasive procedure, in which positron-emitting isotopes in the systemic circulation can be measured as they enter the CNS. BBB permeability can be measured *in vivo*, with combined use of PET technology, and theoretical and physiological information obtained via animal studies (Abbruscato, 1997). PET scans can quantify the activity in specific brain regions, yet cannot differentiate the compartments (brain or blood tissue) in which the activity occurs. However, the blood compartment can be subtracted out by independent measurement of cerebral blood volume, and thereby obtain an estimate the intravascular compartment. Quantification of BBB permeability, using either ^{82}Rb or ^{68}Ga-EDTA in humans, requires accurate

assessment of both plasma AUC and plasma volume, otherwise significant artifacts may result (Pardridge, 1995).

Octanol / Saline Partition Coefficient

Frequently, a compounds ability to diffuse across a membrane can be predicted by the partition between lipophilic (i.e. octanol) and hydrophilic (saline) phases. Predicted lipophilicity as a percent ratio of the amount of compound in the octanol phase to that in the saline phase is referred to as a partition coefficient. This is a simple and fast chemical assessment method used to screen compounds, which provides a rough indication of membrane diffusibility (Habgood et al., 2000). However, this method does not take into account the ability of specific carriers to transport a compound and is pH dependent. This method may not accurately correlate ionizable compounds, as the ionic state is contingent on ambient pH.

HPLC capacity factor

Capacity factors calculate from high performance liquid chromatography (HPLC) retention times are used to assess lipophilicity of various organic compounds. Capacity factors (k) are determined on a pre-established HPLC gradient via the following equation:

$$\text{Capacity factor: } k = (t_r - t_o) / t_o$$

where t_r is the retentions time of the retained peak and t_o is the retention time of the unretained peak (Weber et al., 1993).

Cerebral Microvascular Endothelial Cell Cultures

Cerebral microvessels were first isolated from human or bovine brain using a combination of mechanical homogenization and sieving techniques (Siakotos et al., 1969). Several *in vitro* BBB models have been described in detail by de Boer and Sutanto (1997). These model systems differ with respect to isolation procedures, culture conditions and model preparations. These systems are further complicated by use of primary, subpassaged, and immortalized cell lines from multiple tissue types (i.e. brain capillaries, aortic endothelial cells, umbilical vein endothelial cells) and tissue origins (i.e. human, primate, rodent, bovine, porcine). Recent *in vitro* BBB modeling has centered on the used of astrocyte co-culture and conditioned media, to enhance the *in vivo* BBB characteristics (Dehouck et al., 1990; Abruscatto et al., 1999). The diversity of current *in vitro* BBB models often makes comparison of data difficult, as each model is functionally characterized and optimized to the needs of the research group.

In regards to transport assessment, the strength of *in vitro* blood-brain barrier models is the ability to test of large numbers of non-radiolabeled compounds in a quick and efficient manner. A prevalent *in vitro* BBB model employs the use of primary cultures of brain endothelial cells grown on filters, with measurement of test compounds across the brain endothelial monolayer (Audus and Borchardt, 1986; van Bree et al., 1989). Several potential draw-backs to in vitro BBB models exist. First is the possibility for extensive de-differentiation of brain capillary endothelial cells when grown in culture (Laterra and Goldstein, 1993). Second, down-regulation of nutrient transport, as much as 100-fold (Pardridge et al., 1990), may result in underestimation of BBB permeability of

compounds that utilized carrier mechanisms. Third, compounds that undergo lipid-mediated transport have over-estimated BBB permeability (Pardridge et al., 1990). Fourth, tight junction formation between endothelial cells is greatly reduced (Brightman and Tao-Cheng, 1993). A comparison of *in vitro* vs. *in vivo* BBB models is shown in *table 1.2*.

In vitro	***In vivo***
ADVANTAGES	
Rapid, Sensitive, Simple	Takes into account full physiology
Use of non-radiolabeled compounds	Fully functioning intact BBB
Screens large number of compounds	More accurate assessment of uptake
Pure cell population	More accurate assessment of pathology
Specifically modify parameters of analysis	
DISADVANTAGES	
Dedifferentiation	Greater number of variables
Decrease in carrier mediated mechanisms	More labor intensive
Decrease in tight junction integrity	Greater time for analysis
Altered cell-cell interactions	Peripheral effects on drug
Enhanced lipophilic compound transport	Requires radiolabeled drug
Cell proliferation	

Table 1.2 *In vitro* vs. *in vivo* BBB models

Passive Entry of Drugs into the Brain

The BBB functions as a diffusional restraint, with selective discrimination based on lipid solubility, molecular size, and charge. Lipid solubility has long since been recognized as an important factor for entry across cells (Davson and Danielli, 1943). Lipid solubility is in part a factor of hydrogen bonding affinity. The greater the number and strength of hydrogen bonds the lower its solubility in non-polar solvents. Additionally, a molecular weight threshold (Levin, 1980) limiting BBB transport for molecules exceeding a mass of 400-600 Da has been theorized. The effect of molecular weight / volume on solute diffusion has been consistently noted as a significant factor affecting passive diffusion of drugs (Pardridge, 1998). Yet, it is not clear whether the observed inverse relationship between molecular size and BBB permeability is a true effect or a factor of the specific compounds assessed. Although diffusion coefficients are inversely related to molecular size (Sutherland, 1905), the major step in crossing the BBB is most likely partitioning into the cell membrane. It has been suggested (Habgood et al., 2000) that molecular size may not be as important for determining BBB permeability or that a positive effect of high lipid solubility may counterbalance any negative effect of large molecular size. Additionally, drugs pass through membranes more readily if they are uncharged. "Ion trapping" of a drug, based on the pH of the surrounding fluid and pKa of the drug (pKa is the measure of strength of the interaction of a compound for a proton), results in a net decrease in diffusion across membranes and is a function of charge.

Current Strategies to Enhance Brain Uptake of Peptide Drugs

Transport of peptide based drugs into the brain is greatly limited, primarily due to the existence of the BBB. To date, numerous strategies have been developed to enhance entry of peptide drugs to the brain. These strategies are divided into seven categories: (i) invasive procedures, (ii) blood-brain barrier junctional disruption, (iii) vector based methods, (iv) transnasal delivery, (v) pegylation, nanoparticles, and liposomal delivery systems, (vi) efflux transporter inhibition, and (vii) chemical modification.

Invasive Procedures

Direct delivery into the brain via injection has been proposed, to avoid problems associated with systemic delivery (Carvey et al., 1994). Direct injections via lumbar puncture, via Ommaya reservoir (with catheter to the lateral ventricle), and epidural catheters are being used for the administration of anesthetics and narcotics. However, multiple injections of peptide drugs would be necessary to maintain therapeutic concentrations and would thereby lead to increased risk of infection and patient discomfort (Prokai, 1998). Additional obstacles to this approach are those of diffusibility of large molecular weight drugs, continual efflux out of brain via CSF flow, and enzymatic breakdown. While intraventricular injection of drugs is a poor mode of delivery to the brain parenchyma, this approach does allow for adequate drug distribution to the brain surface (Pardridge, 1995). Therefore diseases with a disposition for the brain surface are more responsive to intraventricular drug administration (i.e. meningitis, meningeal leukemia). Chronic pain may also be amenable with intraspinal morphine

injections owing to the high concentration of opioid receptors on the surface of the spinal cord (Otsuka and Yanagisawa, 1988)

Controlled-release polymeric implants can be used to deliver peptides directly to the brain tissue (Domb et al., 1994), with no associated toxic by-products, and can release drugs over a time course. These pumps have the advantage of a sustained-release delivery of drug. Such implants have been shown to be an effective strategy for the delivery of chemotherapeutics, in a site-specific manner, for treatment against brain cancer (Brem et al., 1991).

Blood-Brain Barrier Junctional Disruption

Osmotic disruption of the BBB is a concept initially conceived and characterized by Rapoport and colleagues (1970). In this method, direct carotid infusion of a hypertonic solution (mannitol, arabinose, lactamide, saline, urea, glycerol) is used to withdraw water from the endothelial cells of the brain capillaries, shrinking the endothelial cells and weakening the tight junction interface. This facilitates the paracellular transport of small and large molecules (Neuwelt et al., 1987), as well as virus sized iron oxide particles (Neuwelt et al., 1994). The hyperosmolar solution draws water out of the brain, and is rapidly rehydrated when infusion is terminated by way of return of water from the vascular space, also facilitating influx of water soluble substances into the brain (Bartus, 1999). However, there are considerable toxic effects associated with generalized opening of the BBB, which can produce inflammation, encephalitis, and seizures in up to 20% of applications (Prokai, 1998).

Vasodilators such as bradykinin and histamine are known to enhance the permeability of capillaries. Bradykinin is an endogenous vasodilator that increases blood-flow and permeability of blood capillaries. Intracarotid infusion of bradykinin, in micromolar quantities (Nomura et al., 1994), was shown to be sufficient to increase permeability in blood-tumor barriers. Bradykinin, in larger concentrations, has also shown to induce increases in pinocytotic vesicles (Raymond et al., 1986). RMP-7 (a.k.a. Labradimil or Cereport) a synthetic analogue of bradykinin selective for the B2 receptor, has been developed to increase the permeability of the BBB. Electron microscopy demonstrated that intravenous RMP-7 increases the permeability of the BBB by "disengaging" the tight junctions at the blood-brain tumor barrier (Emerich et al., 2001).

It should also be noted that rapid increases in arterial blood pressure (Hardebo and Nilsson, 1981), protein kinase C stimulation (Yamada et al., 1990), and systemic cytokine administration (Saija et al., 1995) will disrupt BBB tight junctions. However, the therapeutic potential of these modalities is limited, though they are of importance when considering delivery of drug during a disease state.

Vector Based Methods

Physiologic vector based strategies involve the use of existing BBB transport properties to enhance brain entry of a specific drug. This may employ coupling a peptide drug to a substance that is normally transported through the BBB via a receptor mediated or absorptive mediated endocytosis. These coupled drugs are referred to as "vector-mediated" or "chimeric" peptides. After entry into the brain these chimeric drugs release

from the biologically active compound that allowed their entry, via enzymatic cleavage in a prodrug manner. The drug is then free to initiate a pharmacological action in the brain. This technology may be adapted for use with peptide pharmaceuticals, nucleic acid therapeutics, and small molecules. Multiple concepts for such systems exist (Pardridge, 1999), with present focus on antibody attachment and chemical linker strategies.

This method of delivery is plagued with numerous obstacles. Receptor mediated vectors must be relatively specific for brain uptake. Receptor ligands, such as insulin and transferrin, have been used in several vector mediated delivery strategies, yet they are non-CNS specific and can be taken up by other tissues. Also, there exists a potential competition between the chimeric drug with the endogenous ligand for the receptor. This may result in a decrease in vector transport and / or decrease in the concentration of a required nutrient to the brain resulting in a subsequent pathology. Serum transferrin has shown to actively compete with radiolabeled transferrin (Skarlatos et al., 1995). Absorptive mediated endocytotic strategies have been proposed (i.e. cationized albumin) due to the greater capacity over receptor-mediated strategies. However, cationized albumin is extensively cleared (Pardridge et al., 1990a). A relatively recent technology using receptor-specific antibodies has a great deal of promise. OX26 is a transferrin receptor antibody (rat) that has been covalently conjugated to NGF (neuronal growth factor), resulting in a significant increase in rat brain uptake (Freiden et al., 1994; Pardridge et al., 1994). Nevertheless, a specific receptor antibody for human use has not been assessed. The use of linkers such as avidin-biotin (Yashikawa and Pardridge, 1992; Bickel et al., 2001) and polyethylene glycol (Zhang and Pardridge, 2001) to OX26 and a

peptide drug have shown to enhance the pharmacokinetic profiles of drug vectors. However, linking such complexes is difficult and must be optimized and assessed on an individual basis, as these complexes also add to the molecular mass of the drug. Furthermore, enhanced pharmacokinetics alone, via polyethylene glycol attachment, may account for effects observed. Additional complications revolve around the ability of the conjugated drugs to release a biologically active moiety after enzymatic cleavage. Lastly, the quantity of drug for delivery to brain is directly limited to the transporter concentration. Transporter capacity may become significantly saturated, or down-regulated over time, decreasing the ability to deliver an adequate and consistent dosage to bring about the appropriate pharmacological effect. Therefore, the limited amount of delivery requires extremely potent therapeutic peptides.

Transnasal Delivery

Delivery of narcotic drugs, such as cocaine and amphetamine, have long been shown to rapidly enter into the brain via the nasal route. Nasal delivery appears to be a fast and effective route of administration, suitable for drugs that must act rapidly and are taken up in small amounts. The advantage of such an approach is that it achieves high drug availability to the surface of the brain and results in a substantial drug delivery to the general blood stream, via CSF outflow. Intranasal administration of the highly lipophilic drug progesterone has shown to gain access to the CSF directly, without entry into the peripheral blood compartment (Keck et al., 1989). Transnasal delivery of peptides has been assumed to provide a direct route of the peptide to the CSF compartment,

circumventing the systemic circulation (Cool et al., 1990). However, peptide movement into the CSF is greatly limited by a nasal epithelial barrier. This barrier consists of three types of cells: sensory bipolar neurons, supporting epithelium, and basal epithelium. Tight junctions exist between sensory and supporting epithelium, preventing proteins in the blood from crossing into the nasal cavity (Brightman et al., 1970; Mathison et al., 1998). These tight junctions would additionally prevent transit of peptides from the apical side of the nasal epithelium to the submucous space, where the peptide might diffuse into the microvessels of the olfactory epithelium (Pardridge, 1991). However, the arachnoid membrane that surrounds olfactory lobe also contains tight junctions that may prevent entry into the brain. If a drug does gain access to the CSF it must further contend with the relatively rapid bulk flow out of the CNS into the systemic circulation. Lastly, the significant enzymatic activity (i.e. aminopeptidase) within the nasal cavity requires peptide analogues that are relatively resistant to enzymatic breakdown (Hussain et al., 1995; Khanvilkar et al., 2001).

Many peptides are highly hydrophilic and their ability to diffuse through the barriers necessary for intranasal delivery is log orders slower than more lipid soluble compounds. The use of absorption enhancers may greatly enhance the bioavailability of peptides following intranasal administration. Classes of enhancers include surfactants, chelating agents, cyclodextrins, dihydrofusidates, and bile salts. Several peptide drugs are presently being investigated and / or are currently used, that are administered via the transnasal route (i.e. insulin, calcitonin, secretin, oxytocin, enkephalins, etc.).

Pegylation, Nanoparticles, and Liposomal delivery systems

Drug delivery systems are designed to alter the delivery of injectable drugs. Three new approaches involve pegylation, nanoparticles, or liposomes. Peptides are particularly suited for such mechanism because they are rapidly hydrolyzed, often have poor stability, and are readily cleared.

Pegylation is a procedure of growing interest for enhancing the therapeutic and biotechnological potential of peptides and proteins. When poly(ethylene glycol), or PEG, is correctly linked to a peptide it will modify many of the pharmacokinetic features, while theoretically maintaining the primary biological activity (i.e. enzymatic activity or receptor recognition). PEG chains can contain linear and branched structures, which can be conjugated directly to the peptide drug or linked in a "prodrug" manner. PEG conjugation masks the peptide's surface and increases the molecular size, thereby reducing immune response, enzymatic degradation, toxicity, and renal ultrafiltration (Reddy, 2000). PEGs may also produce improved physical and thermal stability, as well as increased solubility (Veronese, 2001). The principle disadvantage of pegylation is the potential loss of activity with improper choice of PEG (i.e. length, branching, chemical design) or unfavorable choice of attachment site. Another considerable disadvantage to pegylation, in regard to CNS focused drug delivery, is the enhanced hydrophilicity and molecular size that can bring about significant reductions in passive diffusion.

Nanoparticles are polymeric particles made of natural or artificial polymers ranging in size between 10 and 1000 nm. Drugs can be bound in the form of a solid solution, dispersion, or absorbed to the surface of the particle or chemically attached.

Nanoparticle mediated drug transport into the brain depends on the polysorbate overcoating, with polysorbate-80 being the primary form used in nanoparticle technology. Polysorbate-80 nanoparticles have shown to enhance delivery of the Leu-enkephalin analogue dalargin (Kreuter et al., 1995), as well as loperamide, tubocurarine, doxorubicin, and the NMDA receptor antagonist MZ 2/576 (Kreuter, 2001). This material has been theorized to act as an anchor for apolipoprotein E (apo E) or other substances after injection into the blood stream. The particles may act to mimic low density lipoproteins (LDL) and could thus be taken up into the endothelial cells of the BBB via LDL receptor. Other theories of enhanced transport across the BBB by nanoparticles involve tight junction modulation (Kreuter, 2001) or P-gp inhibition (Woodcock et al., 1992). A generalized surfactant effect may also occur, with solubilization of the endothelial cell membrane lipids that could lead to membrane fluidization and enhanced drug entry (Kreuter, 2001). Additionally, enhanced retention of drug-nanoparticle in the blood-stream would allow a decrease in drug clearance. Nanoparticles have not been fully assessed for potential toxicologic ramifications.

Liposome preparations can be designed for drug targeting or continuous release. Liposomes are composed of a phospholipid bilayer that may act as a carrier for both hydrophilic and hydrophobic drugs. There are several beneficial characteristics of liposomes, such as enhanced drug half-life in blood, decreased clearance, and decreased toxicity (Reddy, 2000). Unfortunately, such preparations have shown to be extensively sequestered in the liver, spleen, reticuloendothelial system; general "leak" of drug while in circulation; and lack of long-term physiological stability (Gabizon et al., 1994;

Gabizon and Martin, 1997). Liposomes, as vehicles for transport of drugs across the BBB, have had limited success. Liposome-like micellular formulations with polyethylene glycol (or equivalent) attachment have shown some success in transport of drug across the BBB. One such formulation is the pluronic copolymer P85, a self-forming micelle preparation that encapsulates a drug, has shown to enhance delivery of digoxin into the brain (Batrakova et al., 2001); the mechanism of action is believed to be the inhibition of P-gp. Brain directed immunoliposomes (antibody-directed liposomes) can be used for the delivery of drugs, based on antisense targeting. Immunoliposomes, conjugated to OX26 transferrin antibody, were shown to significantly enhance brain delivery of [^{3}H]-daunomycin (Huwyler et al., 1996), however problems similar to those stated above for *vector-based methods* may also occur.

Efflux Transporter Inhibition

The BBB contains a number of efflux transporters that reduce the influx of certain lipid soluble compounds able to diffuse through cell membranes (Tatsuta et al., 1992). The natural multidrug resistance that they confer to the brain is a significant consideration in the targeting of drugs at the CNS. The coadministration of other substrates, or an inhibitor, of the efflux transporters to competitively saturate the efflux capacity of these "pumps" is a currently investigated strategy to enhance drug transport at the BBB (Drion et al., 1997; Habgood et al., 2000). However, the capacity of these mechanisms appears to be extremely high and their competitive saturation would involve concentrations of drug (i.e. other substrate or inhibitor) in toxic doses. Substrates /

inhibitors need to have lower toxicity than those that have been thus far investigated (i.e. cyclosporin A, vincristine, verapamil, colchicine). One such inhibitor currently under development by Glaxo Wellcome Inc., is GF120918. GF120918 has shown promise as a potent and specific P-GP inhibitor at the BBB and has shown to increase morphine analgesic effect (Letrent et al., 1999), as well as to significantly increase the systemic exposure to oral paclitaxel in cancer patients (Malingre et al., 2001).

Chemical Modification

Drug design as a mode to enhance BBB transport and pharmacological actions can be generally divided into six categories: prodrugs, lipidization, structural modification, enzyme stability, use of nutrient carriers (mimetics), and cationization. *These categories are not exclusive.*

Lipid solubility is a key factor in determining the rate at which a drug passively crosses the BBB, the concept of lipidization focuses on this aspect. Peptide drugs generally contain polar functional groups that impart a degree of dipolarity and hydrogen bonding, thereby reducing their partition into non-polar solvents. Reduction of the relative number of polar groups results in enhanced partition into non-polar solvents, and thereby an improved entry into lipid membranes. The overall balance of polar to non-polar groups within a drug molecule can be reduced either by removal or by the addition of a polar or nonpolar group (Habgood et al., 2000). The removal of two polar hydroxyl groups from dopamine, resulting in phenethylamine, has shown to increase the lipid solubility approximately 50-fold, with subsequent enhancement of brain entry (Fischer et al., 1972). This removal not only reduced the hydrogen binding affinity, but also

effectively reduced the molecular volume. *Table 1.3* lists several strategies for lipidization (***not necessarily enhanced brain uptake***).

Drugs containing only polar groups essential for pharmacological effect, can be modified by addition of extra non-polar groups at sites that do not interfere with

Drug	Modification / Moiety	Reference
Azidothymidine (AZT)	Adamantane	Tsuzuki et al., 1994
Azidothymidine (AZT)	Phosphatidylation	Hostetler et al., 1990
Leucine-enkephalin	Amantadine	Kitagawa et al., 1997
Leucine-enkephalin	Cholesterol ester	Bodor et al., 1992
Leucine-enkephalin	1,4-Dihydrotrigonellinate	Bodor et al., 1992
TRH	Lauric acid	Muranishi et al., 1991
TRH	N-acylation	Bundgaard and Moss, 1990
Estradiol	methyldihydropyridine	Brewster et al., 1988
GABA	Fatty acid or cholesterol ester	Shashoua et al., 1984
Codeine	O-methylation	Oldendorf et al., 1972
Heroin	O-acetylation	Oldendorf et al., 1972
Biphalin	Halogenation (Cl)	Abbruscato et al., 1996
Calcitonin	liposomes	Chen and Lee, 1993
3-hydroxypyridinone	Increase alkyl chain length	Dobbin et al., 1993
DPDPE	Amino acid addition (Phe)	Greene at al., 1996
DPDPE	Stereoselective positioning of lipophilic moiety	Witt et al., 2000

Table 1.3 Strategies to enhance lipid solubility. TRH: Thyrotropin-releasing hormone; GABA: γ-aminobutyric acid; Phe: phenylalanine

appropriate receptor binding region. This effect can be demonstrated by increasing the length of the aliphatic chain of n-alcohols from 1 (methanol) to 8 carbons (octanol), resulting in a four-fold increase in lipid solubility. This effect is more a result of increased molecular volume (i.e. increase in ratio of non-polar to polar constituents) rather than a reduction in hydrogen bonding effects (Hansch et al., 1987; Habgood et al., 2000). However, this strategy may result in a drug that is large, thereby excluding entry across the BBB, or potentially hindering receptor binding of the drug.

Hydrogen bonding effects may be reduced via a number of strategies. Polar functional groups of drug molecule form hydrogen bonds with water. Masking of these groups will result in a reduction of hydrogen bonds and an enhanced lipophilicity. Total number of hydrogen bonds (N) formed in a molecule has been established by the rules according to Stein (1967): 0 for ethers; ½ for esters; 1 for carbonyls, aldehydes, or ketones; 2 for amine, amide, and hydroxyl groups. Hydroxyl groups can be irreversibly blocked by methylation or reversibly blocked by esterification. Morphine, which shows very little BBB uptake (~ 0.02%), contains two hydroxyl groups and a high degree of water solubility. When one of the hydroxyl groups is methylated, resulting in codeine, membrane permeability is enhanced ~10-fold. When both hydroxyl groups are acetylated, resulting in heroin, membrane permeability is enhanced ~100-fold (Oldendorf et al., 1972). Furthermore, heroin has low receptor affinity and actually acts as a prodrug. When deacetylated within the brain it becomes morphine, which maintains high affinity for the μ-receptor. Placement of methyl groups on the phenylalanine of DPDPE, a δ-opioid selective met-enkephalin analogue peptide, induced changes in lipophilicity based

on diastereoismer conformation (Witt et al., 2000). Hydrogen-bonding potential should also be assessed along with the configuration of a peptide, as intramolecular H-bonds will be less able to act with surrounding polar solutes.

Halogenation is another chemical addition that enhances lipophilicity and has shown to enhance BBB permeability (Weber et al., 1991; Gentry et al., 1999). The choice of halogen (Cl, Br, F, or I), as well as placement on the peptide drug, was directly related to the degree of lipophilic enhancement. BBB permeability was related to lipophilicity, molecular weight of compound and halogen, conformation, and effect of the respective halogen on hydrogen bonding.

Amantadine (1-amino-adamantane) and adamantane derivatives are used as lipidization moieties to enhance lipid solubility of azidothymidine (AZT) (Tsuzuki et al., 1994) and leucine enkephalin (Tsuzuki et al., 1991). While leucine enkephalin showed enhanced pharmacological effect when attached to amantadine, AZT with adamantane resulted in no significant increase in brain concentrations. The slow hydrolysis of the AZT/adamantane moiety within the brain may have resulted in low brain concentration, as the moiety may efflux out of the brain with relative ease owing to the enhanced lipophilicity.

Prodrugs provide another strategy to increase brain uptake of peptide drugs. Prodrugs contain a pharmacologically active moiety that is either conjugated to a molecule with a known transporter or to a lipophilicity enhancer, which is cleaved at or near the site of action, allowing drug to induce its effect. Esters have shown particular promise in this arena, due to the abundance of endogenous esterases in the CNS that are

available for cleavage. Both aromatic benzoyl esters (Horn et al., 1979) and branched chain tertiary butyl esters (Greig et al., 1990) have shown to be sufficiently stable in plasma, while still adequately cleaved within the CNS. Another avenue is use of lipophilic amino acids, such as phenylalanine (Phe) as the cleavable unit. The addition of a Phe group to the opioid peptide DPDPE at the amino terminal resulted in enhanced permeability at the *in vitro* BBB (Greene et al., 1996). Furthermore, the high concentration of degradative endopeptidase EC3.4.24.15 in neurons and glial cells (Healy and Orlowski, 1992) could be used to target lipid-soluble enkephalin analogs to the CNS (Greene et al., 1996).

A further prodrug design focuses on the redox system (Simpkins et al., 1986), in which a lipophilic attachment (i.e. 1,4-dihydro) is converted, *in vivo*, to the hydrophilic quaternary form, effectively "locking" (Bodor and Buchwald, 1999) the drug in the tissue. When estradiol is conjugated to the methyldihydropyridine carrier and subsequently oxidized by NADH-linked dehydrogenases in the brain resulting in a quaternary ammonium salt, which will not cross back through the endothelium (Brewster et al., 1988). Enhanced delivery of ganciclovir and zidovudine to the brain was also demonstrated by a redox-based chemical delivery system (Brewster et al., 1994, 1997). The use of the 1,4-dihydrotrigonelline system, as well as similar designs, has been explored with a wide variety of drugs, such as steroids, antivirals, neurotransmitters, anticonvulants, and peptides (Lue-enkephalin analogue and Thyrotropin-releasing hormone analogue) (Bodor and Buchwald, 1999). The primary difficulty with this design

is the any tissue may take up the lipophilic moiety, as well as potential rapid elimination of the charged salt form.

Another strategy of drug design is to incorporate specific molecular characteristics that enable the drug to be transported by one or more of the inwardly directed nutrient carriers. These drugs must have a molecular structure mimicking the endogenous nutrient. The prototypical example is levodopa, a lipid-insoluble precursor of dopamine that has been used for the treatment of Parkinson's disease, because it contains the carboxyl and α-amino groups that allow it to compete for transport across the blood-brain barrier by the large neutral amino acid carrier (Wade and Katzman, 1975). The enzyme that converts levodopa to dopamine is in abundance in both the peripheral and central nervous systems. Therefore, levodapa is administered with an inhibitor of dopa-decarboxylase that does not enter the CNS, allowing greater uptake of non-degraded drug. Biphalin, an opioid peptide, is another example of a drug which uses the neutral amino acid carrier system (Abbruscato et al., 1997) to gain entry into the brain.

Gylcosylation has shown to be a potential modification of peptide drugs to enhance brain uptake (Fisher et al., 1991; Tomatis et al., 1997; Bilsky et al., 2000; Egleton et al., 2000). Originally theorized to have an increased uptake at the BBB via GLUT-1 transporter, it is now believed that this not the case. Glycosylation has shown to improve peptide bioavailability via increased metabolic stability (Powell et al., 1993), and attenuating *in vivo* clearance (Fisher et al., 1991). Lipophilicity and receptor binding affinity were generally observed to decline with glycosylation (Egleton et al., 2000).

Structural design to reduce enzymatic degradation is also method to enhance bioavailability to the brain. It is necessary to define the site of enzymatic cleavage as well as the enzyme. These strategies include modification of amino acid terminus, with N-acylation or use pyroglutamyl residues (Veber and Freidlinger, 1985) to reduce aminopeptidase M activity. However, opioid peptides require the amino terminus to be free for effective receptor binding (Bewley and Li, 1983). Alternative modification for opioids to reduce aminopeptidase activity is to substitute the Gly^2 residue with a $D\text{-}Ala^2$ residue. Other opioid enkephalin degrading enzymes are dipeptidyl aminopeptidase, which cleaves enkephalins at the Gly^2-Gly^3 bond, and enkephalinase and angiotensin converting enzyme (ACE), which cleave enkephalins at Gly^3-Phe^4. Modifications of amino acid or attachment of secondary structures in these regions may reduce degradation. Conformationally constrained analogues have been shown to have significantly reduced enzymatic degradation (Greene et al., 1996), with the additional advantage of enhanced specificity for receptor subtypes (Hruby and Mosberg, 1982).

Cationization of peptides or peptide vectors is a manner of increasing membrane entry via absorptive-mediated endocytosis (AME). Dynorphin-like analgesic peptide E-2078 (pI=10) is a polycationic peptide at physiologic pH shown to internalize into brain capillaries by AME (Terasaki et al., 1989; Yu et al., 1997). Cationized albumin, as a vector strategy, has been employed to enhance absorptive mediated endocytosis. Cationized albumin vector attachment to β-endorphin (Kumagai et al., 1987) showed significant increases in uptake in *in vitro* cultures. The degree of cationization is crucial to the pharmacokinetic profile, as heavy cationization has elevated first pass effects.

Cationized albumin displayed longer serum half-life and general selectivity to the brain (Bickel et al., 2001). Additionally, the cationized albumin has shown to be cleared to a considerable degree by the kidney and liver, posing a potential toxicological threat. Toxic effects of various cationized proteins include immune complex formation with membranous nephropathy (Alder et al., 1983; Huang et al., 1984) as well as increased cerebral and peripheral vascular permeability (Nagy et al., 1983; Vehaskari et al., 1984; Bickel et al., 2001).

Pathophysiology of the BBB

The development of new drugs and drug vectors must also contend with potential pathological conditions of the patient. Several disease states result in enhanced BBB permeability to fluid and / or solutes (Banks and Kastin, 1996), including hypertension, radioactive exposure, edema, inflammation, ischemia, and reperfusion (reoxygenation). The list of factors that may contribute to changes in drug bioavailability (changes in BBB, protein binding, receptor site, enzymes, etc.) during a pathologic state is extensive and must be taken into account for appropriate drug design. Specific changes at the BBB, such as opening of tight junctions, increased pinocytosis, decrease in membrane rigidity, changes in nutrient transport, and pore formation may enhance/reduce drug uptake. *Table 1.4* lists several potential conditions and factors shown to induce changes at the BBB.

Opening of Tight Junctions:	Hyperosmolarity; acidic pH; burn encephalopathy; autoimmune encephalitis; multiple sclerosis; inflammation (chemical mediators of inflammation: TNFα, IL-1β, histamine, serotonin, bradykinin, Thrombin, adenine nucleotides, arachidonic acid, and reactive oxygen species); ischemia; lead (increase protein kinase C with increase in intracellular Ca^{+2}); post-ischemia reperfusion
Increased Pinocytosis:	Acute hypertension; microwave irradiation; hepatic encephalopathy; ischemia; seizures; heat stroke; brain injury, regeneration; tumors; development; hypervolemia; immobilization stress; hypothermia (<16°C); post-radiation; hyperbaric conditions; lead encephalopathy; mercury; Angiotensin II; Tricyclic antidepressants; meningitis; multiple sclerosis; inflammation (mediators listed above); lymphostatic encephalopathy
Decreased membrane rigidity:	Sufactants and solvents (ethanol; propanol; butanol; DMSO)
Pore Formation:	Tricyclic antidepressants (chlorpromazine, nortriptyline)
Disease / toxicant induced nutrient transport changes:	Diabetes (GLUT-1); Alzheimer's disease (β-amyloid); Wernickes-Korsakoff syndrome (thiamine); familial mental retardation (glucose); Eating / weight disorders (insulin & leptin); Stroke (GLUT-1); multiple sclerosis (ICAM-1); aluminum (inhibits protein transporters with potential link to Alzheimer's disease and amyotrophic laterscleros is and increases permeability of lipophilic compounds; also CSF peptide efflux mechanism)

Table 1.4 Causes of blood-brain barrier alteration (adapted from Audus et al., 1992; Pardridge 1995; Banks and Kastin, 1996; Abbott, 2000). TNFα: tissue necrosis factor-α; IL-1β: interleukin-1β; DMSO: dimethylsulfoxide; GLUT-1: glucose transporter type-1; ICAM-1: intracellular adhesion molecule-1

Opioids and Pain

History of Opioids

Extracts from *Papaver somniferum* (opium poppy) have been used for thousands of years. Opium is the Greek word for "juice", which is obtained from the poppy, and first referenced by Theophrastus in the third century B.C. It was found that slicing the fruit of the unripened plant resulted in the secretion of a tar-like sap, which contains over twenty opiate alkaloids, including morphine and codeine. In 1806 the German chemist Friedrich Sertürner isolated pure opium, that he named *morphine*, after Morpheus the Greek god of dreams. Codeine was later isolated by Robiquet in 1832, and papaverine by Merck in 1848. Heroin was marketed as an analgesic in the late 1800s by the German company, Bayer, but was shown to posses even greater addiction liability than morphine. By the middle of the nineteenth century pure alkaloid extracts began to spread throughout the world. Presently, morphine, codeine, methadone, and meperidine are still used in the United States as analgesics, antitussives, and for the treatment of opiate withdrawn. In addition to the abuse liability, other side effects associated with currently used opioids include constipation, respiratory depression, and tolerance. Opioid peptide development centers on both appropriate induction of analgesia and mitigation of side effects.

Endogenous Opioid Peptides

Three distinct opioid families have been identified: the enkephalins ("in the head"), the endorphins (a contraction of "endogenous morphine-like"), and the dynorphins (from the Greek work dynos, meaning "powerful"), all of which fall into the

category of Endorphins. These families are derived from a particular precursor polypeptide and have characteristic anatomical distribution.

Enkephalins were the first class discovered (Hughes et al., 1975) and are derived from the precursor protein proenkephalin A. The principle enkephalins, methionine enkephalin and leucine enkephalin, which are found predominately in areas associated with pain pathways (laminae I and II of spinal cord, spinal trigeminal nucleus, and periaqueductal gray region), emotional behavior (limbic system), motor control (basal ganglion), and autonomic reflexes (nucleu tractus solitarious) (Holtzman and Sung, 1998).

The second class belongs to the proopiomelanocortin (POMC) family (Watson et al., 1977). β-Endorphin is found in high concentrations in the arcuate nucleus of the hypothalamus, and the anterior pituitary where it is co-released with adrenocorticotropin hormone (ACTH). POMC also gives rise to melanocyte-stimulating hormone and ACTH.

The third class belongs to the dynorphins family (Goldstein et al., 1979) and is processed from prodynophin. Prodynorphin gives rise to dynorphin A (1-17), which co-localizes with vasopressin in the magnocellular cells of the hypothalamus and posterior lobe of the pituitary gland. Dynorphin A (1-8) are distributed in a manner similar to the enkephalins, with prevalence in laminae I and II of the spinal cord (Holtzman and Sung, 1998).

Opioid Receptors

The complex interaction of morphine and drugs with mixed agonist / antagonist properties lead to the proposed existence of multiple types of opioid receptors (Martin and Sloan, 1977). Three major classes of opioid receptors have been identified, designated as mu (μ; after the prototype agonist morphine), delta (δ; discovered in mouse vas deferens), and kappa (κ; after the prototypical agonist ketocyclazocine). The homology between the three opioid receptor types is ~65% with little sequence similarity to other G protein-coupled receptors. The regions of highest similarity lie in the seven transmembrane-spanning regions and the intracellular loops. Indications of subtypes within each class have been identified on the basis of their specific drug selectivity. Most clinically used opioids to date have high μ-receptor affinity (morphine, fentanyl, methadone, meperidine, buprenorphine), however higher doses may induce other opioid receptor interaction. Using μ-antagonists investigators have established, in animal models, that morphine can elicit analgesia either spinally (μ_2) or supraspinally (μ_1), with predominate supraspinal analgesia when morphine is given systemically (Pasternak, 1993). Enkephalins and β-endorphin are endogenous ligands for both μ and δ-receptors, whereas dynorphins show the greatest selectivity for κ_1-receptors.

Opioid receptors are coupled negatively to adenylyl cyclase by G proteins (G_i). Activation of an opioid receptor by an agonist results in stimulation of GTPase activity (Koski and Klee, 1981), that is regulated by guanine nucleotide (Blume, 1978) and decreases activity of adenylyl cyclase, resulting in a decrease in production of cyclic adenosine monophosphate (cAMP). This leads to an increase in the efflux of K^+

(primarily with μ and δ-opioid receptors), cellular hyperpolarization, a decrease in Ca^{2+} influx (primarily with κ-opioid receptors), and a lower intracellular concentration of free calcium. This results in a net decrease in neurotransmitter release and decrease in pain pathway stimulation (*Figure 1.8*).

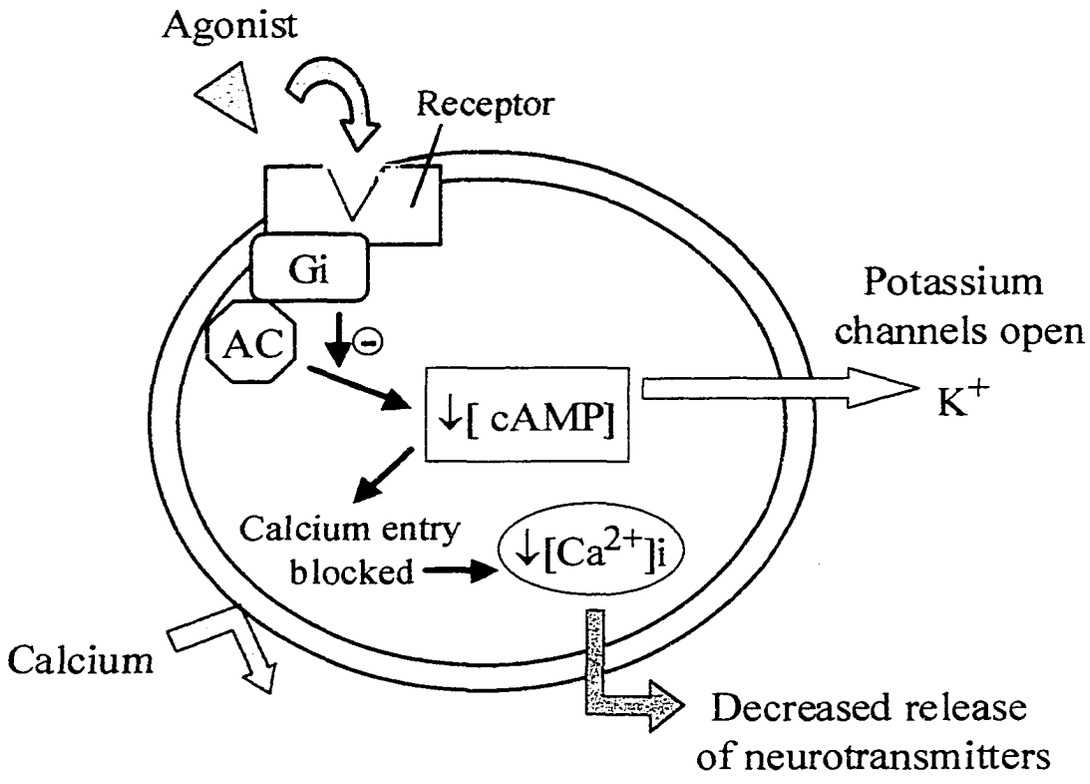

Figure 1.8 Mechanism of action of agonist at opioid receptor on cell. Agonist binds to G-protein, which reduces activity of adenylate cyclase, resulting in decreased production of cAMP, enhanced potassium efflux, and decrease Calcium entry.

Neurophysiology of Pain

The sensation of pain is modulated through both ascending and descending pathways in the CNS. Nociceptors (i.e. pain receptors) on primary afferent neurons, are stimulated by noxious stimuli. Transduction of these stimuli results in action potentials that are transmitted along the afferent neuron into the dorsal horn of the spinal cord. A-delta (Aδ) fibers are small, thinly myelinated, rapidly conducting afferent neurons, that terminate in lamina I of spinal chord. They are activated by mechanical and thermal stimuli, as well as mediate sharp and localized pain (Adriaensen et al., 1983). C fibers are large unmyelinated afferent neurons with slower conduction and are activated by mechanical, thermal, or chemical stimuli. The C fibers terminate in lamina II of the spinal chord and mediate dull, diffuse, or burning pain (i.e. visceral pain) (Bessou and Perl, 1969; Geogopoulous, 1974; Torebjork, 1974).

Descending pain-inhibitory pathway originates in the pariaqueductal gray region of the midbrain and from several nuclei of the rostroventral medulla oblongata, and project caudal to the dorsal horn. The descending pathway releases substances, such as norepinephrine and serotonin, which inhibit activity of ascending pain pathways, either through direct synaptic contacts or by indirect activation of inhibitory interneurons (Basbaum and Fields, 1979).

P-glycoprotein

Originally connected to resistance of tumor cells to chemotherapeutic agents, P-glycoprotein (P-gp; multidrug resistance transporter mdr1a) belongs to the ATP-binding

cassette family of proteins. P-gp, located on the apical surface of the BBB and the blood-cerebrospinal fluid barrier, pumps drugs out which are generally hydrophobic (Cordon-Cardo, et al., 1989). The P-gp transporter has been suggested to act as a "translocase" or "flipase", moving substrates from the inner leaflet to the outer leaflet of the membrane (Higgins and Gottesman, 1992). Linear and cyclic peptides have been indicated as substrates of P-gp (Sharom et al., 1998). Morphine and its glucuronide metabolites have shown to be substrates for P-gp (Drewe et al., 2000). Additionally, synthetic opioid peptides have also shown affinity for P-gp efflux (Chen and Pollack, 1997; King et al., 2001).

DPDPE

DPDPE (H-Try-D-Pen-Gly-Phe-D-Pen-OH) is a cyclic δ-opioid-selective enkephalin analogue (Vanderah *et al.*, 1994) of linear methionine enkephalin (H-Try-Gly-Gly-Phe-Met-OH). DPDPE (*Figure 1.9*) is conformationally constrained between the penicillamines, at position 2 and 5, via a disulfide bridge (Mosberg *et al.*, 1983). This cyclization has shown to provide a greatly enhanced enzymatic stability ($t_{1/2} > 500$ min) (Hambrook *et al.*, 1976; Weber *et al.*, 1991, 1992; Brownson *et al.*, 1994). DPDPE is present as a zwitterion (a dipolar ion that contains positive and negative charges of equal strength) at physiologic pH (pI~6.8) (Abbruscato, et al., 1997). DPDPE has shown increased bioavailability and BBB permeability in both *in vivo* (Williams et al., 1996) and *in vitro* (Weber et al., 1993) systems. It has also shown to be taken up into the brain via both saturable and diffusion processes (Thomas et al., 1997). Despite its metabolic

stability, extensive biliary excretion of DPDPE results in a rapid clearance (Weber *et al.*, 1992; Chen and Pollack, 1997). It also has shown limited uptake into the CNS (Williams et al., 1996), thus requiring high peripheral concentrations to achieve analgesic effect. Additionally, DPDPE has shown affinity for P-gp mediated efflux at the BBB (Chen and Pollack, 1998). Recent investigation has shown DPDPE to be a substrate for the organic anion transporting polypeptide system in rat (Oatp2) and in human (OatA) (Gao et al., 2000), which are expressed at the BBB and liver. It is currently theorized that the saturable uptake of DPDPE at the BBB exists via the organic anion transporter (Dagenais et al., 2001).

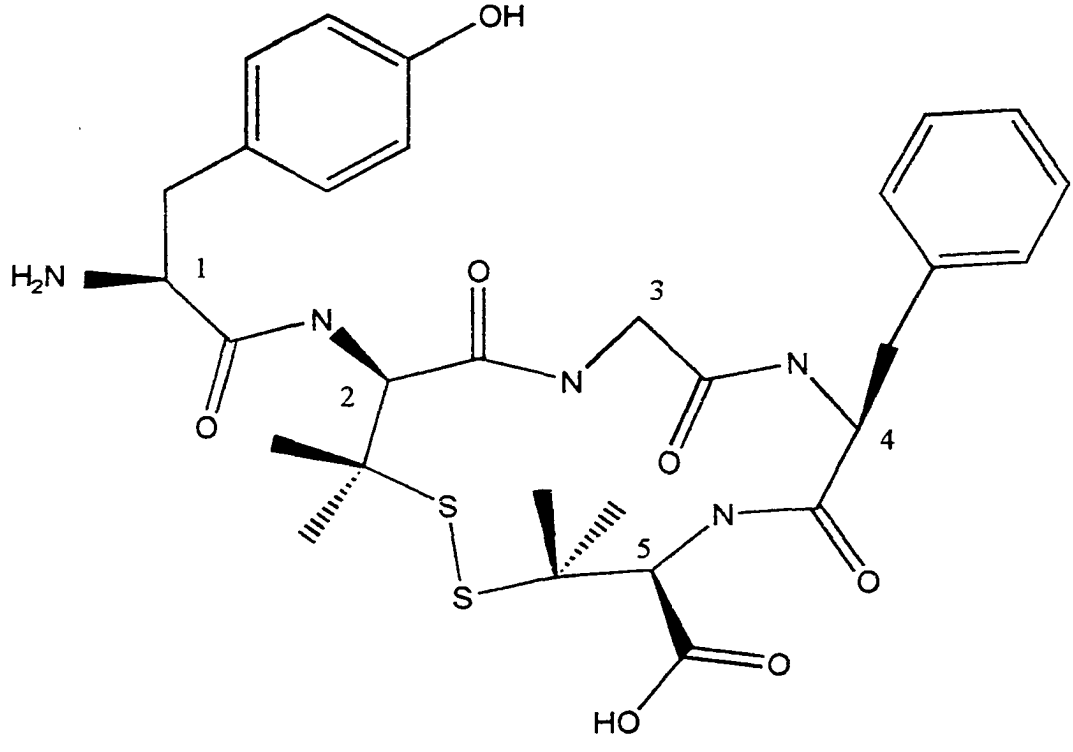

Figure-1.9 Structure of DPDPE; Tyrosine (1), Penacillamine (2), Glycine (3), Phenylalanine (4) and Penacillamine (5). Disulfide bond between the Penacillamines to enhance stability. Structure according to *Liao et al.* (1998).

PRESENT STUDY

Since the discovery of the enkephalins (Hughes, 1975) there have been numerous studies examining the various structural elements which determine protein binding capacity, enzymatic affinity, absorptive capacity, and receptor specificity and efficacy (reviews: Begley 1996; Davis *et al.*, 1995; Hruby 1995; Quock *et al.*, 1999). Although many of peptide analogues have been synthesized, few efficacious and receptor selective analogues are able to gain access to the CNS. Since its creation, DPDPE has become the prototypical δ-opioid receptor agonist and has served as a valuable tool for the characterization of the δ-opioid receptor (Hruby, 1988; Knapp *et al.*, 1989, 1991). Additionally, DPDPE shows promising therapeutic potential as an analgesic without the adverse side effects associated with morphine and other opioid drugs selective for the μ-opioid receptor (Heyman *et al.*, 1986). However, in spite of its attributes, DPDPE has shown limited uptake into the CNS (Williams *et al.*, 1996), thus requiring relatively high peripheral concentrations to achieve analgesic effect.

This dissertation focuses on opioid peptide transport into the brain. Using the δ-opioid peptide analogue of met-enkephalin, DPDPE, this examination will assess the different attributes of two methods by which bioavailability to the brain is enhanced. The two hypotheses are divided into separate chapters, with an introduction covering the current literature, methods, results, assessment of the respective specific aims, and a conclusion of research.

Overlying Hypothesis: **DPDPE delivery to the brain can be enhanced via chemical modification. Stereoselective positioning of methyl groups and conjugation of poly(ethylene glycol) are two such modifications.**

Hypothesis #1: (Chapter 2) Addition of methyl groups on the phenylalanine[4] of δ-receptor selective opioid, DPDPE, alters bioavailability, blood-CNS penetration, and analgesic effect in a stereoselective manner.

Specific Aims:

1. Characterize the receptor binding of diastereoisomer conformations of trimethylphenylalanine.
2. Examine effects of conformation on plasma protein binding, enzymatic breakdown, lipophilicity, and P-glycoprotein affinity.
3. Assess the effects of conformation on saturable and diffusional components of transport across the blood-brain barrier (BBB), with *in vitro* and *in situ* comparison.
4. Determine the effects of conformation on analgesia.
5. Explain the contributions of each component to final bioavailablity observed.

Hypothesis #2: (Chapter 3) Poly(ethylene glycol), or PEG, conjugation to opioid receptor analogue, DPDPE, alters bioavailability and analgesic effect, via enhanced pharmacokinetics in the systemic circulation.

Specific Aims:

1. Characterize the receptor binding changes involved with PEG-conjugation to DPDPE
2. Examine effects PEG-conjugation on plasma protein binding, enzymatic breakdown, lipophilicity, and P-glycoprotein affinity.
3. Assess the transport changes of PEG-conjugated DPDPE across the blood-brain barrier (BBB), with *in vitro* and *in situ* comparison.
4. Assess the distribution changes of PEG-conjugated DPDPE
5. Determine the effects on PEG-conjugation on analgesia.
6. Explain the contributions of each component assessed to end bioavailablity observed.

Chapter 2. Assessment of Stereoselectivity of Trimethylphenylalinine Analogues of Delta-Opioid DPDPE

Introduction

These studies focuses on the affects of trimethylation of Phe^4 of DPDPE (TMP-DPDPE), with regards to stereoselective characteristics. The primary emphasis of the analyses was placed upon the blood-brain barrier (BBB), as it remains the rate limiting step in the pharmacological treatment of many cerebral maladies due to its ability to prevent relevant drug concentrations from gaining access to the brain parenchyma (Egleton *et al.*, 1997).

Analgesia, via δ-opioid receptors, is understood to be a centrally mediated event. Therefore, only those δ-selective opioids that can cross the BBB intact will achieve biological effect (Frederickson *et al.*, 1981; Shook *et al.*, 1987). Transport of DPDPE into the CNS has been previously investigated by our laboratory using *in vitro*, *in situ*, and *in vivo* techniques. Initial experiments using a primary cell culture model of the BBB indicated that DPDPE could cross the BBB (Weber *et al.*, 1993). Distribution studies examining uptake after oral, subcutaneous, intravenous and intraperitoneal administration have shown that naloxone-displacable DPDPE could accumulate in the brain, indicating CNS uptake (Weber *et al.*, 1991, 1992). The entry of DPDPE has shown saturation and specificity (Thomas *et al.*, 1997), revealing a degree of non-diffusionary transport. Other peptides have shown stereoselective carrier-mediated transport across intestinal epithelial cells (Caco-2) (Ogihara, *et al.*, 1996) and β-endorphins have shown to exhibit

stereoselectivity in regards to analgesia (Tseng *et al.*, 1986). Studies measuring analgesia after intravenous, intracerebroventricular, and intrathecal administration of DPDPE, also indicate CNS mediated effects (Galligan *et al.*, 1984; Weber *et al.*, 1991).

Understanding the passage of opiates and their analogues across membrane systems (i.e. BBB), as well as multiple interactions with physiochemical properties of the body, is critical in drug development. The study of naturally occurring peptides (i.e. met-enkephalin) provides a rational and potentially powerful approach in the design of peptide therapeutics. In this study we use a common structural manipulation in drug development, the incorporation of a methyl group(s) next to a metabolically and/or dynamically important functional group. Methylation is seen to reduce the overall hydrogen bond potential of the peptide and increases permeability via enhanced lipophilicity. Earlier efforts, using NMR and molecular modeling, in the analysis of the four isomers of β-methylphenylalanine-DPDPE led to the conclusion that the gauche (-) conformation was required for interaction of the Phe^4 side chain with the δ-opioid receptor (Hruby *et al.*, 1991a). Here, through constrainment, the side-chain moiety of Phe^4 of DPDPE is biased to a particular side-chain conformation (i.e. guache (-)) while maintaining the intrinsic backbone conformation of the peptide. This modifies the topographical relationship of the side-chain groups, creating varied surface characteristics, which interact differently with alternate receptors for a peptide. Our research group has designed a DPDPE analogue with three methyl groups attached to the phenylalanine residue to yield four purified diastereoisomeric conformations (*Figure-2.1*). This manipulation is designed to enhance our knowledge of the effects of

topography, in an endeavor to direct future enkephalin analogue development and research.

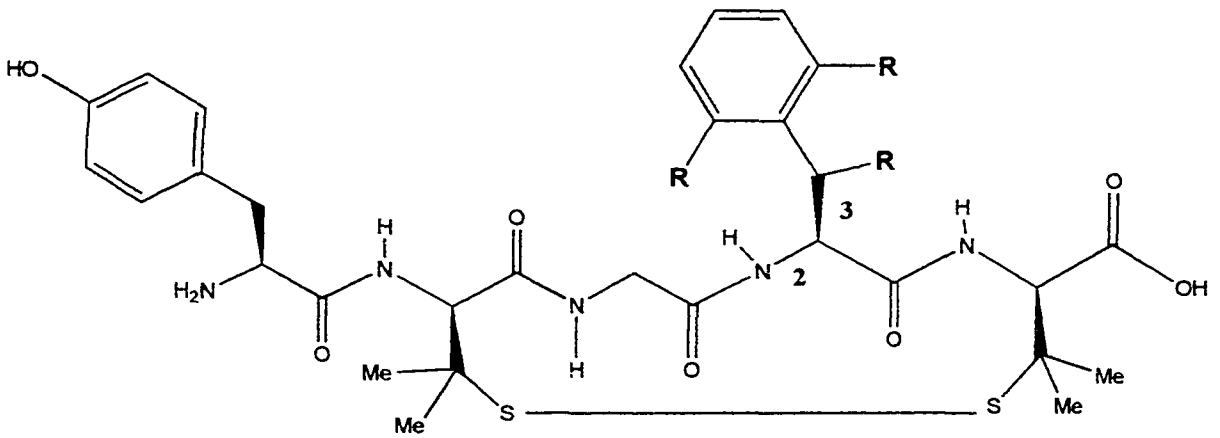

R = H (DPDPE)

R = CH_3 (TMP-DPDPE)

(2S,3S)-β-methyl-2'6'-dimethylphenylalanine^4-DPDPE; (2S,3S)-TMP

(2R,3R)-β-methyl-2'6'-dimethylphenylalanine^4-DPDPE; (2R,3R)-TMP

(2R,3S)-β-methyl-2'6'-dimethylphenylalanine^4-DPDPE; (2R,3S)-TMP

(2S,3R)-β-methyl-2'6'-dimethylphenylalanine^4-DPDPE; (2S,3R)-TMP

Figure 2.1 Structure of DPDPE with trimethylation of the phenylalanine^4 pharmacophore. The diastereoisomeric forms differ in regard to the 2 and 3 position of non-aromatic methyl group.

Methods

Materials

[^{3}H]pCl-Phe^4-DPDPE (47.0 Ci/mmol) and [^{3}H]DAMGO (54.0 Ci/mmol), as well as Na^{125}I were purchased from Dupont NEN Research Products (Boston, MA). All chemicals, unless otherwise stated, were purchased from Sigma (St. Louis, MO).

Animals

Female adult Sprague-Dawley rats (Vendor: Harlan Sprague-Dawley) weighing 250-300 g were used for all appropriate experiments, unless otherwise stated. Rats were housed under standard 12 hr light/12 hr dark conditions and received food *ad libitum*. Approval of protocols was through the Institutional Animal Care and Use Committee at the University of Arizona.

Competition Binding Affinity Studies in Rat Brain

Competition studies were performed according to previous studies (Bylund and Yamamura, 1990; Hruby *et al.*, 1997), using 1.0 nM [^{3}H]DAMGO to label the μ-opioid receptor and 0.75 nM [^{3}H]pCl-DPDPE to label the δ-opioid receptor. Analog concentrations with [^{3}H]DAMGO and [^{3}H]Deltorphin (nM) of: 10,000; 3,000; 1,000; 300; 100; 30; 10; 3; 1; 0.3. Specific binding displacement was defined using 10 μM naltrexone. Incubations took place in a final volume of 1 ml, in a solution consisting of 50 mM Tris/$MgCl_2$ (pH=7.4) with 1 mg·ml^{-1} bovine serum albumin (BSA), 50 μg·ml^{-1}

bacitracin, 30 μM bestatin, 10 μM captopril and 100 μM phenylmethylsulfonyl fluoride. Incubation conditions were 180 min. at 25°C. Final protein concentrations were determined by the Lowry method (Lowry *et al.*, 1951). IC_{50} values were determined using non-linear least-squares regression.

Octanol/Buffer Partition Coefficients

Partition coefficients for DPDPE and the four diastereoisomers of TMP-DPDPE were expressed as the ratio of compound found in the octanol phase to that found in the aqueous phase. Adapted from the method of Collins et al., 1988), equal volumes of octanol and a 0.05 M HEPES buffer in 0.1 M NaCl (pH=7.4) were mixed and allowed to equilibrate for 12 hrs. The layers were separated and stored at 4°C. 50 μg of peptide was added to 500 μl of the HEPES buffer, and mixed with 500 μl of octanol by vortexing (37°C). The sample was centrifuged in a Beckman microfuge for 1 min. at 4000 rpm., and layers separated. The octanol phase was lyophilized and resuspended in NaH_2PO_4 buffer and analyzed via RP-HPLC, (Perkin-Elmer 250 HPLC), as was the aqueous layer. The octanol/buffer distribution coefficient (D) was calculated as the ratio of octanol layer to the aqueous buffer layer. All octanol/buffer distribution studies were performed in triplicate.

Iodination of Compounds

DPDPE and its TMP analogues were monoiodinated on the tyrosine[1] residue using a standard chloramine-T procedure (Bolton, 1986) as adapted by Schetz *et al.*

(1995). Purification of the iodinated peptides was carried out using a reverse-phase Perkin-Elmer 250 HPLC gradient system and a Vydac column (880115-9 #74). The samples were eluted at 37°C using a curvilinear gradient of 0.1% TFA in acetonitrile (10-35%) versus 0.1% aqueous TFA over 20 minutes at a flow-rate of 1.5 ml · min^{-1}.

Protein Binding

The binding affinity of the iodinated peptides to bovine serum albumin in the mammalian-Ringer solution or rat serum was determined by ultrafiltration centrifugal dialysis (Paulus, 1969). Rat serum was obtained by harvesting blood from Sprague-Dawley rats and allowing the blood to clot for 30 min on ice and 30 min at room temperature. The whole blood was then centrifuged (Sorval RC2-B, DuPont Co., Wilmington, DE) at 20,000 x g for 20 min to produce a serum supernatant. Peptides were dissolved in 1 ml of Ringer's solution (see *in situ* methodology) or serum and warmed to 37°C, and then ultrafiltrated using a Centrifree™ micropartition device (Amicon, Beverly MA). Approximately 400 µl of ultrafiltrate was obtained when sample was centrifuged at 2000 x *g* for 10 min. (Sorval RC2-B, DuPont Co., Wilmington, DE). The total concentration (T) of [^{125}I] peptide introduced into the system and the amount found in the ultrafiltrate (F) was determined via counting on a Beckman 5500 gamma counter (Beckman Instruments, Fullerton, CA). The percentage of peptide bound to the serum albumin was calculated as:

$$\% \text{ Bound} = (T-F) / T \times 100$$

In Vitro Bovine Brain Microvascular Endothelial Cell (BBMEC) Uptake Analysis.

BBMECs were isolated from the gray matter of the cerebral cortex and characterized as described by Audus and Borchardt (1986, 1987). Fresh bovine brains (2-3) were obtained from University of Arizona Agricultural Farms. Brain microvessel endothelial cells were then isolated from the gray matter of the cerebral cortex and cryo-preserved. *Table 2.1* outline the isolation procedure.

BBMECs were grown to confluence on 24-well plates precoated with rat tail collagen and fibronectin. After confluence was confirmed microscopically, 10 to 12 days after seeding, growth media was removed and the cells were pre-incubated for 30 min. in assay buffer [122 mM NaCl; 3 mM KCl; 1.2 mM $MgSO_4$; 25 mM $NaHCO_3$; 0.4 mM K_2HPO_4; 1.4 mM $CaCl_2$; 10mM D-glucose; 10 mM HEPES]. The cells were then incubated for 20, 40 and 60 min. time points with each respective iodinated peptide, on a shaker table at 37°C. [^{14}C] sucrose was incubated under the same conditions and time points with the identical batch of confluent BBMECs to serve as control. After the appropriate time, the radioactive buffer was removed and the cells were washed three times with ice-cold assay buffer. Then, 1 ml of 1% Triton-X-100 was placed into each well and shaken for 30 min. A 200 µl portion of the Triton-X was prepared for radioactive counting. The other portion of the sample was assayed for protein concentration using a Pierce BCA-protein kit with analysis on a Beckman UV spectrometer (model 25).

Table 2.1
Protocol for Isolation of Bovine Brain Microvessel Endothelial Cells

1. Clean brains with phosphate buffered saline with 3 x antibiotics (3 mM NaH_2PO_4; 7 mM Na_2HPO_4; 145 mM NaCl; 300 $\mu g \cdot ml^{-1}$ Penicillin G; 300 $\mu g \cdot ml^{-1}$ Streptomycin).

2. Remove surface vessels and meninges from brains, with brain material bathed in a Minimum Essential Medium (MEM) solution.

3. Aspiration of cerebral gray matter from cerebral cortex using a vacuum.

4. Dilute gray matter to 50 g / 500 ml of MEM with dispase (0.5%) and incubate for 3 hrs at 37°C in a shaker water bath.

5. Centrifuge mix after 3 hrs at 1,000 x g for 10 min, discard supernatant, resuspend pellets in 13 % Dextran (MW 70,000).

6. Centrifuge mix at 3,800 rpm for 20 min, discard supernatant. Resuspend crude microvessel pellet in 20 ml of collagenase / dispase (1 $mg \cdot ml^{-1}$) and incubate for 3-4 hrs at 37°C in shaker water bath.

7. Centrifuge after incubation at 1000 x g for 10 min and discard supernatant. Resuspend microvessels in 8 ml of MEM. This suspension is then layered over a 50% Percoll gradient.

8. Centrifuge at 1000 x g over 20 min. Then remove band 2 (see *figure 2.2* below) from the gradient and wash with culture medium. Resuspend cell suspension in freezing medium with 20% equine serum and 10% dimethylsulfoxide. Aliquot for storage in liquid nitrogen.

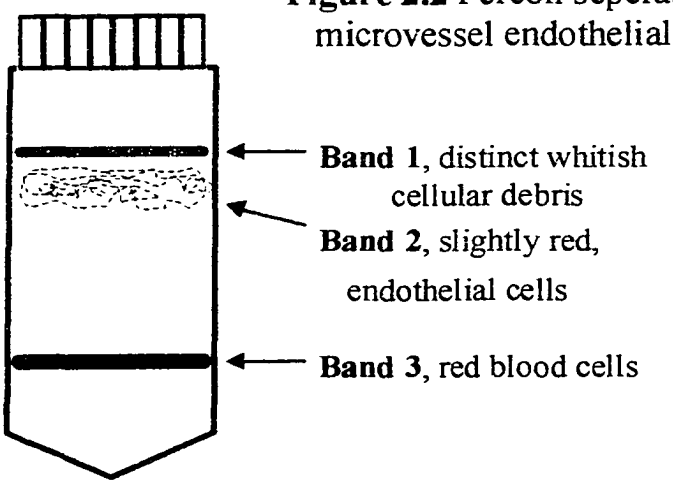

Figure 2.2 Percoll seperation of microvessel endothelial cells

Unidirectional rate constants were determined by multiple time-point analysis and normalized for protein content (Egleton *et al.*, 1998):

$$K_{cell} = \text{Uptake into cell (T)} / \text{Conc. in buffer} \times T$$

where uptake into cell is the dpm radioactivity per mg of protein at time (T), concentration in buffer is the dpm·ml^{-1} of buffer and T is 20 min.

In Situ Brain Perfusion Analysis.

Adult Sprague-Dawley rats (250-350 g) were anesthetized with a 1 ml·kg^{-1} i.m. injection of a cocktail comprised of ketamine (3.1 mg·ml^{-1}), xylazine (78.3 mg·ml^{-1}) and acepromazine (0.6 mg·ml^{-1}), and then heparinized (10,000 U·kg^{-1}). Both common carotids were exposed and cannulated with silicone tubing connected to a perfusion circuit. The perfusate consisted of a protein containing mammalian Ringer (Preston *et al.*, 1995), consisting of a modified Krebs-Henseleit-Ringer's solution [NaCl, 117 mM; KCl, 4.7 mM; $MgSO_4$, 0.8 mM; $NaHCO_3$, 24.8 mM; KH_2PO_4, 1.2 mM; $CaCl_2$, 2.5 mM; D-glucose, 10 mM; 3.9% dextran (MW 70,000); bovine serum albumin- type V, 10 g·L^{-1}]. The addition of Evans blue (0.055 g·L^{-1}) albumin to the Ringer provided a control for BBB integrity. The perfusate was aerated with 95% O_2 and 5% CO_2, and warmed to 37°C. The right jugular vein was sectioned upon the initiation of the perfusion to allow drainage of perfusate as previously described (Takasato et al., 1984). Once the desired perfusion pressure and flow-rate were achieved (85–95 mmHg; at 3.1 ml·min^{-1}), the

contralateral carotid artery was cannulated and perfused in the same manner as described above and the left jugular vein was then sectioned (*Figure 2.3*). Iodinated DPDPE or its iodinated TMP analogues were infused using a slow-drive syringe pump (model 22: Harvard Apparatus, South Natick, MA), into the inflow of the perfusate. After a set perfusion time of 20 min. a cisterna magna CSF sample (~50 μl) was taken with a glass cannula. The animal was decapitated and the brain removed. Choroid plexi were excised and the brain was sectioned and homogenized. The perfusate containing the radiolabeled compounds was collected from each respective carotid cannula at the termination of the perfusion to serve as a reference. The iodinated peptides were then counted on a Beckman 5500 gamma counter. Identical methodology was used in the analysis of P-gp affinity for iodinated DPDPE and (2S,3S)-TMP with 1.6 μM cyclosporin-A, a known P-gp inhibitor (Foxwell *et al.*, 1989; Fontaine *et al.*, 1996), added to the mammalian-Ringer to inhibit the P-gp efflux mechanism.

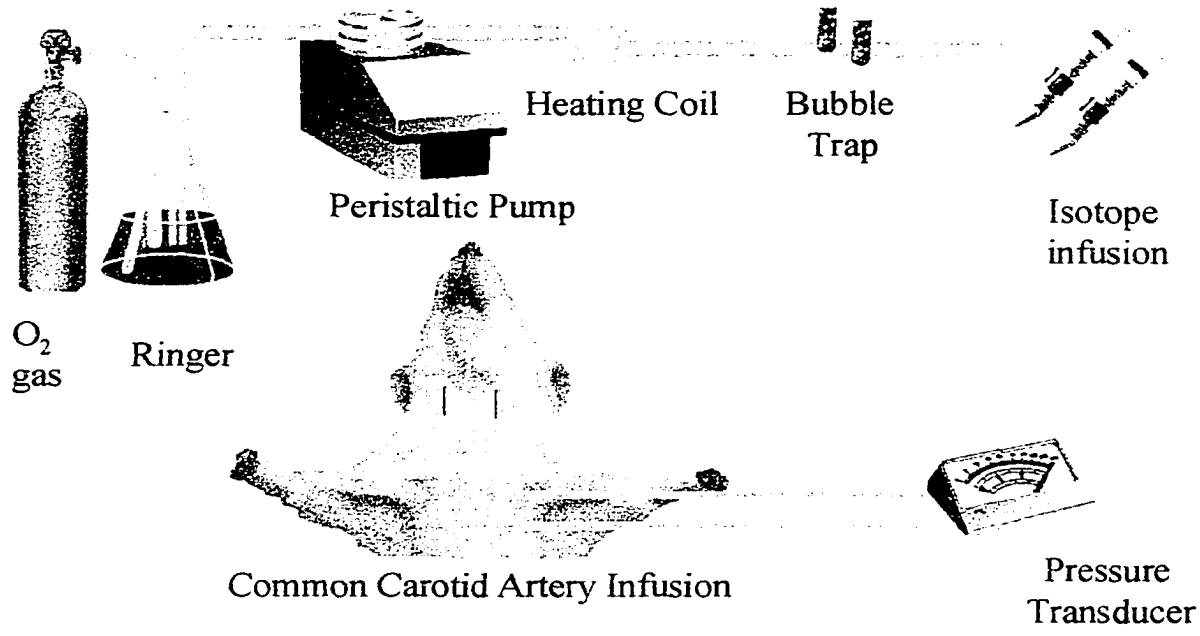

Figure 2.3 A schematic diagram of the in situ brain perfusion circuit. The brain is perfused via both common carotid arteries with oxygenated mammalian Ringer (Gas = 95% O2 and 5% CO2). Radiolabelled compounds can be introduced via a slow drive syringe. Both jugular veins are sectioned to allow outflow of perfusate

Capillary Depletion

Measurement of the vascular component to total brain uptake was performed using capillary depletion (Triguero *et al.*, 1990; Zlokovic *et al.*, 1992). After a 20 min. *in situ* perfusion, the brain was removed and the choroid plexi were excised. The brain tissue (500 mg) was homogenized (Polytron homogenizer, Brinkman Instruments, Westbury NY) in 1.5 ml of capillary depletion buffer [10 mM, 4-(2-hydroxyethyl)-piperaxineethanesulfonic acid; 141 mM, NaCl; 4 mM, KCl; 2.8 mM $CaCl_2$; 1 mM $MgSO_4$; 1 mM NaH_2PO_4; 10 mM, D-glucose; pH 7.4] kept on ice. Two milliliters of ice-cold 26% Dextran (MW 60,000) were then added and homogenization was repeated. Aliquots of homogenate were centrifuged at 5,400 x *g* for 15 min. in a microfuge (Beckman Instruments, Fullerton CA). The capillary-depleted supernatant was separated from the vascular pellet. All of the homogenization procedures were performed within two minutes of sacrificing the animal. The homogenate, supernatant, and pellet were taken for radioactive counting (Beckman 5500 gamma counter).

Expression of In Situ and Capillary Depletion Data

The amount of iodinated DPDPE and TMP analogues in the whole brain, CSF, homogenate, supernatant, and pellet was expressed as the percentage ratio of tissue (C_{Tissue} disintegrations per gram^{-1} of disintegrations per milliliter^{-1}) to plasma activities (C_{Plasma} disintegrations per milliliter^{-1}) and expressed as R_{Tissue} %.

$$R_{Tissue}\ \% = (C_{Tissue} / C_{Plasma}) \times 100$$

The percent inhibition of uptake by an inhibitor can be expressed by the following equation (Williams *et al.*, 1996):

$$\% \text{ Inhibition} = [(R_{Tissue} - R_{Inhibtion}) / R_{Tissue}] \times 100$$

where $R_{Inhibition}$ is the R_{Tissue} uptake in the presence of an inhibitor in the plasma perfusate.

The unidirectional transfer constant, K_{in} ($\mu l \cdot min^{-1} \cdot g^{-1}$), was determined by single time point calculation at 20 min. (Zlokovic et al., 1986).

$$K_{in} = [C_{Tissue} / C_{Plasma}] / \text{time (min)}$$

Integrity of Labeled Compounds

Venous outflow samples were collected from the jugular veins of *in situ* perfused rats. Aliquots of 200 µl were mixed with ice-cold 5% TFA and left on ice for 5 min., followed by a 5 min. centrifugation at 8,000 x *g*. The supernatant was extracted, lyophilized and resuspended in 5% acetonitrile in 0.1 mM acetic acid, prior to HPLC analysis. The analysis was carried out by RP- HPLC (Perkin-Elmer 250) with a Vydac column (940415-21-1 #66). The samples were eluted at 37°C using a curvilinear gradient of 0.1% TFA in acetonitrile (10-50%) versus 0.1% aqueous TFA over 30 min. at 1.5 $ml \cdot min^{-1}$. Data is represented as area under the HPLC peak.

Extraction of Radiolabeled Peptides

Brain extractions were performed using a modified method of Erchegyi *et al.* (1991). Briefly, rats were perfused via *in situ* perfusion for 20 minutes with radiolabeled peptide. At the end of the perfusion period, the animal was decapitated and the brain was removed and immediately placed in 7.5 ml of ice-cold 10% TFA. Each sample was homogenized (Polytron homogenizer) and centrifuged at 20,000 x *g* for 20 min. The supernatants were collected and an equal volume of ether was added. The ether phase was discarded and the samples were lyophilized to dryness. The samples were diluted to 500 µl with 10% acetonitrile in 0.1 M acetic acid and analyzed via HPLC (as above), with data represented as area under the HPLC peak.

Analgesia Analysis

A radiant-heat tail flick analgesia meter, model-33 (IITC Scientific Products, Woodland Hills, CA) was utilized to assess pain sensitivity following the administration of the test compounds. The analgesia meter was set to produce a baseline latency of 2-3 sec. with a cutoff time of 15 sec. Male ICR mice (20-25g) (Harlan Sprague-Dawley, Inc., Indianapolis, IN) were administered a single i.v. dose of the test compound (6.2 nM) dissolved in sterile saline and injected into the tail vein, with assessment at the 10, 30, 45, 60, and 120 min. time points. The mice (n=5) were placed into plastic restraint holders and their tails were properly placed under the radiant heat beam. The beam was turned on and then automatically shut off upon flicking of the tail. Analysis was stopped at any

given time point in which the maximal possible analgesic effect fell within 5% of the baseline. DPDPE was used to establish the proper dosage level and served as the control.

Nociceptive sensitivity was determined by converting the recorded analgesic tail-flick times to a percent maximal possible effect (% M.P.E.):

% M.P.E. = (recorded flick time – baseline) / (maximum time (15s) – baseline)

Data Analysis

For all experiments, the data are presented as mean ± S.E.M. values. The slopes (K_{cell}) of curves were determined by least squares linear regression analysis, with slopes compared by ANOVA. All other analyses used ANOVA comparison, followed by Newman-Keuls statistical analysis when applicable. Student's t-test was used for the comparison of two means. Analysis was performed using PCS® software (Tallarida & Murray, 1987).

Results

Competition/Binding AffinityAnalysis

DPDPE shows the highest selectivity for the δ-opioid receptor with a μ/δ ratio (IC_{50}) of 181.6. Addition of the methyl groups reduces δ-binding, with respective μ/δ ratios: (2S,3S)-TMP = 0.1; (2R,3R)-TMP = 9.5; (2R,3S)-TMP = 10.8; (2S,3R)-TMP = 2.2. (2S,3S)-TMP exhibits a 6-fold better binding at the μ-opioid receptor, than DPDPE. The other forms, (2R,3R)-TMP, (2R,3S)-TMP and (2S,3R)-TMP, exhibited significantly reduced selectivity for both the δ and μ receptors, respective to both DPDPE and (2S,3S)-TMP.

Octanol / Buffer Distribution

All TMP-DPDPE diastereoisomers partitioned into the octanol phase (i.e. hydrophobic) to a greater extent than the parent (*Figure-2.4*). The addition of the methyl groups onto the Phe^4 residue increased the percentage of (2S,3S)-TMP into the octanol phase approximately 8-fold ($p < 0.01$) over that of the parent DPDPE, and approximately 3-fold over the other conformations. The remaining three TMP forms, (2R,3R)-TMP, (2R,3S)-TMP and (2S,3R)-TMP, have an approximately 3-fold greater octanol association compared to the parent.

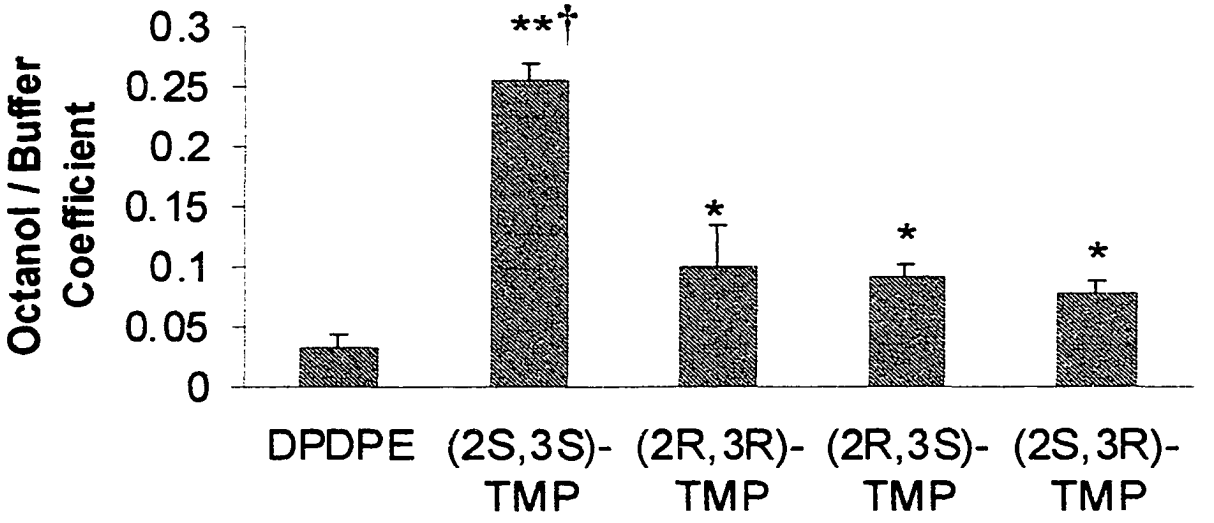

Figure 2.4 Octanol/Buffer distribution (D) expressed as a ratio of peptide in aqueous and organic phases, representing the lipophilicity of each peptide analogue. Each bar represents the mean ± S.E.M. (n=3). Statistical significance of D compared to the parent compound is denoted by $^{**}p < 0.01$; $^{*}p < 0.05$. $^{\dagger}p < 0.01$ signifies D as related to all other analogues in relation to one another, via ANOVA followed by Newman-Keuls post-hoc analysis.

Protein Binding

Iodinated DPDPE and the four iodinated TMP diastereoisomers were found to bind protein in rat serum to a greater degree than to the BSA in mammalian-Ringer perfusion medium, with an average of 45% increased binding for each respective compound in the serum (*Table-2.2*). Statistical significance ($p < 0.01$) was observed with reduced protein binding capacity of the (2R,3S)-TMP and (2S,3R)-TMP form in reference to the parent DPDPE and the other two diastereoisomers. Statistical significance ($p < 0.01$) was shown for (2R,3S)-TMP and (2S,3R)-TMP, as well as

(2R,3R)-TMP ($p < 0.05$) compared to DPDPE, in rat serum. No protein was found in the ultrafiltrate using the Lowry protein assay.

	Binding to BSA-Ringer	Binding to Plasma
DPDPE	46.7 ± 2.8	83.7 ± 4.0
(2S,3S)-TMP	44.2 ± 2.1	75.2 ± 3.4
(2R,3R)-TMP	50.0 ± 4.5	*75.4 ± 0.5
(2R,3S)-TMP	**33.3 ± 1.6	**74.3 ± 1.0
(2S,3R)-TMP	**35.8 ± 1.8	**71.0 ± 1.6

Table 2.2 Protein binding data presented as a percentage of binding to either rat plasma or mammalian BSA-Ringer. Data are mean ± S.E.M. **$p < 0.01$ and *$p < 0.05$ by ANOVA, as referenced to DPDPE; differences between respective compounds determined via Newman-Keuls post-hoc analysis.

BBMEC Uptake

The *in vitro* uptake analysis of iodinated DPDPE and the TMP diastereoisomers (*Table-2.3*) showed a 2-fold increase in the unidirectional rate constant, K_{cell} ($\mu l \cdot min^{-1} \cdot mg^{-1}$), for the (2S,3S)-TMP form over that of the parent. The other three TMP diastereoisomers exhibited a reduced K_{cell} compared to DPDPE.

	K_{cell} ($\mu l \cdot min^{-1} \cdot mg^{-1}$) (n=5)	K_{in} Brain ($\mu l \cdot min^{-1} \cdot g^{-1}$)	n	K_{in} CSF ($\mu l \cdot min^{-1} \cdot g^{-1}$)	n
DPDPE	0.18 ± 0.02	1.06 ± 0.05	10	1.97 ± 0.10	4
(2S,3S)-TMP	0.40 ± 0.10	1.72 ± 0.09	10	2.56 ± 0.13	4
(2R,3R)-TMP	0.004 ± 0.060	0.72 ± 0.04	5	2.19 ± 0.11	4
(2R,3S)-TMP	0.07 ± 0.02	1.11 ± 0.06	5	3.29 ± 0.16	4
(2S,3R)-TMP	0.16 ± 0.10	0.93 ± 0.05	5	3.46 ± 0.17	3

Table 2.3 Calculated unidirectional transfer constants (K) for DPDPE and TMP analogues, with single 20 minute time point analysis for the *in situ* (K_{in}) calculations and multiple time point analysis for *in vitro* (K_{cell}) calculations (determined as the slope of the computed regression line). Data are mean ± S.E.M.

In situ Brain Perfusion

The effects of trimethylating the phenylalanine group of DPDPE were assessed *in situ* (*Table-2.4*) to determine the basal permeability across an intact BBB of each respective compound as a percent ratio of brain uptake (R_{Br} %). The (2S,3S)-TMP configuration exhibited a significant increase in uptake, 1.6-fold ($p < 0.01$), as compared to the parent. Additionally, the (2R,3R)-TMP configuration exhibited a 1.5-fold reduction compared to the parent form ($p < 0.05$). In addition, the (2R,3S)-TMP and (2S,3R)-TMP showed a 3-fold increase in lipophilicity over the parent; however, no significant change was noted in the ratio of brain uptake when compared to DPDPE. The addition of 100 μM unlabeled DPDPE against the iodinated (2S,3S)-TMP revealed a saturable component, which is shared by the parent compound (Thomas *et al.*, 1997). *Figure 2.5* illustrates R_{Br} % of DPDPE, and (2S,3S)-TMP which exhibited the greatest degree of uptake among the trimethylated forms, in the absence and presence of cyclosporin-A. The addition of cyclosporin-A, which competes for the P-glycoprotein efflux mechanism, significantly ($p < 0.01$) increased the uptake of each TMP compound.

	% R_{BR}	n	% CSF	n
DPDPE	2.11 ± 0.08	10	3.94 ± 1.06	4
(2S,3S)-TMP	**3.44 ± 0.23	10	5.11 ± 1.83	4
(2R,3R)-TMP	*1.44 ± 0.11	5	4.39 ± 0.52	4
(2R,3S)-TMP	2.22 ± 0.17	5	6.58 ± 2.40	4
(2S,3R)-TMP	1.86 ± 0.18	5	6.92 ± 2.49	3
(2S,3S)-TMP with 100 μM *unlabeled* DPDPE	$^{\$}$1.93 ± 0.11	5	1.67 ± 0.21	3

Table-2.4 Brain and CSF entry of DPDPE and TMP analogues, post 20 minute *in situ* perfusion with BSA containing mammalian ringer, presented as of uptake a ratio. Data are mean ± S.E.M. *$p < 0.05$ and **$p < 0.01$ by ANOVA, as referenced to DPDPE; differences between respective compounds determined via Newman-Keuls post-hoc analysis. $^{\$}p < 0.01$ by Student's t-test, as referenced to (2S,3S) TMP.

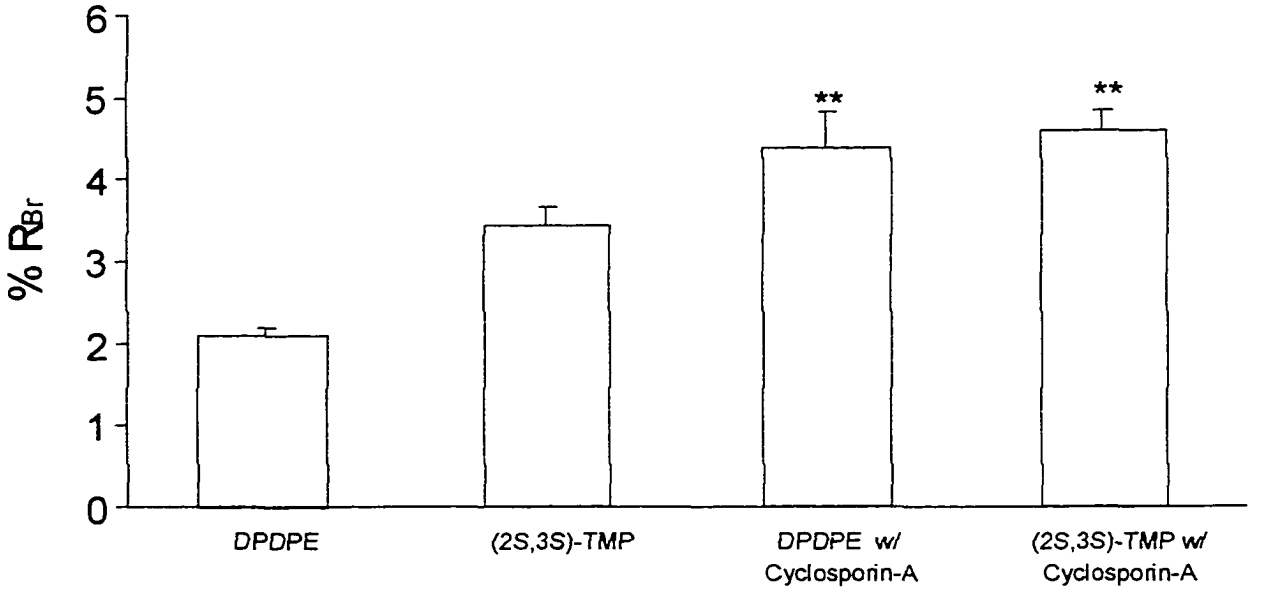

Figure 2.5 Uptake expressed as a percentage ratio of tissue to perfusate radioactivities (R_{tissue}, in milliliters per gram). Perfusion time was 20 minutes and values are the mean ± S.E.M. for ten animals for DPDPE and (2S,3S)-TMP and five animals with both compounds in the presence of 1.6 μM cyclosporin-A (P-gp substrate). **$p < 0.01$ by Student's t-test, as referenced to each respective compound, followed by Newman-Keuls post-hoc analysis.

Capillary Depletion

Capillary depletion analysis (*Table-2.5*) revealed that 39% of the iodinated DPDPE is associated with the vascular component (i.e. pellet) after a 20 min. *in situ* brain perfusion. (2S,3S)-TMP had a 16% association with the capillaries. Additionally, the portion associated with actual entry into the brain parenchyma (i.e. supernatant) was not statistically different from the homogenate. Analysis of the (2R,3R)-TMP configuration revealed an association with the brain vasculature, with no statistical difference shown between the pellet and the homogenate. The (2R,3S)-TMP and (2S,3R)-TMP conformations exhibited a 19% and 21%, respectively, association with the vasculature, with no significant difference between the pellet and homogenate. The addition of cyclosporin-A exhibited significance ($p < 0.01$), with a 15% association with the vasculature for DPDPE and 24% association with the vasculature for (2S,3S)-TMP. No statistical difference was observed between the supernatant and homogenate, for DPDPE and (2S,3S)-TMP, with the coadministration of cyclosporin-A.

Integrity of Labeled Compounds in Venous outflow and Brain Extraction

The percent degradation of each of the iodinated compounds in the brain perfusion procedure was calculated as % AUC from the HPLC analysis (*Table 2.6*), following a 20 min *in situ* brain perfusion. Appendix A shows HPLC figures (*figures 4.1A through 4.10A*) for each venous outflow and brain extraction. Blanks (saline) were run prior to each sample. Unlabeled compound (respective to each iodinated form) was run on UV spectra (214 nm) as additional control. The parent compound showed a 8%

degradation as related to the metabolism within the vascular network, with comparable degradation seen in (2S,3S)-TMP, (2R,3S)-TMP, and (2S,3R)-TMP. Whereas, the (2R,3R)-TMP configuration exhibited an approximate 3-fold greater degree of degradation in outflow metabolism. The brain extraction revealed that (2S,3S)-TMP

	% PELLET (Capillaries)	% SUPERNATANT (Brain Parenchyma)	% HOMOGENATE (Total Brain)
DPDPE	0.88 ± 0.16	1.94 ± 0.11	2.23 ± 0.06
(2S,3S)-TMP	0.43 ± 0.14	2.46 ± 0.99	2.65 ± 0.264
(2R,3R)-TMP	1.23 ± 0.22	*1.23 ± 0.23	*1.48 ± 0.31
(2R,3S)-TMP	0.37 ± 0.15	2.42 ± 0.66	1.99 ± 0.19
(2S,3R)-TMP	0.39 ± 0.16	1.64 ± 0.22	1.84 ± 0.25
DPDPE with 1.6 μM Cyclosporin-A	0.64 ± 0.13	**$4.17 ± 0.45	**$4.35 ± 0.36
(2S,3S)-TMP with 1.6 μM Cyclosporin-A	1.16 ± 0.27	**$3.66 ± 0.38	**$4.78 ± 0.25

Table 2.5 Capillary depletion analysis (N= 4-5) of DPDPE and TMP analogues, post 20 min *in situ* perfusion, presented as a percent ratio of uptake. Data are mean ± S.E.M. *$p < 0.05$ and **$p < 0.01$ by ANOVA and Newman-Keuls post-hoc analysis as referenced to DPDPE. $^{\$}p < 0.01$ by Student's t-test, as referenced to (2S,3S) TMP. DPDPE and (2S,3S)-TMP analyzed with respect to 1.6 μM cyclosporin-A in examination of P-glycoprotein affinity.

had the lowest degree of degradation, with similar results seen for (2S,3R)-TMP. The parent compound exhibited a 2-fold greater degree of degradation as compared to (2S,3S)-TMP, in regards to the brain extract. Only the parent and (2R,3S)-TMP compound differed to any considerable degree as to the degradation, in the venous or brain sampling.

	Venous outflow (% A.U.C.)	Brain Extraction (% A.U.C.)
DPDPE	92.1	78.9
(2S,3S)-TMP	86.5	89.5
(2R,3R)-TMP	69.0	71.8
(2R,3S)-TMP	88.5	78.8
(2S,3R)-TMP	92.0	86.8

Table 2.6 Percentage of Intact compound determined for DPDPE and TMP analogues as area under the HPLC curve (Appendix A). Venous outflow and brain extractions were collected from *in situ* perfused rats, at 20 min.

Analgesia

The i.v. administered doses of each compound showed a time (min) vs. response (% M.P.E.) relationship (*Figure 2.6.1*). The (2S,3S)-TMP conformation exhibited a mild increase in analgesic effect over the parent. The other conformations, (2R,3R)-TMP, (2R,3S)-TMP, and (2S,3R)-TMP, exhibited greatly reduced analgesic effects. The A.U.C. (*Figure 2.6.2*) revealed that the analgesic effect is significantly reduced for (2R,3R)-TMP, (2R,3S)-TMP, and (2S,3R)-TMP when compared to both DPDPE and (2S,3S)-TMP ($p < 0.01$).

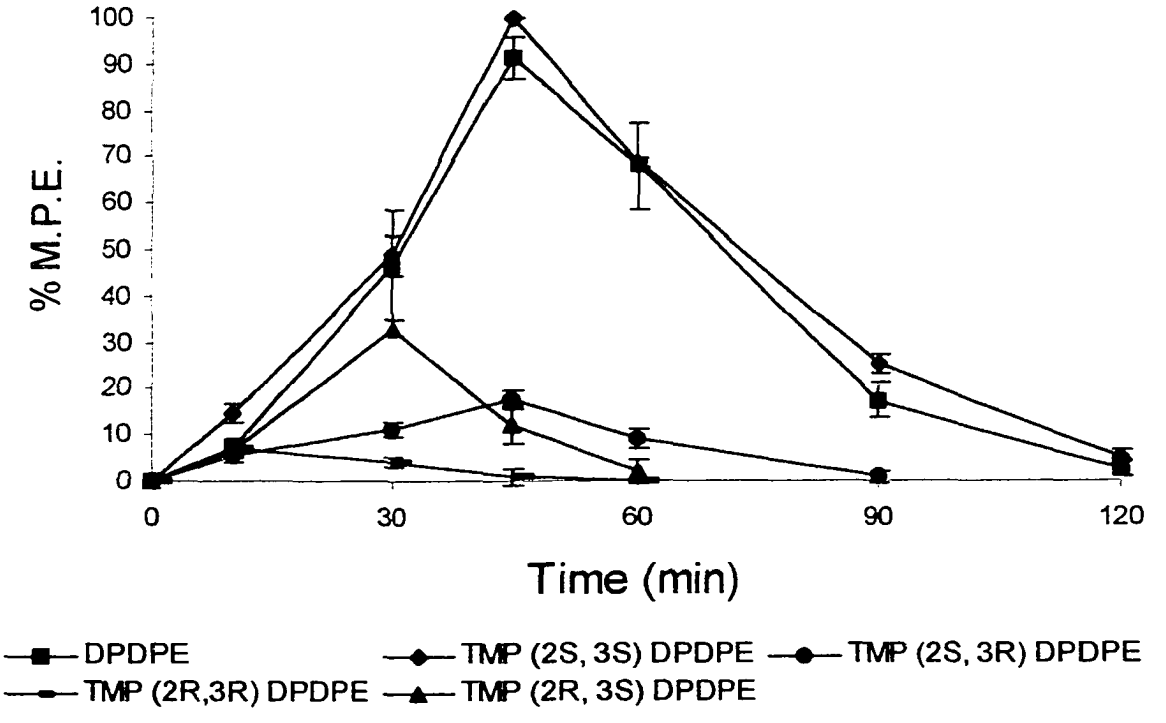

Figure 2.6.1 Data are presented as % maximal possible effect (% M.P.E.) ± S.E.M. at time points of: 30, 45, 60, 90, and 120 min, using a radiant-heat tail flick analgesia meter. ICR mice (20-25g) were administered an i.v. dose of 6.2 nM, 5 animals per time point.

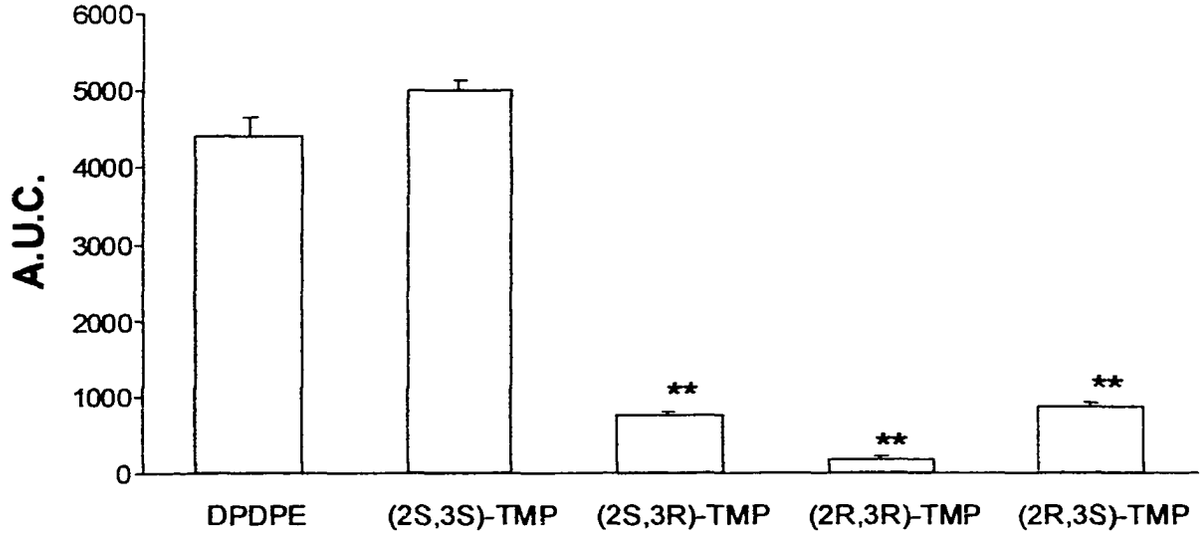

Figure 2.6.2 Analgesia data of DPDPE and TMP analogues represented as area under the curve (A.U.C.), in regard percent maximal possible effect (% M.P.E.) obtained over time course analysis. **p <0.01 by ANOVA, followed by Newman-Keuls post-hoc analysis.

Discussion

The study of conformational constraints in biologically active peptides has been proposed as a means to help design pharmacotherapeutics with specific surface characteristics. This approach has been used to increase selectivity and specificity towards receptors, enzymes and other biological systems where molecular recognition is important to the biological activity and response mechanisms (Hruby, 1982; Kazmierski *et al.*, 1988; Hruby *et al.*, 1991a).

The first paradigm examined in our study was the ligand binding affinities of the trimethylated diastereoisomers to the δ and μ opioid receptors. The trimethylation of the Phe^4 group on DPDPE has a notable effect on the binding affinities and selectivity as shown by competition analyses. While constraining the side-chain of Tyr^1 in DPDPE has been shown to elicit potent and selective δ-opioid receptor affinity (Qian *et al.*, 1996a; 1996b), the same can not be said for constrainment of the Phe^4 of DPDPE. Previous conformational and dynamic examination of DPDPE (Hruby *et al.*, 1988; Nikiforovich *et al.*, 1991) indicates that Tyr^1 and Phe^4 aromatic side chain groups lie in close proximity on the same structural surface, suggesting the topographical relationships between these two aromatic rings are important for receptor recognition and transduction. The introduction of a trimethylated tyrosine [(2S,3R)-β-methyl-2',6'-dimethyltyrosine^1; TMT] (Qian *et al.*, 1996a) and a dimethylated tyrosine [2,6-dimethyltyrosyl^1; DMT] (Hansen *et al.*, 1992) to the DPDPE structure has shown enhancement of ligand binding selectivity and increased potency. The [(2S,3S)-β-MePhe^4]-DPDPE form (mono-β-

methylated) (Hruby et al., 1991a) exhibited a 15-fold increase in selectivity (μ/δ) as compared to DPDPE, in sharp contrast to the trimethylated form. Therefore, the addition of the aromatic methyl groups onto the phenylalanine plays a significant role in reducing δ-receptor selectivity, whereas trimethylation of the tyrosine group of DPDPE enhances selectivity, implying that the phenylalanine is less malleable to manipulation compared to the tyrosine. The trimethylphenylalanine side-chain conformation may simply be excessively bulky (i.e. increased steric hinderance) thus reducing binding efficiency to the respective receptor "inter-lock" (Hruby et al., 1991b) conformation. This indicates that the Phe^4 of DPDPE plays a more significant role in the receptor-binding motif than Tyr^1.

An interesting aspect of the trimethylation of DPDPE is the relative differences in lipophilicity of the diastereoisomers in respect to the parent form, as well as to each other. For drugs, which lack specific transporters for uptake into a cell, transport is mediated by passive diffusion of the compound through apical membrane, cytoplasmic milieu, and across the basolateral membrane in an energy independent process, based in part on the lipophilicity of the compound. Attempts have been made to extend lipophilicity considerations to predicting the permeability of peptides across cellular membranes (Banks and Kastin, 1985; Gentry et al., 1999) with variable success. Methylation has been shown to increase permeability of peptides across endothelial cell monolayers, through the removal of a hydrogen bonding donor group from the peptide and effectively reducing the transfer energy from water into the cell membrane (Burton et al., 1996); however, methylation in and of itself has shown minimal effects on

lipophilicity (Conradi et al., 1992). Therefore, the variation in lipophilicity observed between the parent form and the TMP diastereoisomers was contrary to expectation. The reason for the variation in an already constrained peptide, specifically to that seen with the (2S,3S)-TMP conformation vs. the other forms is not clearly discernable, although it may be a consequence of alterations in how the phenol group of the Phe interacts with the peptide backbone.

Potential CNS targeted prodrugs are often designed with major consideration given to end ligand binding affinity. A complication with this focus is that therapeutic compounds can be degraded by blood, intercytoplasmic and tissue derived enzymes. This is often an important factor for peptides, when they can be proteolytically cleaved into non-functional fragments. The ideal CNS targeted prodrug should have a relatively long half-life in the plasma, tissue and cytoplasmic milieu. The metabolism of the peptides within the in situ venous outflow was ~10% for all the compounds, except for the (2R,3R)-TMP conformation, which had a 3-fold higher degradation. This may be due to the enzymes which are in greater concentration in the blood/vasculature (i.e. leucine aminopeptidase) (Patel et al., 1993). The brain extract, which contains various enzymes including high concentrations of aminopeptidase M (Hui et al., 1983), shows different results in regards to DPDPE as well as the (2R,3S)-TMP conformation. DPDPE and (2R,3S)-TMP both exhibited 2-fold increases in % degradation over that seen in their respective venous outflow data. In both the venous outflow and brain extraction data, the (2S,3S)-TMP configuration seems to provide a greater degree of protection against various enzymatic processes.

It is also important to assess protein binding of peptides, since it is known that protein binding can play a major role in determining CNS uptake (Banks et al., 1990). There was no significant difference between (2S,3S)-TMP and the parent, in terms of protein binding in ringer or plasma, while (2R,3R)-TMP showed a significant increase in plasma as compared to DPDPE. The (2R,3S)-TMP and (2S,3R)-TMP conformations exhibited significance in both Ringer and plasma, respective to DPDPE. Therefore, in the case of binding affinities, the (2R,3S)-TMP and (2S,3R)-TMP conformations should have the greatest likelihood of gaining access to the brain. However, the variations are only 5-10%, and may not be of any practical significance.

The in situ brain perfusion data of the TMP diastereoisomers revealed a significant difference between the uptake of DPDPE and (2S,3S)-TMP, and (2R,3R)-TMP. This increased uptake of (2S,3S)-TMP could be due to a number of factors, such as enhanced stability, lipophilicity and reduced P-gp efflux. Whereas, the (2R,3R)-TMP conformation, exhibiting a decrease in R_{Br} % compared to DPDPE, showed a decrease in stability (venous outflow & brain extraction data), as well as a lower degree of lipophilicity compared to (2S,3S)-TMP. The CSF sampling, although not statistically significant, followed a similar trend respective to DPDPE, (2S,3S)-TMP, and (2R,3R)-TMP. The next step was to determine if the addition of methyl groups would change the saturability characteristics of DPDPE. DPDPE has been shown to have both a diffusional and saturable component (Thomas et al., 1996). To determine whether or not any part of the brain or CSF uptake of (2S,3S)-TMP maintained the saturable component seen previously, the effect of excess unlabeled DPDPE was examined. Excess DPDPE did

induce the in situ uptake inhibition of (2S,3S)-TMP by 44%, revealing the saturable component was still intact. The Thomas et al. (1996) study revealed only a 26% inhibition of [^{3}H]DPDPE using the same concentration of unlabeled compound, revealing that the enhanced uptake of (2S,3S)-TMP is produced in part by the saturable component, rather than solely by the compound's enhanced lipophilicity. The CSF has been referred to as the sink to the brain (Davson et al., 1961), since the rate of bulk flow of the CSF out of the ventricles is considered faster than the diffusion kinetics from fluid to brain (Collins and Dedrick, 1983). CSF data reveals a similar trend to that seen with the R_{Br}%, suggesting that entry into the CSF may also be saturable.

Another factor of importance in relation to conformational adaptations and lipophilicity is the enhanced affinity for the active transport P-glycoprotein (P-gp) efflux system present throughout the capillary endothelium of the BBB (Lum et al., 1995). Although most studies of P-gp have focused on chemotherapeutic substrates, many studies have demonstrated that opioids such as morphine (Letrent et al., 1997) and loperamide (Schinkel et al., 1996) interact with P-gp. Recently Chen et al. (1998, 1999) demonstrated DPDPE as a substrate for P-gp. Here we examined DPDPE and (2S,3S)-TMP using in situ brain perfusion analysis, to examine the potential effect of stereospecific compounds on P-gp. Although the (2S,3S)-TMP conformation exhibited enhanced lipophilicity, its percent enhanced uptake is lower in the presence of Cyclosporin-A respective to the enhanced uptake of DPDPE in the presence of Cyclosporin-A, which is in opposition of what one might theoretically predict. It would appear that the (2S,3S)-TMP conformation has an intrinsic decreased affinity for P-gp, in

spite of its lipophilicity. Therefore, this type of conformational manipulation may have a highly beneficial effect for use with CNS-active chemotherapeutics known to be effluxed from the capillary endothelium by P-gp. Reports of P-gp in glial cells (Dietzmann et al., 1994) and astrocyte foot processes (Golden et al., 1999) may also be affected by such modifications.

The capillary depletion data revealed a ~2-fold lower association with the capillary component for (2S,3S)-TMP as compared to the parent compound. Therefore, the (2S,3S)-TMP conformation, although having a decreased affinity for P-gp over DPDPE, has a lower association with the capillary endothelium, implying that a greater percentage of the (2S,3S)-TMP in situ R_{Br} actually becomes accessible to the target receptors. Whereas the (2R,3R)-TMP form exhibits an almost complete association with the capillary component, vastly decreasing its ability to interact with the appropriate receptor.

The unidirectional transfer constants calculated from the *in situ* (K_{in}; $\mu l \cdot min^{-1} \cdot g^{-1}$) analysis of each TMP diastereoisomer shows an excellent correlate to that resulting from the *in vitro* (K_{cell}; $\mu l \cdot min^{-1} \cdot mg^{-1}$) BBMEC uptake analysis. The *in situ* K_{in} values exhibit smaller increases in permeability as compared to that of the K_{cell} values of the *in vitro* model. The rank order of permeability is preserved across both models, providing validation of the respective models. To understand the differences between the models one needs to realize that K_{cell} is solely representative of luminal membrane permeability, with a greater degree of error as to extracellular surface binding, by volume, as compared to *in situ*. The *in vitro* model provides a quick and relatively accurate examination of

peptide permeability at the cellular membrane without the physiological biodynamics obtainable by use of the *in situ* perfusion technique.

The (2S,3S)-TMP exhibited analgesia comparable to DPDPE, yet showed significantly enhanced lipophilicity, lower degree of degradation, equal protein binding affinity, increased endothelial (i.e. BBB) cell permeability, and a potentially decreased affinity for P-gp. Thus, (2S,3S)-TMP's low affinity for the receptor may be significant enough to impede enhancement of analgesia. Additionally, the analgesic effect observed by the TMP compounds is most likely μ-receptor derived, negating the reduction in μ-receptor derived side-effects.

In this study, we investigated the BBB permeability using iodinated peptides. The iodination of the tyrosine residue of each respective compound will have effects upon both permeability and lipophilicity. Only the analyses of *in vitro* permeability, *in situ* permeability, and protein binding used the iodinated peptide form. The iodination of Tyr^1 of opioid peptides has been shown to reduce the *in situ* K_{in} value, in spite of any enhancement of the distribution coefficient (i.e. lipophilicity). This effect may be due to the large van der Waals volume of iodine (Bondi, 1964) distorting the conformation of tyrosine's aromatic ring as well as the addition of a bulky radioactive group (Iodine M.W. = 125) onto a relatively small peptide (DPDPE M.W. = 646). Therefore the observed K_{in} and K_{cell} values may underestimate the actual uptake of the peptides.

Biological organisms have developed stereospecific receptors, protein-binding regions, and enzymes throughout their evolution to keep the biochemical milieu of the system tightly regulated. It is logical that all aspects of drug disposition (i.e. absorption,

distribution, metabolism, & excretion) are potentially stereospecific (Brocks & Fakhreddin, 1995). Biological activity of peptides is often dependent upon their "functional code" (Hruby *et al.*, 1991b) representative of a three-dimensional configuration. Due to the flexibility of endogenous peptide hormones, multiple conformational states can exist with potentially differing biological significance (i.e. stereoselectivity). The basis of how many pharmacologically active drugs function lie in their ability to interact with specific receptor molecules, which are chiral macromolecules. The resulting conclusion is that the optimum conformation of stereoselectively designed compounds will change in reference to the conformation, placement and amino acid onto which the manipulation is added. With this understanding, it is essential to explore the use of stereoselective manipulation to optimize drug efficacy. In this study, we have shown that alteration in one methyl group alignment can induce significant change in: enzymatic stability, receptor specificity, agonist/antagonist specificity, biological activity, and BBB permeability.

Chapter 3. Poly(ethylene glycol) Conjugation to Met-Enkephalin Analogue DPDPE alters bioavailability, pharmacodynamic and pharmacokinetic profile.

Introduction

Poly(ethylene glycol) (PEG), also known as poly(ethylene oxide) (PEO), is a nontoxic, nonimmunogenic, biocompatable and water-soluble polymer used in biotechnology, biomaterials, and pharmaceutics. PEGs consist of repeating ethoxy subunits with terminal hydroxyl groups that can be chemically activated, and may be attached to a compound at single or multiple sites. PEG derivatives, involveing covalently attached polyethylene glycol to proteins and peptides ("PEGylation"), have been used to enhance drug stability and circulation, while reducing immunogenicity, proteolysis, and clearance (Delgado *et al.*, 1992; Reddy, 2000). Low molecular weight (MW) drugs (< 20kDa) have been attached to PEG to enhance solubility, alter biodistribution, while reducing toxicity and plasma protein binding (Greenwald *et al.*, 2000). The enormous potential of PEGylated proteins as therapeutics was initially assessed in the 1970s, and has since evolved over the past two decades (Harris and Zalipsky, 1997).

Three PEGylated proteins, bovine adenosine deaminase (Adagen®) for the treatment of ADA deficiency, *E.coli* L-asparaginase (Oncaspar®) for the treatment of acute lymphoblastic leukemia, and interferon alpha (PEG-Intron®) for the treatment of hepatitis C have been approved by the FDA, with several other PEG-proteins in clinical

trials by a number of companies. However, no PEG conjugate to a low MW compound has yet been approved by the FDA for therapeutic use.

Peptides bound to PEG often serve as linkers to larger compounds, ideally allowing release of the compound to a target locations, based on pH or enzymatic breakdown of the peptide link. However, peptides serving as the biologically active agent, bound to PEG, have not been fully evaluated. Peptide based therapeutics suffer from a number of drawbacks, principally a lack of enzymatic stability and rapid elimination, both of which could benefit from PEG technology. The use of PEG modified opioid peptides has been shown to significantly enhance analgesia (i.c.v.), however results varied dependent upon the peptide to which the PEG moiety was attached (Maeda *et al.*, 1994). In this study our research group has assessed the pharmacokinetic and pharmacodynamic characteristics of the linear methoxy-PEG (2kDa) conjugate of met-enkephalin analogue DPDPE (*Figure 3.1*). The use of DPDPE provides a number of advantages for the examination of PEGylation. Transport of DPDPE into the CNS has been investigated previously by our laboratory using *in vitro*, *in situ*, and *in vivo* techniques. DPDPE is a low molecular weight peptide (646 Da), which is conformationally constrained via cyclic disulfide bonds providing enhanced stability ($t_{½}$ > 500 min in blood) (Weber *et al.*, 1991). This innate stability allows for a more accurate assessment of the PEG conjugation without added complication of peptide degradation. DPDPE does in effect eliminate one of the primary benefits of PEGylation (i.e. stability), however the degree of stability allows for more accurate quantification. Analgesia, via δ-opioid receptors, is understood to be a centrally-mediated event. Only

those δ-selective opioids that can cross the blood-brain barrier (BBB) intact will achieve biological effect (Frederickson *et al.*, 1981; Shook *et al.*, 1987). This characteristic provides the ability to assess how PEG modification affects BBB transport. DPDPE has also been shown to be a substrate for the P-glycoprotein (P-gp) efflux mechanism at the BBB (Chen and Pollack, 1999; Witt *et al.*, 2000), allowing an opportunity to assess PEG's effect on P-gp efflux. Lastly DPDPE, and other opioids, is known to be rapidly and extensively excreted via the hepto-biliary route of elimination (Weber *et al.*, 1992; Chen and Pollack, 1997). The rapid clearance of DPDPE greatly contributes to limited uptake into the CNS, thus requiring relatively large peripheral doses to achieve analgesic effect. Therefore, DPDPE allows for the evaluation of the PEG moiety when attached to a drug with virtually no renal clearance and its subsequent ability to reduce elimination and promote the necessary analgesic response.

Numerous alterations have been introduced into peptides, both to gain greater understanding of biological activity and to increase potency and bioavailability. Modification of drug molecules with PEG results in altered properties of the compound, such as steric interference, changed electrostatic binding properties, and conformational alterations (Reddy, 2000). Thus, not all PEGylated proteins are alike, and each requires optimization on an individual basis to derive the maximum clinical benefit. In this study we analyzed the contribution of PEGylating of DPDPE in a series of established techniques in an endeavor to develop strategies for future peptide drug development paradigms.

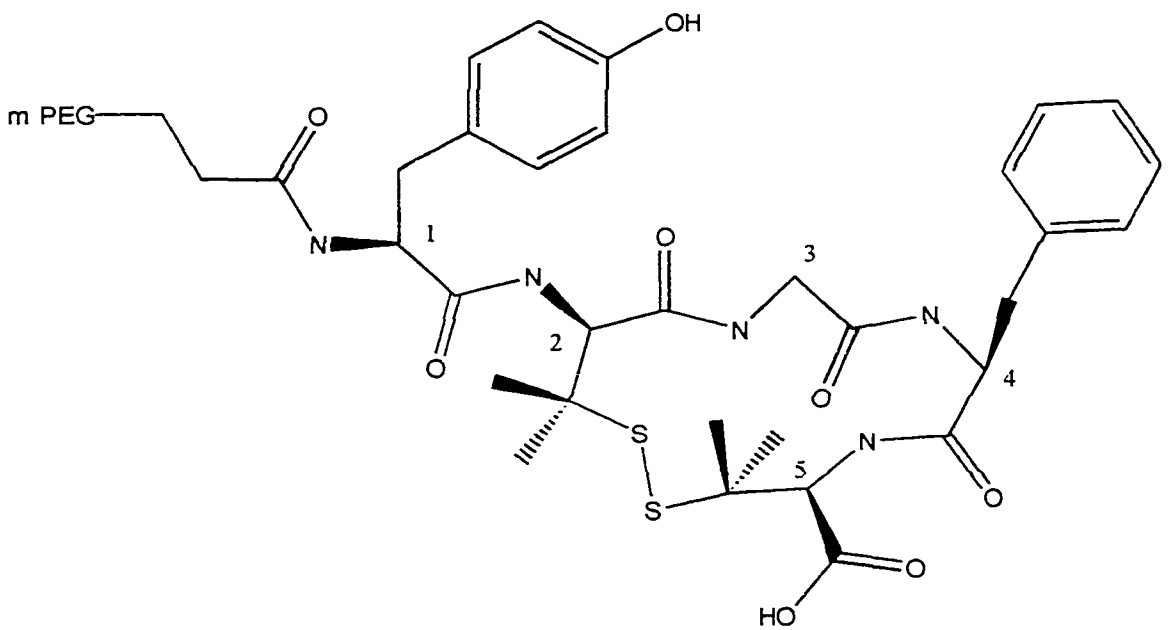

Figure 3.1 Structure of PEG conjugated DPDPE; Tyrosine (1), Penacillamine (2), Glycine (3), Phenylalanine (4) and Penacillamine (5). Disulfide bond between the Penacillamines to enhance stability. Poly(ethylene)-glycol (mPEG) attachment at the amino group of Tyrosine, CH_2-$(OCH_2CH_2)_n$- , (n = 45). Structure according to *Liao et al.* (1998).

Methods

Radioisotopes/Chemicals

[^{3}H]Deltorphin-II (41.0 Ci/mmol) and [^{3}H]DAMGO (50.0 Ci/mmol), and Na^{125}I (107 mCi/ml) were purchased from Dupont NEN Research Products (Boston, MA). DPDPE was obtained from Multiple Peptide Systems (San Diego, CA). mPEG-DPDPE was supplied by Shearwater Corp. (Huntsville, AL). All other chemicals, unless otherwise stated, were purchased from Sigma Corp. (St. Louis, MO.)

Iodination of Compounds

DPDPE and PEG-DPDPE were monoiodinated on the tyrosine[1] residue using a standard chloramine-T procedure (Bolton, 1986), as adapted in our laboratory by Schetz *et al.* (1995). Purification of iodinated peptides was carried out using a reverse-phase Perkin-Elmer 250 HPLC gradient system and a Vydac™ column (880115-9 #74). Samples were eluted at 37°C using a curvilinear gradient of 0.1% TFA in acetonitrile (10-35%) versus 0.1% aqueous TFA over 20 minutes at a flow-rate of 1.5 ml · min^{-1}.

Animals

Adult female Sprague-Dawley rats weighing 250-300 g were used for *in situ* brain perfusion analysis; male adult ICR mice weighing 25-30 g were used for all other analyses unless otherwise noted. Rats and mice were housed separately under standard 12 hr light/12 hr dark conditions and received food and water *ad libitum*, unless

otherwise noted. All protocols were approved through the Institutional Animal Care and Use Committee at the University of Arizona.

Intracerebroventricular Injections

Intracerebroventricular (i.c.v.) were performed in the manner described by Porreca et al. (1984). Mice were lightly anesthetized with ether. A longitudinal incision was then made in the scalp and the bregma suture identified. A 25-gauge needle, attached to a 25 µl syringe, was inserted 2 mm through the skull in a position 1 mm lateral to the midline and 2 mm caudal to bregma in order to reach the lateral ventricle. Injection depth was controlled by a plug on the needle. Drugs were injected in a volume of 5 µl.

Analgesia Analysis

Radiant-heat tail flick analgesia meter, model-33 (IITC Scientific Products, Woodland Hills, CA), was utilized to assess antinociceptive (i.e. analgesic) profile following administration of DPDPE or PEG-DPDPE. PEG was also assessed without conjugated peptide. The analgesia meter was set to produce a baseline latency of 2-3 sec with a cutoff time of 15 sec. Male ICR mice (~25g) (n = 5, per time point) were administered a single dose. Intravenous (i.v.) dose (25 µmole/kg), via tail vein, of each respective test compound dissolved in sterile saline and injected into the tail vein, with assessment at 15, 30, 45, 60, 90, 120, 150, 180, 210 and 240 min time points. I.c.v. dose (3.1 µmole/kg) of each respective compound was assessed at 15, 30, 45, 60, 90, 120, and

180 min. Analyses were stopped at any time point in which the maximal possible analgesic effect fell within 5% of the baseline.

Nociceptive sensitivity was determined by converting the recorded analgesic tail-flick times to a percent maximal possible effect (% M.P.E.):

% M.P.E. = [(recorded flick time – baseline) / (maximum time (15s) – baseline)] x 100

Competition Studies in Rat Brain

Competition studies were performed *ex situ* according to previous studies (Hruby *et al.*, 1997), using 1.0 nM [^{3}H]DAMGO to label the μ-opioid receptor and 0.75 nM [^{3}H]Deltorphin II to label the δ-opioid receptor. Rat brains are removed and immediately homongenized in 50 mM Tris buffer. Analog concentrations with [^{3}H]DAMGO and [^{3}H]Deltorphin (nM) of: 10,000; 3,000; 1,000; 300; 100; 30; 10; 3; 1; 0.3. Specific binding displacement was defined using 10 μM naltrexone. Incubations took place in a final volume of 1 ml, in a solution consisting of 50 mM Tris/$MgCl_2$ (pH=7.4) with 1 mg·ml^{-1} bovine serum albumin (BSA), 50 μg·ml^{-1} bacitracin, 30 μM bestatin, 10 μM captopril and 100 μM phenylmethylsulfonyl fluoride. Incubation conditions were 180 min at 25°C. Final protein concentrations were determined by Lowry method (Lowry *et al.*, 1951). IC_{50} values were determined using non-linear least-squares regression.

Octanol/Buffer Partition Coefficients

Partition coefficients for [^{125}I]DPDPE and [^{125}I]PEG-DPDPE were expressed as the ratio of compound found in the octanol phase to that found in the aqueous phase. Briefly, equal volumes of octanol and a 0.05 M HEPES buffer in 0.1 M NaCl (pH=7.4) were mixed and allowed to equilibrate for 12 hr. The layers were separated and stored at 4°C. At testing, 1 μCi of respective peptide was placed in 1 ml of buffer and added to 1ml of octanol (n = 4). The octanol/buffer solution was vigorously shaken (~2 min) and centrifuged at 1,000 rpm for 5 min (37 °C). The octanol and buffer phases were separated and analyzed via Beckman 5500 gamma counter. The octanol/buffer distribution coefficient was calculated as the ratio of octanol layer to aqueous buffer layer. All octanol/buffer distribution studies were performed in triplicate.

Protein Binding

The binding affinity of [^{125}I]DPDPE and [^{125}I]PEG-DPDPE to mouse plasma was determined by ultrafiltration, centrifugal dialysis (Abbruscato *et al.*, 1996). Peptides were dissolved in 1 ml of plasma (37°C), and ultrafiltrated using a Centrifree™ micropartition device (Amicon, Beverly MA) (n = 4). Respective compounds were also dissolved in saline (0.9%) in an identical manner for determination of non-specific binding. Ultrafiltrate was obtained after the sample was centrifuged at 2000 x *g* for 10 min (Sorval RC2-B, DuPont Co., Wilmington, DE). Total concentration (T) of iodinated peptide introduced into the system and the amount found in the ultrafiltrate (F) was

determined via counting on a Beckman 5500 gamma counter. The fraction of peptide unbound (f_u) in plasma was calculated as:

$$f_u = 1 - [(T-F) / T]$$

Non-specific binding was calculated in an identical manner as plasma binding and subsequently subtracted from total binding, resulting in a specific plasma protein bound concentration.

Time Course Distribution

Mice were deprived of food 12 hr before the start of distribution studies. Mice (n = 4-5 per time point) were anesthetized with sodium pentobarbital (80 mg/kg) and administered [^{125}I]DPDPE or [^{125}I]PEG-DPDPE via the tail vein (~1.5 μCi per animal). After 15, 30, 45, 60, 90, 120, 180, and 240 min, the chest cavity was opened and a blood sample (~500 μl) was taken from the left ventricle of the heart. Blood samples were divided and analyzed as whole blood and plasma, heparin was used as the anticoagulant. The animal was perfused with 0.9% saline via the left ventricle, with the right ventricle cut for outflow; blanching of brain and clearing of all blood from systemic circulation was accomplished in this manner.

Immediately following perfusion, the brain, gallbladder, liver, GI Tract, GI content (flushed with ~1 ml of saline), spleen, kidneys, urine, and tail (to determine the degree of compound remaining at point of injection) were removed and concentration of

iodinated compound in each was counted on a Beckman 5500 gamma counter (Beckman Instruments, Fullerton, CA). The entire procedure lasted 15 ± 3 min.

Plasma half-life (t½) in min^{-1}, determined via a plot of concentration (DPM % · ml^{-1}) vs time (min). The elimination rate constatn K (min^{-1}) is determined by the slope of the plasma concentration vs. time curve. The area under the curve (AUC) in DPM%·min·ml^{-1}, determined by the trapezoid rule, plotted on Excel™ and manually. The volume of distribution (Vd) in ml, is determined by the i.v. dose injected, divided by the AUC and slope. Clearance (CL) in ml·min^{-1}, determined by volume of distribution multiplied by 0.693 and divided by plasma half-life. Volume of distribution and clearance adjusted to weight (kg), based on average weights of mice used during procedure.

$$K\ (min^{-1}) = \frac{0.693}{t½}$$

$$Vd\ (ml) = \frac{i.v.\ dose\ (DPM\ \%)}{(AUC) \cdot (K)}$$

$$CL\ (ml \cdot min^{-1}) = \frac{0.693 \cdot Vd}{t½}$$

Extraction of Radiolabeled Peptides

Extractions of [^{125}I]DPDPE or [^{125}I]PEG-DPDPE from brain and plasma (at 30 min), and feces and urine (at 120 min) were performed to determine the % intact (i.e. stability) of the respective compound in each region specified. Briefly, four mice were injected i.v. via the tail vein with iodinated drug for each respective assessment. At the appropriate time point, each respective sampling had 1-3 ml of 50 mM phosphate buffer (3:1 Na_2HPO_4 to NaH_2PO_4) with 5% Acetonitrile solution (kept on ice) added. Brain and fecal content samples were homogenized (Polytron™ homogenizer). All samples were centrifuged at 20,000 x *g* for 20 min. Supernatant was decanted and the pellet resuspended in phosphate/acetonitrile solution. Samples were again centrifuged and the two supernatants combined and immediately analyzed by RP-HPLC. Controls for each compound included an aliquot of iodinated compound in phosphate/acetonitrile solution vigorously homogenized, centrifuged and run on RP-HPLC (Davis and Culling-Berglund, 1985) and detected as dpm. Analysis was carried out by RP-HPLC (Perkin-Elmer 250) with a Vydac™ analytical column (940415-21-1 #66). Samples were eluted at 37°C using a curvilinear gradient of 0.1% TFA in acetonitrile (10-60%) versus 0.1% aqueous TFA over 30 min at 1.5 $ml \cdot min^{-1}$. Data is represented as area under the RP-HPLC peak (Davis and Culling-Berglund, 1985).

In Situ Brain Perfusion Analysis

Adult Sprague-Dawley female rats (n = 5; 250-350 g) were anesthetized with a 1 $ml \cdot kg^{-1}$ i.m. injection of cocktail comprised of ketamine (3.1 $mg \cdot ml^{-1}$), xylazine (78.3

$mg \cdot ml^{-1}$), and acepromazine (0.6 $mg \cdot ml^{-1}$), and then heparinized (10,000 $U \cdot kg^{-1}$) via i.p. injection. Both common carotids were exposed and cannulated with silicone tubing connected to a perfusion circuit. The perfusate consisted of a protein containing mammalian Ringer's solution (Preston *et al.*, 1995) [117 mM NaCl; 4.7 mM KCl; 0.8 mM $MgSO_4$; 24.8 mM $NaHCO_3$; 1.2 mM KH_2PO_4; 2.5 mM $CaCl_2$; 10 mM D-glucose; 3.9% dextran (MW 70,000); bovine serum albumin- type V, 10 $g \cdot L^{-1}$]. The addition of Evans blue (0.055 $g \cdot L^{-1}$) albumin to Ringers solution provided a control for BBB integrity. Perfusate was aerated with 95% O_2 and 5% CO_2, and warmed to 37°C. The right jugular vein was sectioned upon initiation of perfusion to allow drainage of perfusate. Once the desired perfusion pressure and flow-rate were achieved (85–95 mmHg; at 3.1 $ml \cdot min^{-1}$), the contralateral carotid artery was cannulated and perfused in the same manner as described above and the left jugular vein was then sectioned. [^{125}I]DPDPE or [^{125}I]PEG-DPDPE was infused using a slow-drive syringe pump (Model 22: Harvard Apparatus, South Natick, MA), into the inflow of the perfusate. After a set perfusion time of 20 min, a cisterna magna CSF sample (~50 µl) was taken with a glass cannula (n = 3). The animal was decapitated and the brain removed. Choroid plexi were excised and brain sectioned and homogenized. Perfusate containing the radiolabeled compounds was collected from each respective carotid cannula at termination of the perfusion to serve as a reference. Iodinated peptides were counted on a Beckman 5500 gamma counter.

Capillary Depletion

Measurement of the vascular component to total brain uptake of [^{125}I]DPDPE or [^{125}I]PEG-DPDPE was performed using capillary depletion (n = 3) (Triguero *et al.*, 1990; Zlokovic *et al.*, 1992). After a 20 min *in situ* perfusion, the brain was removed and choroid plexi were excised. Brain tissue (500 mg) was homogenized (Polytron homogenizer, Brinkman Instruments, Westbury NY) in 1.5 ml of capillary depletion buffer [10 mM, 4-(2-hydroxyethyl)-piperaxineethanesulfonic acid; 141 mM, NaCl; 4 mM, KCl; 2.8 mM $CaCl_2$; 1 mM $MgSO_4$; 1 mM NaH_2PO_4; 10 mM, D-glucose; pH 7.4] kept on ice. Two milliliters of ice-cold 26% Dextran (MW 60,000) were added and homogenization repeated. Aliquots of homogenate were centrifuged at 5,400 x *g* for 15 min (Beckman Instruments, Fullerton CA). Capillary-depleted supernatant was separated from the vascular pellet. All of the homogenization procedures were performed within two min of sacrificing the animal. The homogenate, supernatant, and pellet were taken for radioactive counting (Beckman 5500 gamma counter).

Expression of In Situ and Capillary Depletion Data

The amount of [^{125}I]DPDPE or [^{125}I]PEG-DPDPE in whole brain, CSF, homogenate, supernatant, and pellet was expressed as the percentage ratio of tissue (C_{Tissue} disintegrations per minute per gram^{-1}) to Ringers activities ($C_{Perfusate}$ disintegrations per minute per milliliter^{-1}) and expressed as R_{Tissue} %.

$$R_{Tissue}\ \% = (C_{Tissue} / C_{Ringer}) \times 100$$

In Vitro Bovine Brain Microvascular Endothelial Cell (BBMEC) Uptake Analysis

BBMECs were isolated from gray matter of cerebral cortices as previously detailed and characterized (Audus and Borchardt, 1986, 1987). BBMECs were grown to confluence on 24-well plates precoated with rat-tail collagen and fibronectin. At confluence, confirmed microscopically 10 to 12 days after seeding, growth media was removed and the cells were pre-incubated for 30 min in assay buffer [122 mM NaCl; 3 mM KCl; 1.2 mM $MgSO_4$; 25 mM $NaHCO_3$; 0.4 mM K_2HPO_4; 1.4 mM $CaCl_2$; 10 mM D-glucose; 10 mM HEPES]. Cells were incubated for 20 min with [^{125}I]DPDPE or [^{125}I]PEG-DPDPE (n = 6), with and without cyclosporin A (1.6 μM), on a shaker table at 37°C. 1.6 μM cyclosporin A is a concentration which inhibits the P-gp efflux protein without affect upon other transporters at the membrane (Legrand et al., 1998). BBMECs were also incubated for 20 min with [^{125}I]DPDPE or [^{125}I]PEG-DPDPE (n = 6), with and without 100 μM DPDPE, to determine saturability. [^{14}C] Sucrose was incubated under the same conditions and time points to serve as control. This was performed to verify that cells were viable and not damaged through during analysis, as no increase in sucrose should be observed over the time course if cells maintain their integrity. After the appropriate times, the radioactive buffer was removed and the cells washed three times with ice-cold assay buffer. 1 ml of 1% Triton-X-100 was placed into each well and shaken for 30 min. A 200 μl portion of Triton-X was prepared for radioactive counting (Beckman 5500 gamma counter). The other portion of the sample was assayed for protein concentration using a Pierce BCA-protein kit with analysis on a Beckman UV

spectrometer (model 25). R_{cell} % is the percent ratio of labeled compound taken up by the cell, relative to concentration of the labeled compound in buffer.

Data Analysis

For all experiments, data were presented as mean ± S.E.M. Student's t-test was used for comparison of two means. Area under curve analysis was calculated via the Trapezoid Rule. Analysis of variance (ANOVA) comparison, followed by Newman-Keuls Post-hoc test was used when applicable. Analyses were performed using PCS software (Tallarida and Murray, 1987).

Results

Analgesia

I.v. administration of DPDPE and PEG-DPDPE via tail vein was evaluated (*Figure 3.2.1*). A significant increase in analgesic effect of PEG-DPDPE was shown, with a 3.3 fold increase in the area under the curve (*Figure 3.2.2*) ($p < 0.01$). A rightward shift (15 min) in analgesic effect, in the percent maximum possible effect (% M.P.E.) curve, was also observed with PEG-DPDPE compared to DPDPE. However, i.c.v administration showed no significant analgesic difference between the two compounds (*Figure 3.3*). No analgesia resulted from PEG administered alone (i.e. without peptide conjugate), either i.v. or i.c.v.

Competition/binding affinity

DPDPE was shown to be selective for the δ-opioid receptor, with a 172-fold greater affinity ($p < 0.01$) than PEG-DPDPE (*Table 3.1*). Neither compound was shown to be selective for the μ-opioid receptor.

Octanol/Buffer Partition Coefficient

The octanol/buffer distribution shows that [^{125}I]PEG-DPDPE has 36-fold lower affinity ($p < 0.01$) for the octanol (i.e. hydrophobic) phase than [^{125}I]DPDPE (*Table 3.2*).

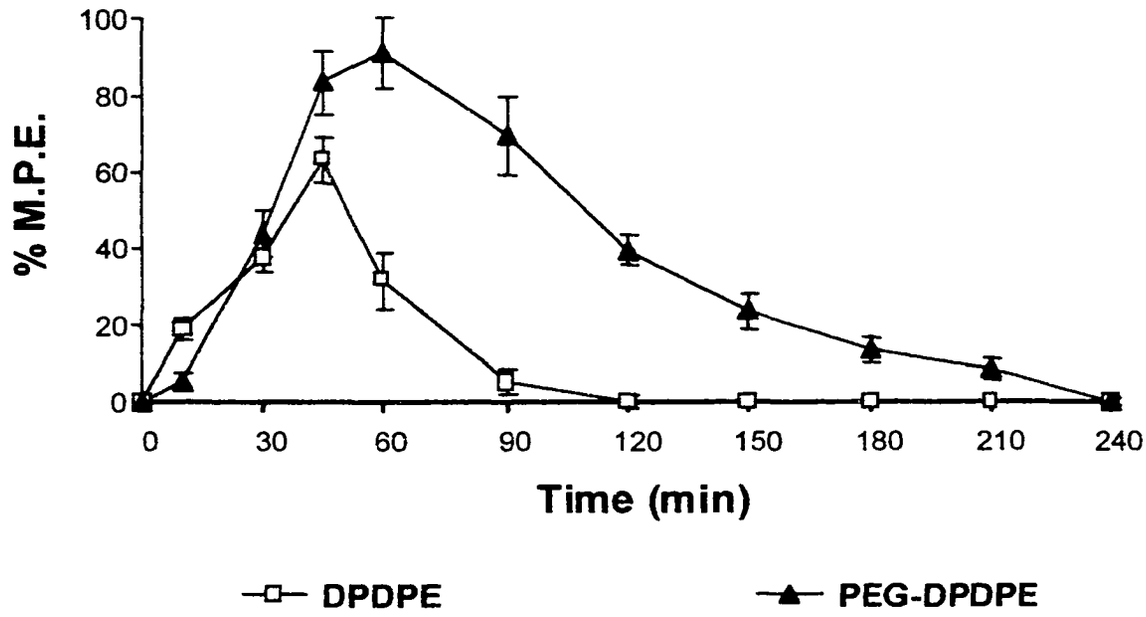

Figure 3.2.1 Data are presented as % maximal possible effect (% M.P.E.) ± S.E.M. at time points of: 15, 30, 45, 60, 90, 120, 150 and 180 min (time points for PEG-DPDPE also assessed at 210 and 240 min), ICR mice (~25g) were administered an i.v. dose of 25 μmole/kg, 5 animals per time point.

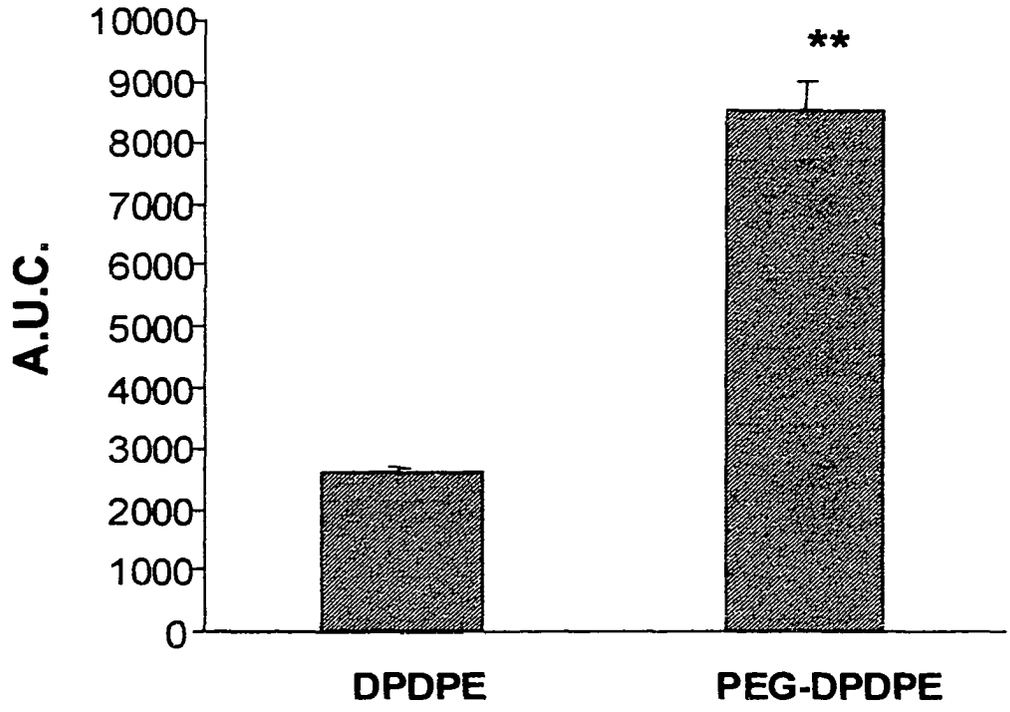

Figure 3.2.2 Analgesia data represented as area under the curve (A.U.C.), in regard percent maximal possible effect (% M.P.E.) obtained over time course analysis. **p <0.01 by Students' t test.

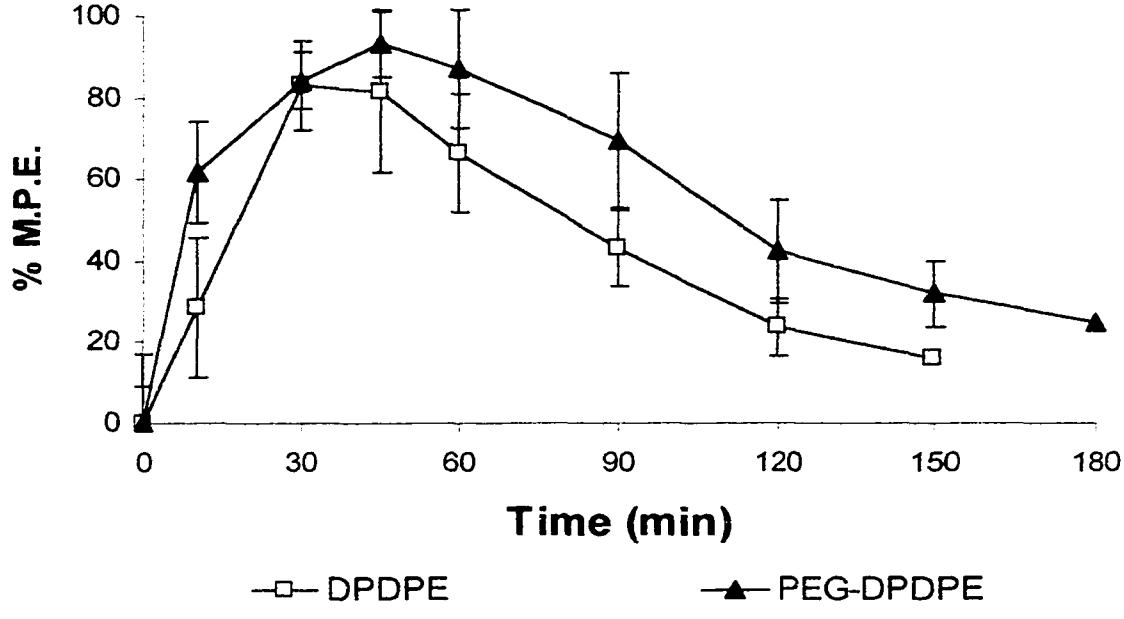

Figure-3.3 Data are presented as % maximal possible effect (% M.P.E.) ± S.E.M. at time points of: 15, 30, 45, 60, 90, 120, 150 and 180 min, ICR mice (~25g) were administered an i.c.v. dose of 3.1 μmole/kg, 5 animals per time point

	[^{3}H] Deltorphin II IC_{50}, nM	[^{3}H] DAMGO IC_{50}, nM
DPDPE	20.2 ± 5.35	>10000
PEG-DPDPE	3436.5 ± 211**	>10000

Table 3.1 DPDPE or PEG-DPDPE binding affinities and selectivity in competition with [^{3}H] Deltorphin II (δ-opioid specificity) or [^{3}H] DAMGO (μ-opioid specificity) in rat brain receptor binding assays. Data are mean ± S.E.M. **$p < 0.01$ by Student's t test.

Protein Binding

[^{125}I]PEG-DPDPE was found to have a 12% greater unbound fraction (f_u) than [^{125}I]DPDPE ($p < 0.01$), as seen in mouse plasma (*Table 3.2*). Similar results were found, under identical conditions, when BSA-containing mammalian Ringer (used for *in situ* brain perfusion analysis) was used (data not shown).

Time Course Distribution

Log plasma concentration vs. time data (*Figure 3.4*) show a significant difference in pharmacokinetics of [^{125}I]DPDPE and [^{125}I]PEG-DPDPE (*Table 3.2*). Elimination half-life ($t_{½}$) increased 2.5-fold ($p < 0.01$) for the [^{125}I]PEG-DPDPE over [^{125}I]DPDPE. Volume of distribution (V_d) for [^{125}I]PEG-DPDPE had a decrease of 2.7-fold ($p < 0.01$) compared to [^{125}I]DPDPE. Clearance rate (CL) of [^{125}I]PEG-DPDPE had a 7-fold decrease ($p < 0.01$) over [^{125}I]DPDPE.

Figure 3.5 shows distribution time course of [^{125}I]DPDPE (□) and [^{125}I]PEG-DPDPE (▲), following i.v. tail vein injection, in mice organs, urine, feces, whole blood and plasma. In plasma (*Figure 3.5.1*) and whole blood (*Figure 3.5.2*), levels of [^{125}I]PEG-DPDPE were higher ($p < 0.01$, A.U.C.) at all time points than [^{125}I]DPDPE. Equivalent plasma concentrations for the two peptides were reached at the 240 min time point.

[^{125}I]DPDPE was eliminated / excreted predominately via the hepato-biliary route, whereas [^{125}I]PEG-DPDPE exhibited significantly lower liver (*Figure 3.5.3*), gall-bladder

	$t_{½}$ (min)	V_d ($ml \cdot kg^{-1}$)	CL ($ml \cdot min^{-1} \cdot kg^{-1}$)	f_u	Octanol/ Buffer Coefficient
DPDPE	21 ± 2.9	1390 ± 130	46.2 ± 4.2	0.451 ± 0.022	0.328 ± 0.005
PEG-DPDPE	54 ± 4.4**	510 ± 46.6**	6.54 ± 0.59**	0.572 ± 0.054**	0.009 ± 0.001**

Table 3.2 Pharmacokinetic parameters of [^{125}I]DPDPE and [^{125}I]PEG-DPDPE in mice Data are mean ± S.E.M (n = 4-5 mice per time point). Elimination half-life ($t_{½}$), volume of distribution (V_d), and clearance (CL) calculated from linear portion of log plasma concentration curve. Unbound fraction (f_u) in plasma and Octanol/Buffer coefficient of respective compounds also shown. **$p < 0.01$ by Student's t test.

(*Figure 3.5.4*), GI tract (*Figure 3.5.5*), and GI content (*Figure 3.5.6*) concentration ($p < 0.01$, A.U.C.) via this route.

Kidney concentration was significantly greater ($p < 0.01$, A.U.C.) for [^{125}I]PEG-DPDPE than for [^{125}I]DPDPE (*Figure 3.5.7*). [^{125}I]PEG-DPDPE showed consistent accumulation in the urine over the time course (*Figure 3.5.8*), with significantly greater ($p < 0.01$, A.U.C.) concentrations than [^{125}I]DPDPE. [^{125}I]PEG-DPDPE concentration in the urine plateau at ~ 67% of the initial dose administered.

Spleen concentrations of [^{125}I]DPDPE and [^{125}I]PEG-DPDPE (*Figure 3.5.9*) were significantly different ($p < 0.01$, A.U.C.) over the time course. [^{125}I]PEG-DPDPE concentration in the spleen decline past min 120, whereas [^{125}I]DPDPE concentrations were seen to decline gradually from initial time point.

Brain concentrations of [^{125}I]DPDPE and [^{125}I]PEG-DPDPE (*Figure 3.5.10*) were significantly different ($p < 0.05$, A.U.C.) over the time course. [^{125}I]PEG-DPDPE showed increasing concentration in the brain up to 45 min and then declined. [^{125}I]DPDPE showed increasing concentration in the brain up to 30 min and then declined.

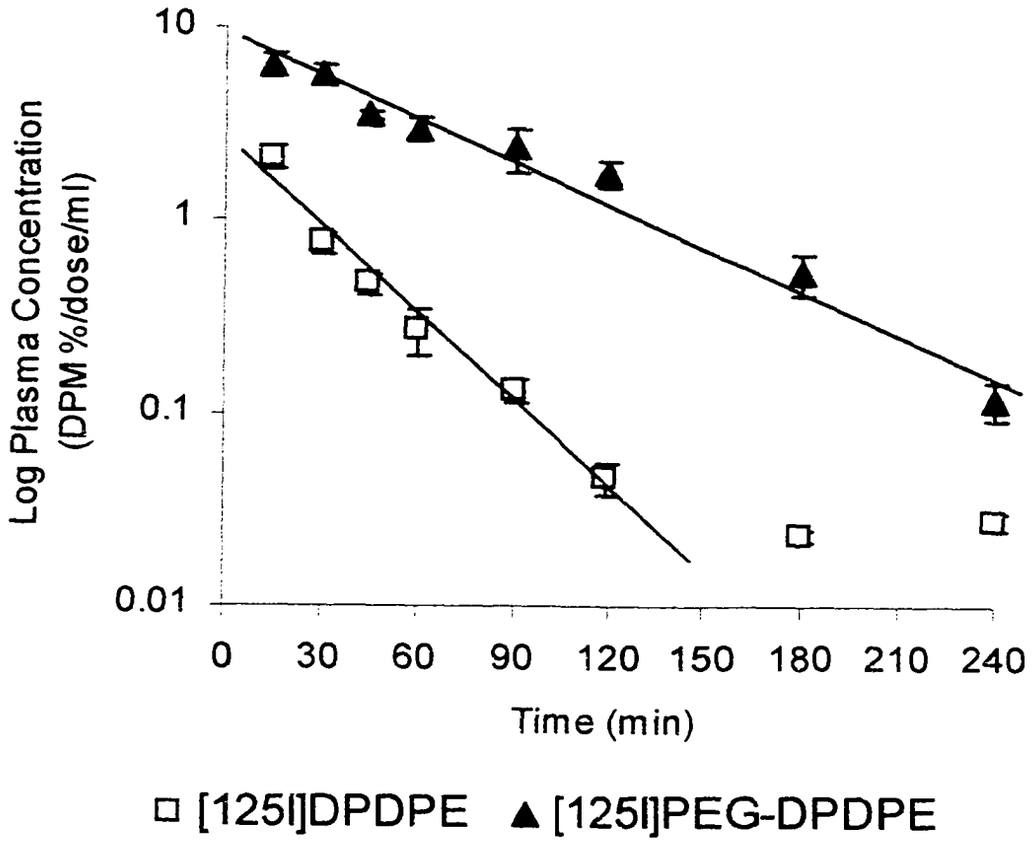

Figure 3.4 Logarithmic plasma concentrations of [^{125}I]DPDPE and [^{125}I]PEG-DPDPE, at each time point with trend line. DPDPE time points 180 and 240 fall outside of log plasma linearity (assay limitation at low concentration)

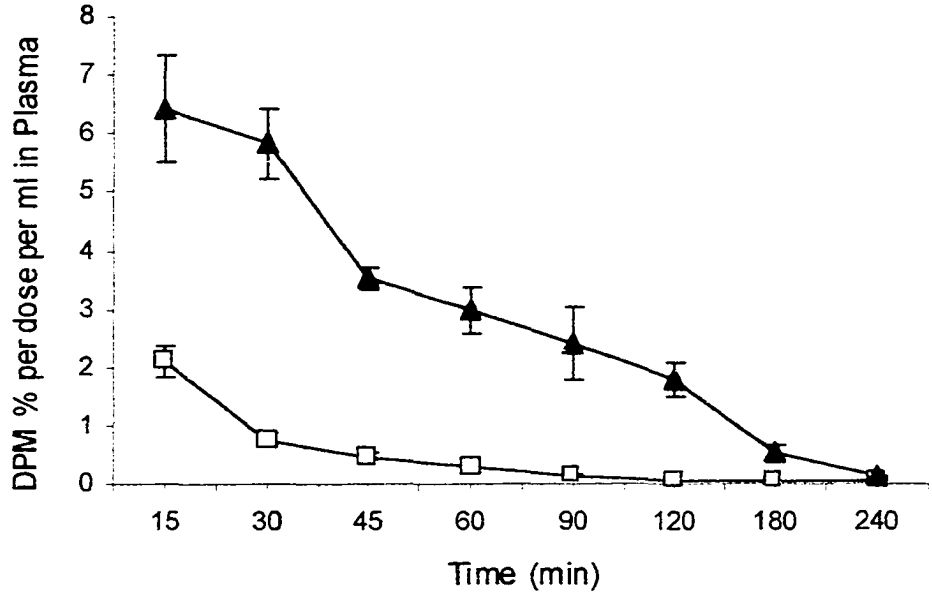

Figure 3.5.1 Tissue distribution, after i.v. tail vein injection, of [^{125}I]DPDPE (□) and [^{125}I]PEG-DPDPE (▲) at 15, 30, 45, 60, 90, 120, 180 and 240 min time points in Plasma.

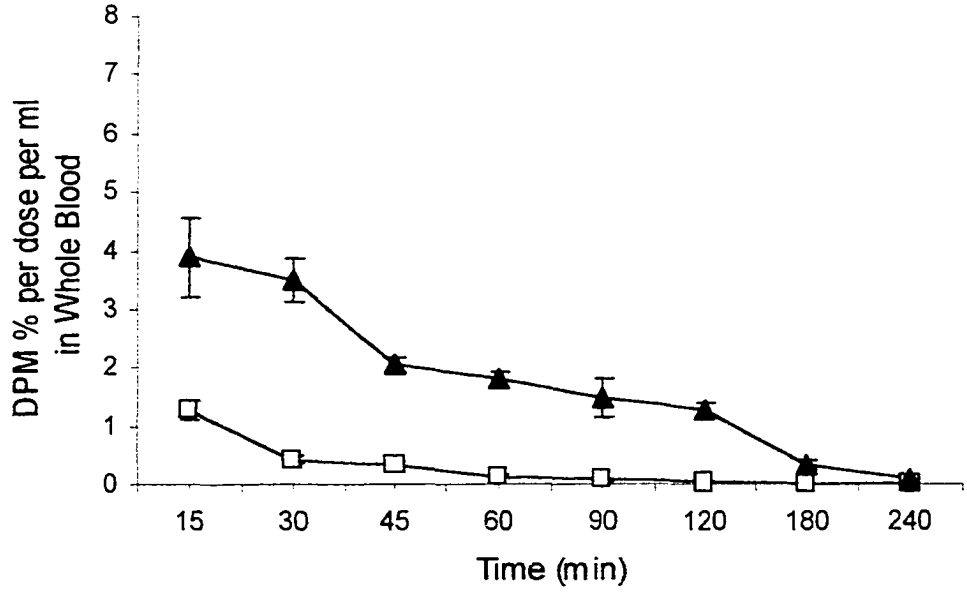

Figure 3.5.2 Tissue distribution, after i.v. tail vein injection, of [^{125}I]DPDPE (□) and [^{125}I]PEG-DPDPE (▲) at 15, 30, 45, 60, 90, 120, 180 and 240 min time points in whole blood.

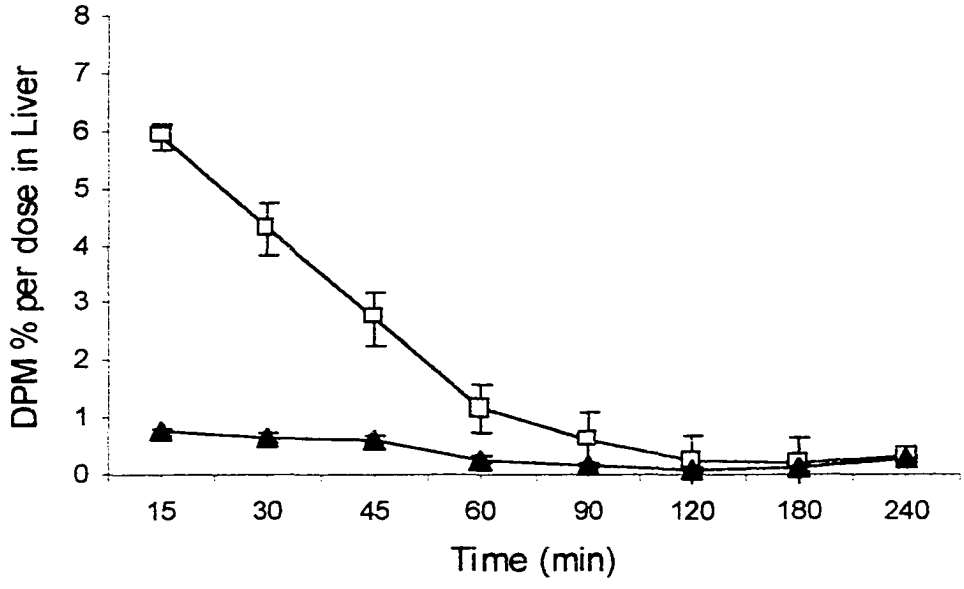

Figure 3.5.3 Tissue distribution, after i.v. tail vein injection, of [^{125}I]DPDPE (□) and [^{125}I]PEG-DPDPE (▲) at 15, 30, 45, 60, 90, 120, 180 and 240 min time points in liver.

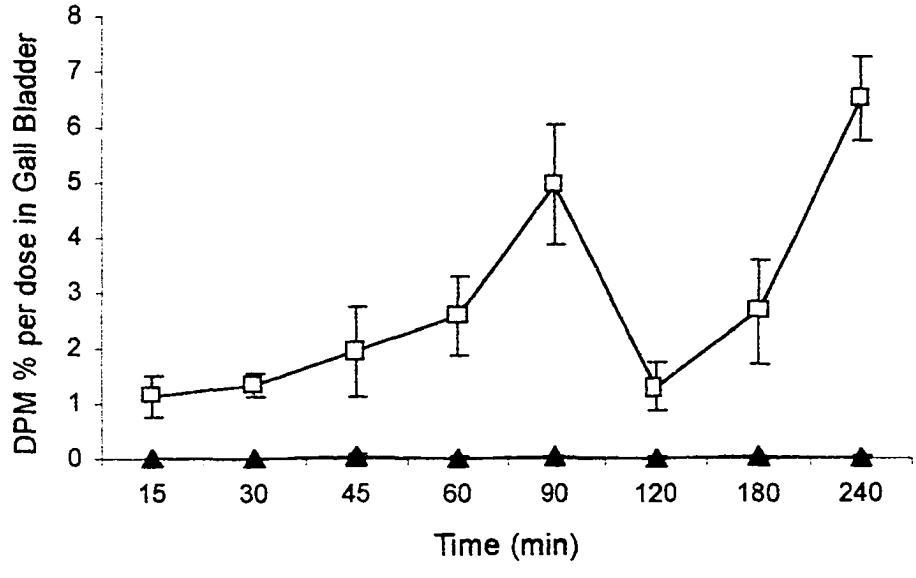

Figure 3.5.4 Tissue distribution, after i.v. tail vein injection, of [^{125}I]DPDPE (□) and [^{125}I]PEG-DPDPE (▲) at 15, 30, 45, 60, 90, 120, 180 and 240 min time points in bladder.

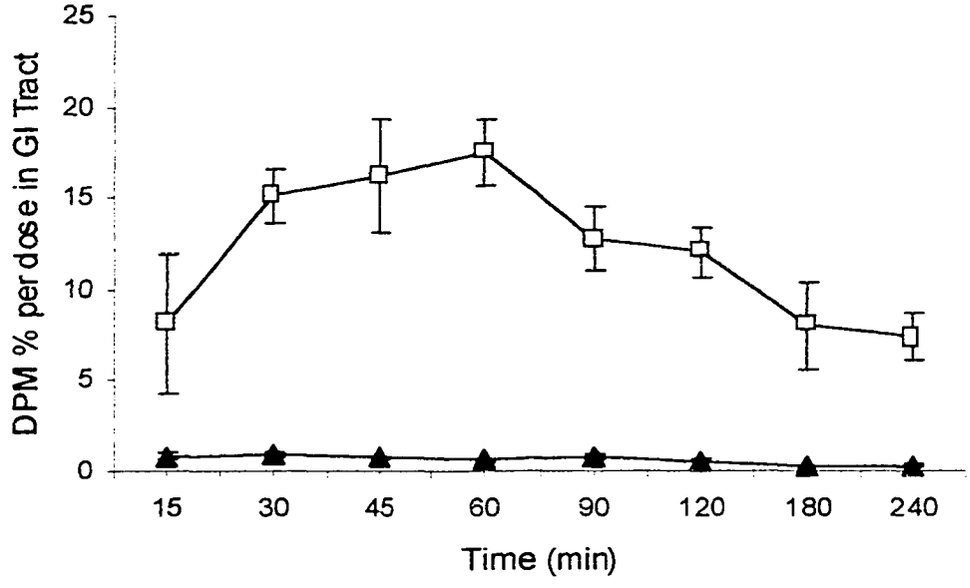

Figure 3.5.5 Tissue distribution, after i.v. tail vein injection, of [^{125}I]DPDPE (□) and [^{123}I]PEG-DPDPE (▲) at 15, 30, 45, 60, 90, 120, 180 and 240 min time points in GI tract.

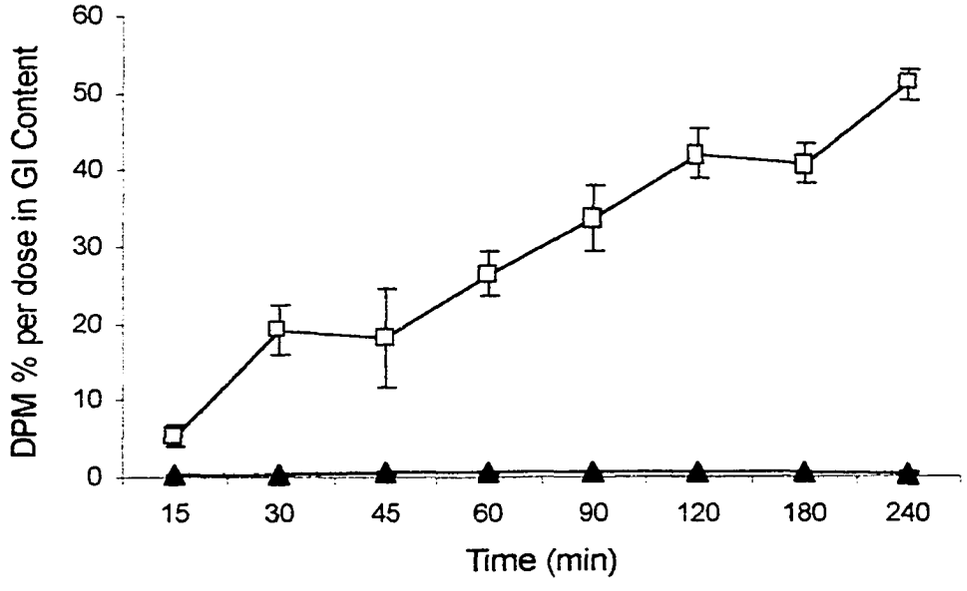

Figure 3.5.6 Distribution, after i.v. tail vein injection, of [^{125}I]DPDPE (□) and [^{125}I]PEG-DPDPE (▲) at 15, 30, 45, 60, 90, 120, 180 and 240 min time points in GI content.

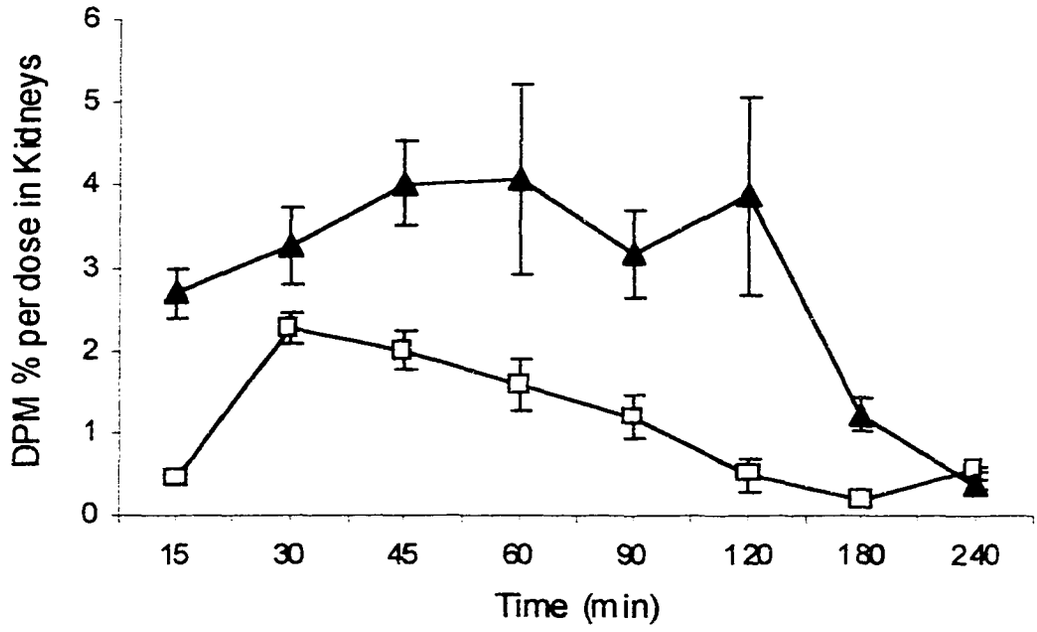

Figure 3.5.7 Tissue distribution, after i.v. tail vein injection, of [^{125}I]DPDPE (□) and [^{125}I]PEG-DPDPE (▲) at 15, 30, 45, 60, 90, 120, 180 and 240 min time points in kidneys.

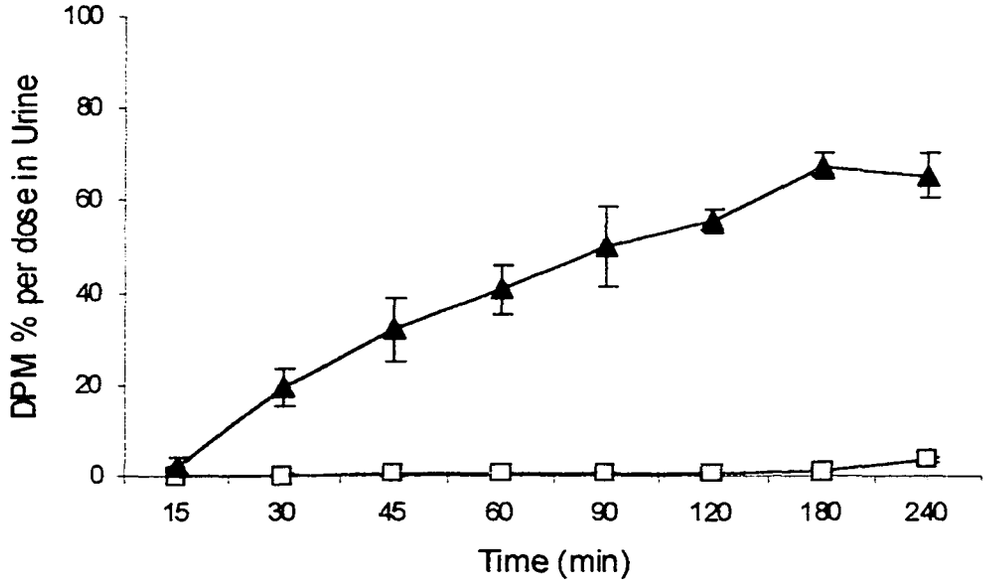

Figure 3.5.8 Distribution, after i.v. tail vein injection, of [^{125}I]DPDPE (□) and [^{125}I]PEG-DPDPE (▲) at 15, 30, 45, 60, 90, 120, 180 and 240 min time points in urine.

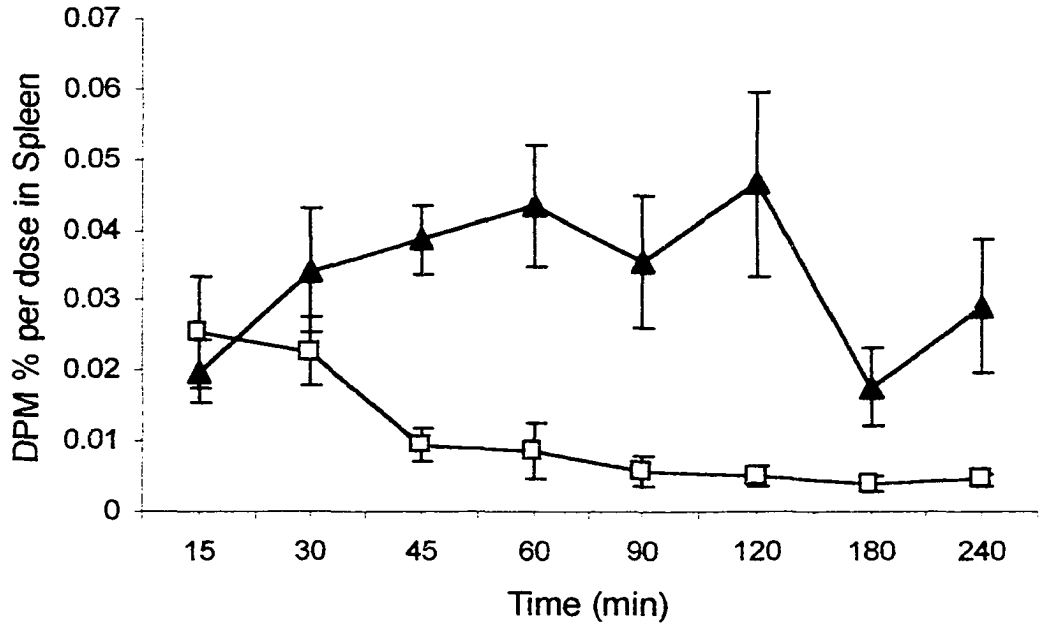

Figure 3.5.9 Tissue distribution, after i.v. tail vein injection, of [^{125}I]DPDPE (□) and [^{125}I]PEG-DPDPE (▲) at 15, 30, 45, 60, 90, 120, 180 and 240 min time points in spleen.

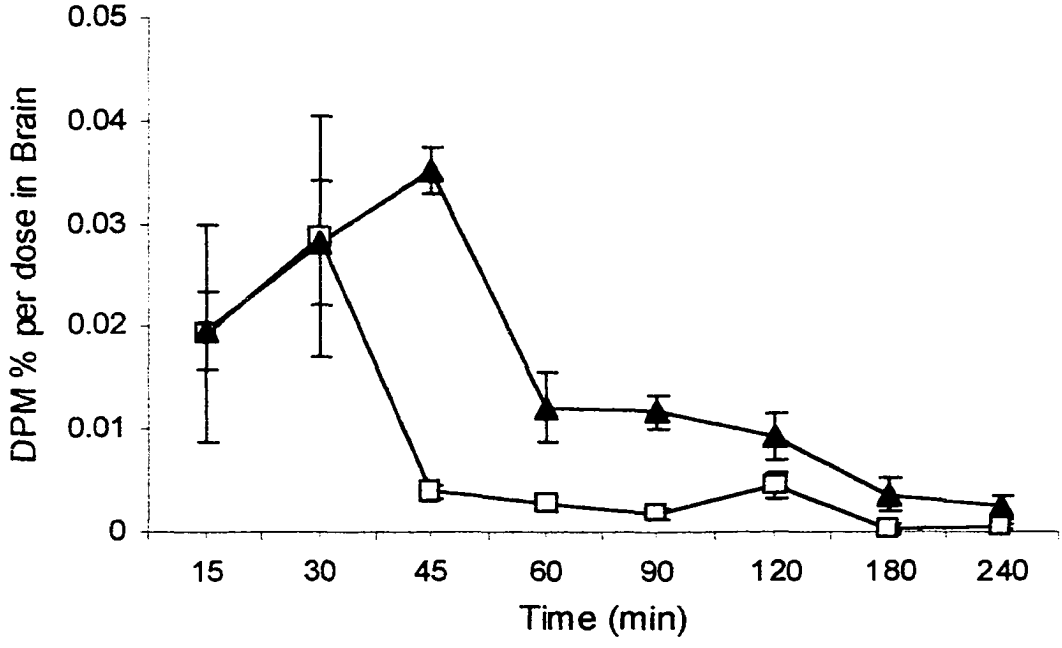

Figure 3.5.10 Tissue distribution, after i.v. tail vein injection, of [^{125}I]DPDPE (□) and [^{125}I]PEG-DPDPE (▲) at 15, 30, 45, 60, 90, 120, 180 and 240 min time points in brain.

Extraction of Radiolabeled Peptides

The percent of iodinated compound found intact, of total found within the brain and plasma (at 30 min), and feces and urine (at 120 min), after an i.v. administration, was assessed via RP-HPLC (*Table 3.3*). Appendix B shows the HPLC chromatographs (figures 5.1B through 5.10B) for the percent intact peptide shown in table 3.3. [^{125}I]DPDPE content found in the brain was 25.7% intact, with one major metabolite. [^{125}I]DPDPE content found in plasma was greater than 99.0% intact, and in feces greater than 98.0% intact. [^{125}I]DPDPE found in the urine was 33.0% intact with five metabolites. [^{125}I]PEG-DPDPE found in plasma and urine was greater than 99.0% intact. [^{125}I]PEG-DPDPE found in brain consisted of 58.9% [^{125}I]PEG-DPDPE and 41.1% [^{125}I]DPDPE. [^{125}I]PEG-DPDPE found in feces consisted of 53.4% [^{125}I]PEG-DPDPE and 37.4% [^{125}I]DPDPE, with one other metabolite.

In Situ Brain Perfusion and Capillary Depletion

The uptake of [^{125}I]DPDPE and [^{125}I]PEG-DPDPE into rat brain were assessed via *in situ* brain perfusion, at 20 min (*Table 3.4*). There was no significant difference in uptake to the brain, or accumulation in the CSF, for either compound. Capillary depletion analysis also revealed no significant difference in compound concentration contained within the capillary (i.e. pellet) or supernatant (i.e. brain parenchyma).

	[^{125}I] DPDPE		[^{125}I] PEG-DPDPE		
	Parent form	**Number of metabolites (>1.0%)**	**Parent form**	**DPDPE metabolite**	**Number of metabolites (>1.0%)**
Control	> 96.0	2	> 99.0	< 1.0	0
Brain	25.7	1	58.9	41.1	1
Plasma	> 99.0	0	> 99.0	< 1.0	0
Feces	> 98.0†	1	53.4	37.4	2
Urine	33.0	5	> 99.0†	< 1.0	0

Table 3.3 Percent intact [^{125}I]DPDPE and [^{125}I]PEG-DPDPE, found in each of the respective region after i.v. dose, by HPLC after i.v. administration. Brain and Plasma sampling taken at 30 min time point, Fecal and Urine sampling taken at 120 min time point. Iodine^{125} tag was found intact in each respective sampling to > 99%.Pooled extraction from n = 4 mice. †Signifies primary route of elimination for parent form, with > 95% of initial total dose eliminated via that route.

	R_{Br} %	CSF %	Pellet % (Capillaries)	Supernatant % (Brain Parenchyma)	Homogenate % (Total Brain)
[^{125}I] DPDPE	3.54 ± 0.30	2.53 ± 0.45	1.35 ± 0.40	3.12 ± 0.45	3.52 ± 0.43
[^{125}I]PEG -DPDPE	3.41 ± 0.16	3.63 ± 0.41	1.37 ± 0.26	2.70 ± 0.75	3.13 ± .019

Table 3.4 *In situ* brain perfusion (20 min) characteristics of [^{125}I] DPDPE and [^{125}I] PEG-DPDPE, presented as a ratio of uptake (n =5) in brain and CSF (n = 3); Capillary depletion analysis (n = 3) represented as ratio of uptake in pellet, supernatant and homogenate. Data are mean ± S.E.M.

BBMEC Uptake

The BBMECs were shown to maintain their integrity over time course, as determined by no change in [^{14}C]sucrose uptake. Assessment of the effects of PEGylation on the P-glycoprotein efflux mechanism was assessed *in vitro* at a 20 min time point. [^{125}I]DPDPE and [^{125}I]PEG-DPDPE cellular uptake were analyzed with P-gp inhibitor cyclosporin-A (*Figure 3.6*). [^{125}I]DPDPE, a known P-gp substrate, showed a significant ($p < 0.01$) increase in BBMEC uptake when coadministered with cyclosporin-A. [^{125}I]PEG-DPDPE, showed a significant increase ($p < 0.01$) over [^{125}I]DPDPE at the single 20 min time, however did not have any change in uptake when coadministered with cyclosporin-A. Saturable transport exhibited for DPDPE *in situ* (Williams *et al.*, 1996), was assessed for [^{125}I]PEG-DPDPE in BBMECs. Significant reduction ($p < 0.05$) in [^{125}I]PEG-DPDPE uptake was observed with 100 μM DPDPE (*Figure 3.7*), suggesting that [^{125}I]PEG-DPDPE is taken up into the endothelial cells via the same mechanism as DPDPE.

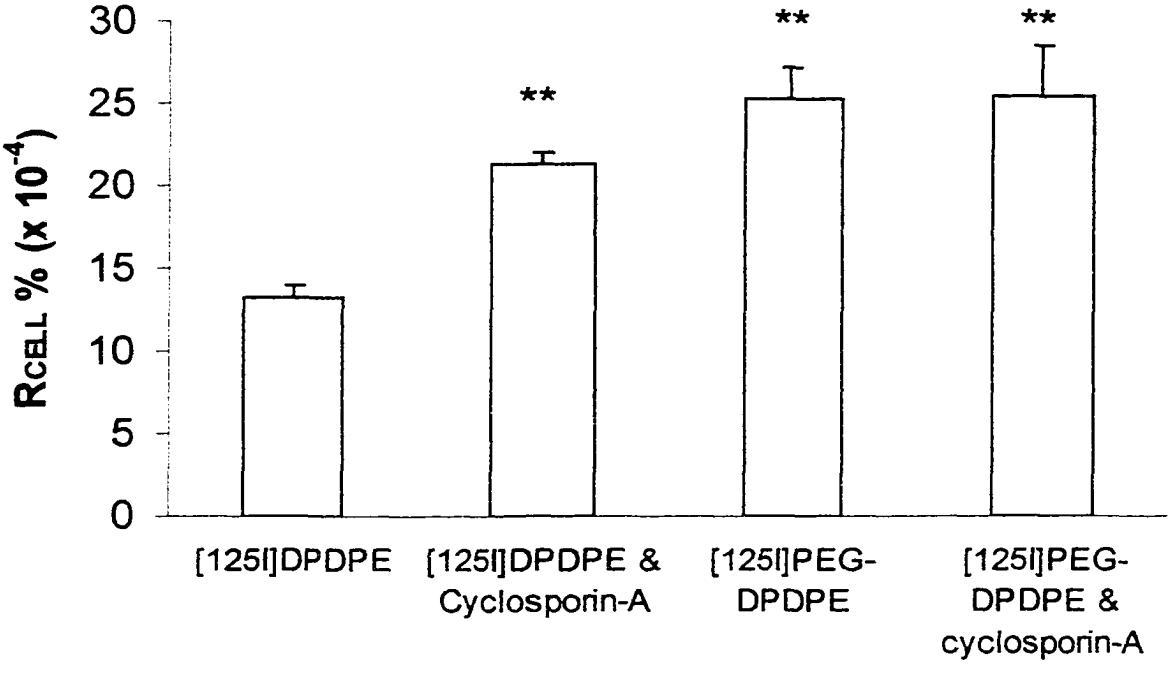

Figure 3.6 BBMEC uptake expressed as a percent ratio of cellular uptake (R_{cell} %). Time was 20 min, values are the mean ± S.E.M. (n = 6). Cyclosporin-A (1.6 μM) was used to assess effects of P-glycoprotein inhibition on [^{125}I]DPDPE and [^{125}I]PEG-DPDPE cellular uptake. Data are mean ± S.E.M. Significance determined by ANOVA, followed by Newman-Keuls post-hoc analysis, denoted by **$p < 0.01$, with respect to DPDPE.

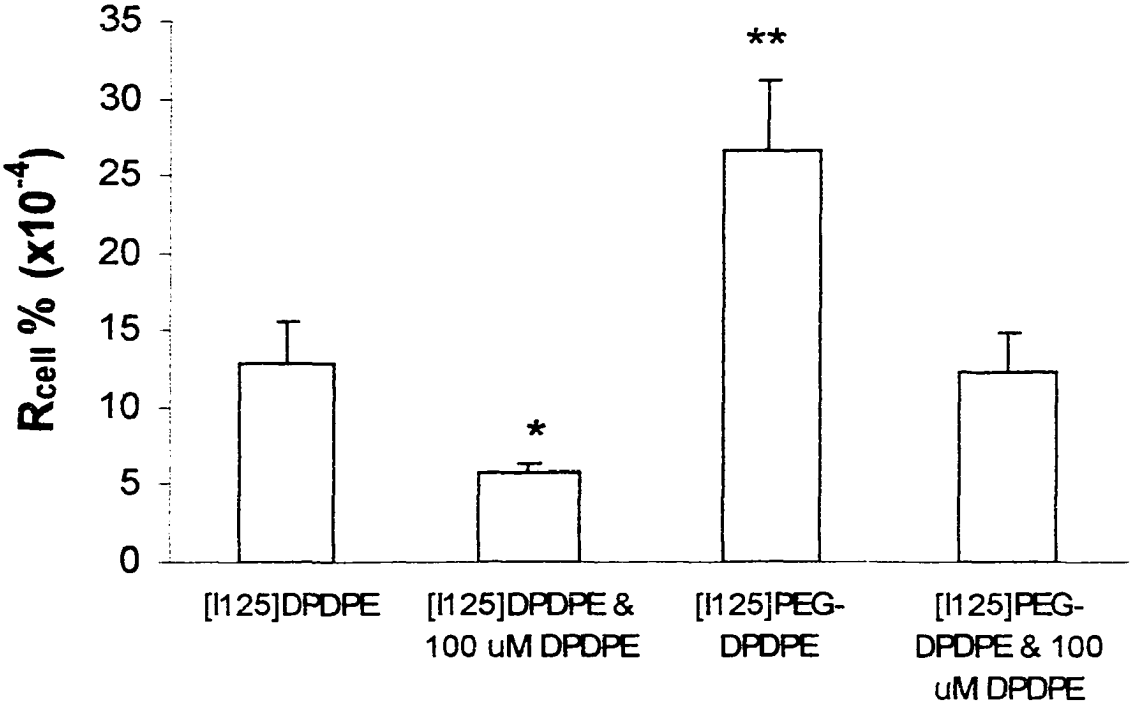

Figure 3.7 BBMEC uptake expressed as a percent ratio of cellular uptake (R_{cell} %). Time was 20 min, values are the mean ± S.E.M. (n = 6). 100 μM DPDPE was used to assess saturable uptake on [^{125}I]DPDPE and [^{125}I]PEG-DPDPE cellular uptake. Data are mean ± S.E.M. Significance determined by ANOVA, followed by Newman-Keuls post-hoc analysis, denoted by **$p < 0.01$and *$p < 0.05$ with respect to [^{125}I]DPDPE, †$p < 0.05$ with respect to [125]PEG-DPDPE.

Discussion

In this study we have used PEGylation in an attempt to enhance the pharmacodynamic profile and analgesic effect of DPDPE. PEG conjugated to DPDPE enhanced analgesic effect (i.v.), increasing maximal response as well as the duration (*Figure 3.2*). I.c.v. injection of PEG-DPDPE showed no significant difference in analgesia to that of DPDPE (*Figure 3.3*), while receptor binding data indicated significant reduction of δ-opioid receptor binding affinity with PEG conjugation. It would be expected that i.c.v. administration would result in decreased analgesia, given the significant reduction in receptor binding. However, enzymes within the brain parenchyma may contribute to the hydrolysis of PEG-DPDPE, resulting in a non-conjugated DPDPE that is able to interact with the receptor. Additionally, the PEG moiety would likely prevent the rapid efflux of DPDPE out the brain via P-gp, allowing more time to act at the receptor. Thus, the improved analgesia of i.v. administered PEG-DPDPE, to DPDPE (i.v.), is likely due to improved bioavailability, either via increased brain uptake or altered peripheral pharmacokinetics.

We conducted biodistribution studies in mice to investigate the effects of PEGylation on DPDPE availability to the brain. The amount of [^{125}I]PEG-DPDPE in the systemic circulation available for transport to the brain is significantly greater than non-conjugated DPDPE for all time points (*Figures 3.4 & 3.5*). The greater concentration within the systemic circulation was not necessarily indicative of greater bioavailability to the target organ (i.e. brain). Binding of the peptide to red-blood cells and serum proteins can play a significant role in determining CNS uptake (Banks *et al.*, 1990). The plasma

concentration of both [^{125}I]DPDPE and [^{125}I]PEG-DPDPE (*Figure 3.5.1*) was approximately twice that of whole blood (*Figure 3.5.2*), indicating the majority of compound is in the plasma portion of the blood. Protein binding analysis shows [^{125}I]PEG-DPDPE has a significantly greater unbound fraction in the plasma than DPDPE (*Table 3.2*). Therefore, [^{125}I]PEG-DPDPE has not only a greater concentration in the systemic circulation, but it also has a greater unbound portion within the systemic circulation.

It has been theorized that an "exclusion-effect", also referred to as " steric-stabiliziation", via the PEG moiety results in repulsion of other macromolecules and particles (Lasic *et al.*, 1991). It is believed that the heavy hydration, good conformation flexibility and high chain mobility are primarily responsible for this exclusion effect. This aspect of PEG, along with its greater circulation time, would result in a large free concentration of PEG-DPDPE reaching capillary endothelial cells of the BBB.

The liver, GI tract, GI content, gallbladder, kidney, urine, spleen, and brain concentration-time profiles of [^{125}I]DPDPE correspond well to previous studies (Weber *et al.*, 1992; Chen and Pollack, 1997). Conjugation of the PEG moiety greatly reduced hepato-biliary elimination of DPDPE. This effect likely results from enhanced hydrophilicity. Additionally, the amount of [^{125}I]PEG-DPDPE that was found within the feces (<5%) was only 53.4% intact (*Table 3.3*). The PEG conjugation shifted elimination almost completely to the renal pathway. PEGs with a molecular weight of 4000 Da, or less, have been shown to be excreted via the renal route, at a rate equivalent to creatinine (Shaffer *et al.*, 1948). Higher molecular weight PEGs (>20KDa) alternatively reduce

glomerular/renal elimination. This reversal of elimination routes may be limited to low molecular weight peptides attached to low molecular weight PEGs. [^{125}I]PEG-DPDPE found in the urine at 120 min was greater than 99.0% intact (*Table 3.3*), indicating that breakdown products are eliminated via another route (i.e. hepato-biliary).

Distribution analysis indicates that similar amounts of [^{125}I]DPDPE and [^{125}I]PEG-DPDPE are taken up into the brain for the first 30 min. [^{125}I]PEG-DPDPE concentrations continue to increase in the brain up to 45 min, while [^{125}I]DPDPE concentrations decrease significantly after the 30 min time point. This trend corresponds well with the analgesia data. The increased circulation time of [^{125}I]PEG-DPDPE allows for a given concentration of drug to be exposed to the capillary endothelial cell surface of the BBB over a longer period of time. *In situ* brain perfusion analysis (*Table 3.4*) indicated that no difference exists in ratios of brain uptake (R_{Br} %), or capillary endothelial cell concentration, between the PEGylated and non-PEGylated forms. This corresponds with the theory that PEG-DPDPE has an increased uptake into the brain via a longer circulation time.

In vitro analysis (% R_{cell}) indicated a significant increase in [^{125}I]PEG-DPDPE uptake, compared to [^{125}I]DPDPE, at 20 min. This result was unexpected, with the significant variation in lipophilicity (i.e. octanol/buffer coefficients) between the two DPDPE forms, a difference in permeability would be expected. PEGylation increased hydrophilicity would likely reduce compound uptake at the BBB. The reason for these variable effects may be due to multiple factors. First, *in vitro* analysis is solely representative of luminal membrane permeability, with a greater degree of error as to

extracellular surface binding (by volume) as compared to *in situ* brain perfusion. Secondly, DPDPE has been shown to have a saturable mechanism of transport at the BBB (Williams *et al.*, 1996), this transport also has affinity for the PEG-DPDPE conjugate (*Figure 3.7*), thereby potentially offsetting a reduced diffusion resultant of PEG's enhancement of hydrophilicity. This saturable transport occurred at a concentration greater than 100 μM DPDPE (concentrations far above those used in this study). Thirdly, DPDPE has been identified as a substrate for the P-gp efflux mechanism (Chen and Pollack, 1999; Witt *et al.*, 2000). In this study [^{125}I]DPDPE and [^{125}I]PEG-DPDPE were coadministered with P-gp inhibitor cyclosporin-A to assess uptake into BBMECs (*Figure 3.6*). [^{125}I]DPDPE with cyclosporin-A showed increased uptake into the cells; whereas [^{125}I]PEG-DPDPE with cyclosporin-A showed no change in cell uptake. This data indicates that [^{125}I]PEG-DPDPE uptake into the brain may be aided by a reduced affinity for P-gp. *In vitro* models which include astrocytes or astrocyte-conditioned media may exhibit a greater expression of P-gp at the BBB (Gaillard *et al.*, 2000); therefore, non-astrocyte conditioned models used in this analysis may underestimate P-gp efflux of DPDPE. The PEG moiety, which conveys steric hindrance and added hydrophilicity, may also inhibit the attachment/identification of DPDPE to the P-gp efflux mechanism, thus allowing a greater concentration to gain entry into the brain. This effect could also counterbalance the hydrophilicity of the PEG moiety. Finally, the hydrophilicity appears to be of secondary importance to chain conformational flexibility and mobility (Blume *et al.*, 1993; Torchilin *et al*, 1994).

Breakdown of [^{125}I]DPDPE in brain (*Table 3.3*), examined at 30 min, found only 25.7% intact; whereas [^{125}I]PEG-DPDPE was 58.9% intact, with 41.1% identified as [^{125}I]DPDPE (metabolite). This idea that the PEG moiety acts in a "prodrug" manner is further supported by the ligand binding profile. PEG-DPDPE shows a 172-fold decrease in δ-opioid receptor affinity over DPDPE, with no enhancement of μ-opioid receptor binding affinity. It has been indicated that the flexible chain of mPEG polymers can sterically interfere with active binding sites of compounds (Marshall *et al.*, 1996). Therefore, in this instance the PEG moiety is likely removed from DPDPE via hydrolysis, leaving the native peptide to react at the receptor.

A number of caveats exist which need to be addressed. The peak effect of analgesia onset for both compounds appears to be 15 min after peak brain uptake, as measured in the distribution assessment. The reason for this disparity is likely the effect of the radioactive tag used in the distribution analysis, but not the analgesia analysis. Iodination of tyrosine residues has effects on permeability. Reduced *in situ* brain uptake occurs with the use of radioactive iodine tagging (Witt *et al.*, 2000). This effect is thought to occur via the large van der Waals volume of iodine (Bondi, 1964) distorting the conformation of tyrosine, as well as the addition of a bulky radioactive group onto a relatively small compound. For each analysis in this study, both the PEGylated and non-PEGylated DPDPE were treated in an identical manner (i.e. either both were iodinated or non-iodinated). Iodine^{125} tag was found intact in each respective sampling to > 99%.

We also performed the investigation with a number of established models using correlations drawn between animal models and sexes, with examination of bovine (*in vitro*), female rat (*in situ*, receptor competition), and male mouse (distribution, serum binding, analgesia, peptide enzymatic integrity). BBB permeability variations between mice and rats have been examined *in situ* (Murakami *et al.*, 2000), with over 20 different compounds, finding similar (1:1) permeabilities across species. Additionally, variations in sex and species have been reported for opioid response, with links to the estrus cycle (Mogil *et al.*, 2000). Studies have also shown a larger number of δ-opioid receptors in mouse brain, compared with similar concentrations of μ-opioid receptor (Yoburn *et al.*, 1991). Despite the variations between models, the study focus was on differences between the PEGylated and non-PEGylated form of drug, with both forms treated in an identical manner within each model.

PEGylation of peptide-based drugs has the potential to overcome many of the problems associated with achieving adequate therapeutic effect. The key to optimizing a clinically beneficial drug revolves around the elucidation of the pharmacodynamic and pharmacokinetic effects that the PEG moiety induces upon the conjugated compound. The chemical composition of the PEG, how and where the PEG is linked to the drug, the drug's composition, and where the drug induces it's receptor mediated effect are also significant considerations. In this study, we have shown that conjugation of PEG to DPDPE induced significant changes in a number of factors, including elimination half-life, volume of distribution, protein binding, hydrophilicity, receptor binding, P-gp affinity, metabolism and membrane transport resulting in an improved analgesic effect.

Chapter 4. General Discussion and Conclusions

The present studies demonstrate that chemical modification, both trimethylation and poly(ethylene glycol) conjugation, alter the brain uptake, lipophilicity, plasma protein binding, stability, receptor binding, distribution, and resultant analgesic effect of the opioid peptide DPDPE.

Chapter 2 centered on the investigation of trimethylation of DPDPE, with subsequent analyses focused on each diastereoismer formed. The tri-methylation of the Phe^4 group of DPDPE brought about significant alterations in δ-opioid receptor binding, with a uniform decrease in δ-selectivity for each of the four diastereoisomers. Only the (2S,3S)-TMP form exhibited an increase in μ-opioid receptor selectivity compared to the parent form, DPDPE. Plasma protein binding analysis on each form did exhibit significance, yet the actual variation between each form was not such that it would result in any observable or significant changes in bioavailability. Lipophilicity of all four diastereoismer forms was increased compared to the parent form, which would result in enhanced transport via passive diffusion. The (2S,3S)-TMP form exhibited the greatest degree of enhanced lipophilicity, as well as the greatest degree of increased transport across the blood-brain barrier (BBB). Brain uptake, both *in vitro* and *in situ*, shown to be significantly enhanced for the (2S,3S)-TMP form compared to the parent. Whereas the (2R,3R)-TMP form shown to be significantly decreased compared to the parent. The two remaining forms, (2S,3R)-TMP and (2R,3S)-TMP, exhibited no significant change in brain uptake, *in vitro* or *in situ*, compared to the parent. Integrity (i.e. stability) of the compounds within the venous blood shown all diastereoismers, with exception to

(2R,3R)-TMP, to be equivalent to the parent form. (2R,3R)-TMP exhibited an ~4-fold greater instability than the parent form in the venous outflow. The stability within the brain extracts revealed an approximate 2-fold increase in stability for both (2S,3S)-TMP and (2S,3R)-TMP, and (2R,3R)-TMP exhibited an ~0.75-fold decrease in stability, compared to the parent. Comparison of the parent form and (2S,3S)-TMP as to P-glycoprotein (P-gp) affinity revealed that (2S,3S)-TMP was less of a substrate for the efflux mechanism than DPDPE. The parent compound and the (2S,3S)-TMP form were approximately equivalent in their ability to inhibit a nociceptive response, whereas the remaining three diastereoisomers had a significant reduction in their ability to inhibit the nociceptive response compared to the parent.

The data indicated that the positioning of the methyl groups on the Phe^4 of DPDPE resulted in alterations in receptor binding, lipophilicity, stability, brain uptake, P-gp affinity, and plasma protein binding, which in combination contribute to altered analgesic effect. Although (2S,3S)-TMP exhibited significantly enhanced stability, lipophilicity, and brain uptake, as well as reduced P-gp affinity, its greatly reduced affinity for the δ-opioid receptor eliminated the potential benefit of these factors, resulting in no enhance of analgesia over the parent. Conversely, (2R,3R)-TMP exhibited significantly reduced stability and brain uptake, with a much reduced affinity for the δ-opioid receptor, yet an enhance lipophilicity compared to the parent, resulted in a significant reduction in analgesia compared to the parent.

This project has provided important preliminary work toward the understanding and characterization of stereoselective positioning of molecules on peptides, with

intention to enhance bioavailability and end effect. The positioning of molecules about a peptide can result in the alteration of lipophilicity, stability, plasma protein binding, receptor affinity, membrane permeability, and general bioavailability. Each of these factors is of considerable importance in the process of drug design and must be weighed accordingly. This work provides the first semi-comprehensive assessment of stereoselective positioning of methyl groups on a CNS acting peptide, using *in vitro*, *in situ*, and *in vivo* methodologies

Chapter 3 centered on the investigation of poly(ethylene glycol), or PEG, conjugation to DPDPE. Pegylation of proteins and peptides is a relatively new field with little assessment to date on BBB permeability, biodistribution, and pharmacokinetics. PEG-DPDPE showed a significant increase in analgesic response (i.v.) compared to the non-conjugated form, despite a 172-fold lower binding affinity for the δ-opioid receptor. PEG-DPDPE also showed a 36-fold greater hydrophilicity and 12% increase in the unbound plasma protein fraction, compared to DPDPE. PEG-DPDPE had a 2.5-fold increase in elimination half-life, a 2.7-fold decrease in volume of distribution, as well as a 7-fold decrease in plasma clearance rate to DPDPE. Time course distributions in mice showed significant concentration differences in plasma, whole blood, liver, gall-bladder, GI content, GI tract, kidneys, spleen, urine, and brain, between the conjugated and non-conjugated forms. PEG-DPDPE was >99% eliminated via the kidneys, whereas the DPDPE was >99% eliminated via the GI tract. Increased brain uptake of PEG-DPDPE corresponded to analgesia data. PEG-DPDPE recovered from brain was shown to be 58.9% intact, with 41.1% existing as DPDPE (metabolite); whereas DPDPE was 25.7%

intact in the brain. *In vitro* P-gp affinity shown for DPDPE, but not shown for PEG-DPDPE. *In vitro* saturable uptake, with 100 μM DPDPE, shown for PEG-DPDPE, indicating affinity for the same endocytotic process that contributes to DPDPE uptake at the BBB.

The enhanced pharmacokinetic profile of the pegylated form completely changes the route by which DPDPE is eliminated as well as significantly increases the time profile of the drug in the systemic circulation. The reduced lipophilicity of PEG-DPDPE, compared to DPDPE, did not resulted in a change in BBB permeability (*in vitro* or *in situ)*. This is likely the result of the decreased affinity for the P-gp efflux mechanism of the PEG-DPDPE and the continued affinity for the endocytotic mechanism present for DPDPE at the BBB. In this study PEG conjugated DPDPE seems to act as a prodrug, enhancing peripheral pharmacokinetics, while undergoing hydrolysis in the brain allowing non-conjugated DPDPE to act at the receptor. This conclusion is supported by both the extremely low binding affinity of the PEG-DPDPE at the δ-opioid receptor and the assessment of breakdown of the PEG-DPDPE within the brain. Furthermore, the prolonged *in vivo* half-life and reduced plasma protein binding would additionally contribute to the enhancement of analgesia observed.

This project has provided important preliminary work toward the understanding and characterization of poly(ethylene glycol) attachment to CNS acting peptides. The use of PEG in peptide based pharmaceutics is limited, with little knowledge to date on PEG effects on BBB permeability. The use of PEG conjugation must be weighed according to the drug assessed, location of conjugation to the drug, where the drug acts in

body, the stability of the bond, the make-up of the PEG polymer, and the end receptor binding affinity. This work provides the first assessment of PEG conjugation to a CNS acting peptide, using *in vitro*, *in situ*, and *in vivo* methodologies.

Chromatography analysis for the TMP study was carried out by RP- HPLC (Perkin-Elmer 250) with a Vydac column (940415-21-1 #66). The samples were eluted at 37°C using a curvilinear gradient of 0.1% TFA in acetonitrile (10-50%) versus 0.1% aqueous TFA over 30 min. at 1.5 $ml \cdot min^{-1}$.

Appendix A
(HPLC chromatographs for TMP study)

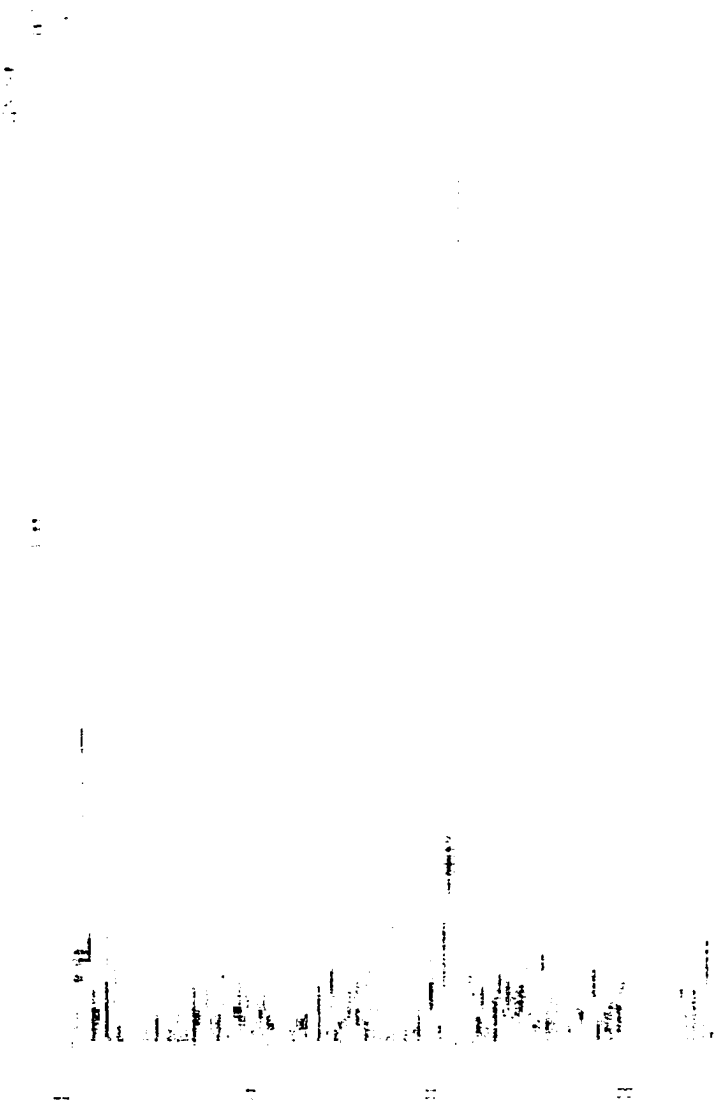

Figure 4.1A DPDPE Brain Extract TMP Study

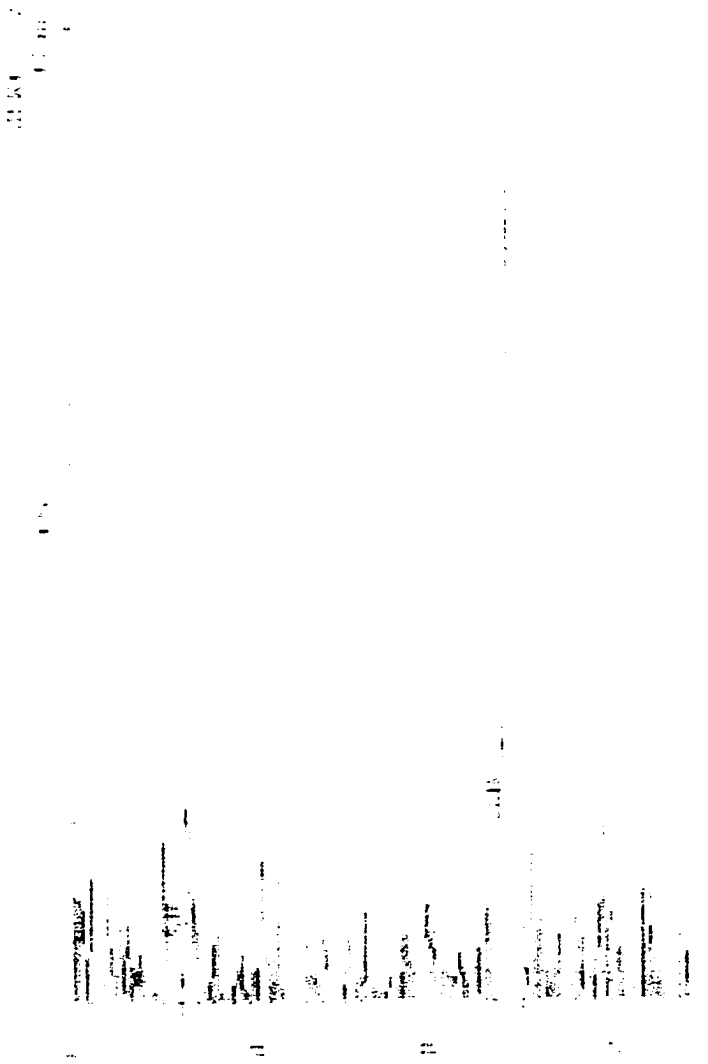

Figure 4.2A 2S,3S-TMP Brain Extract

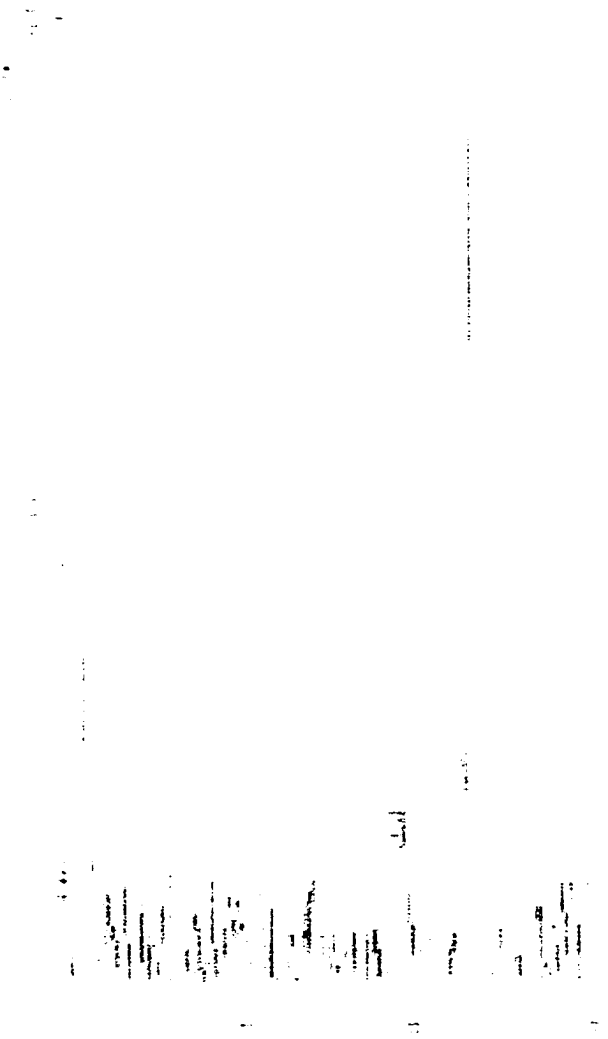

Figure 4.3A 2R,3S-TMP Brain Extract

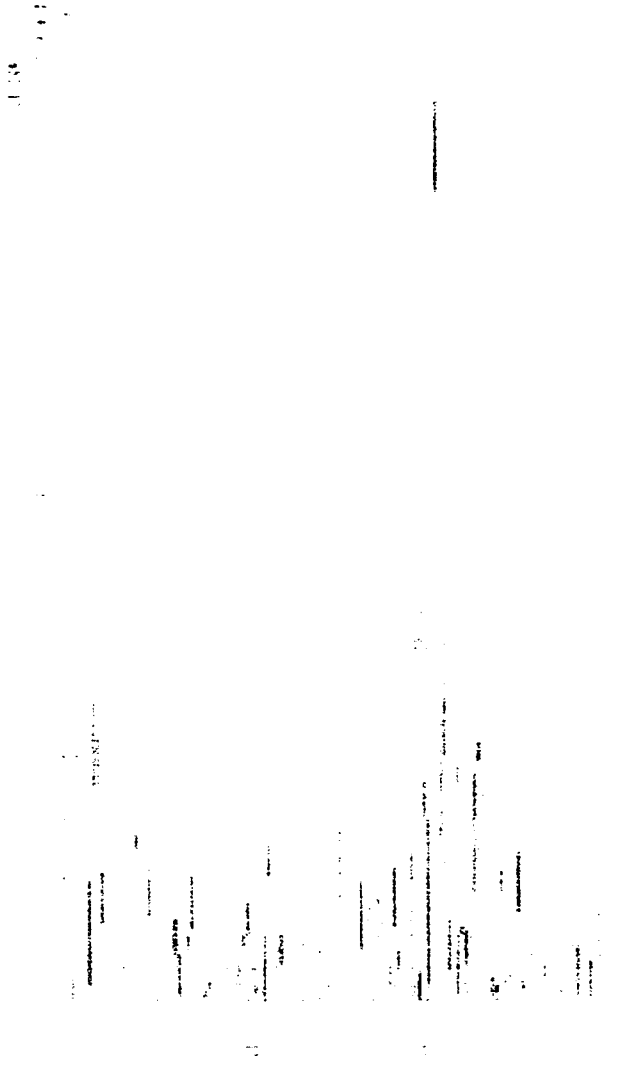

Figure 4.4A 2S,3R-TMP Brain Extract

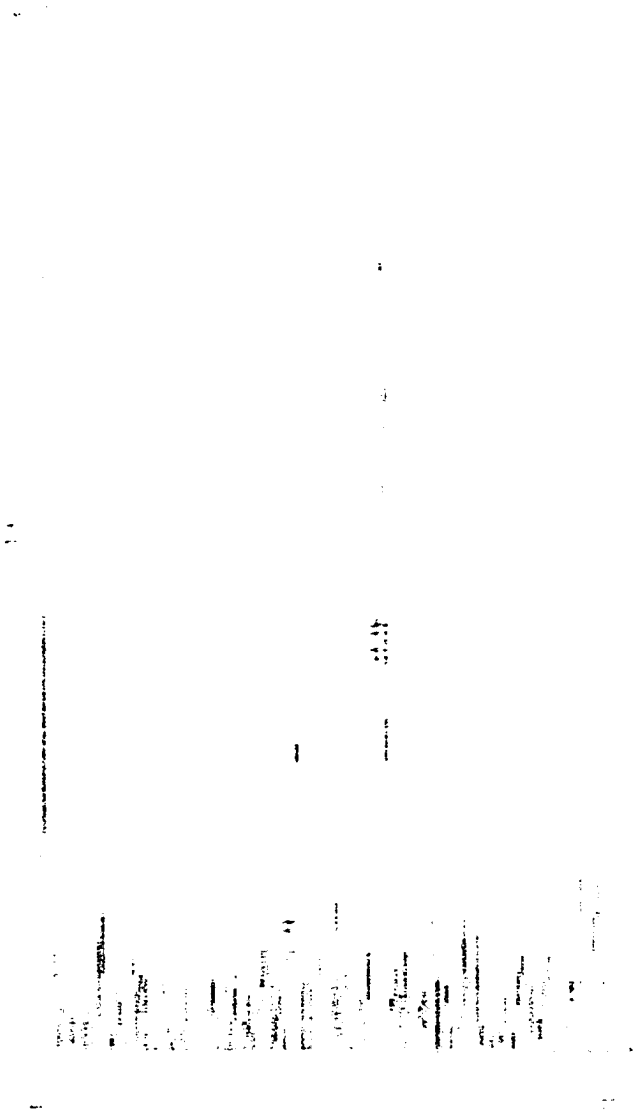

Figure 4.5A 2R,3R-TMP Brain Extract

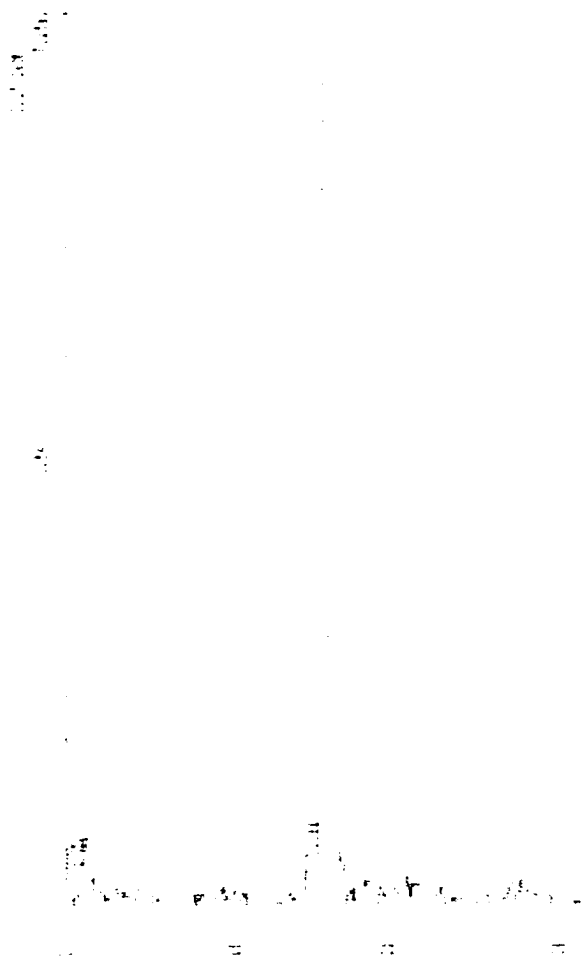

Figure 4.6A DPDPE venous outflow

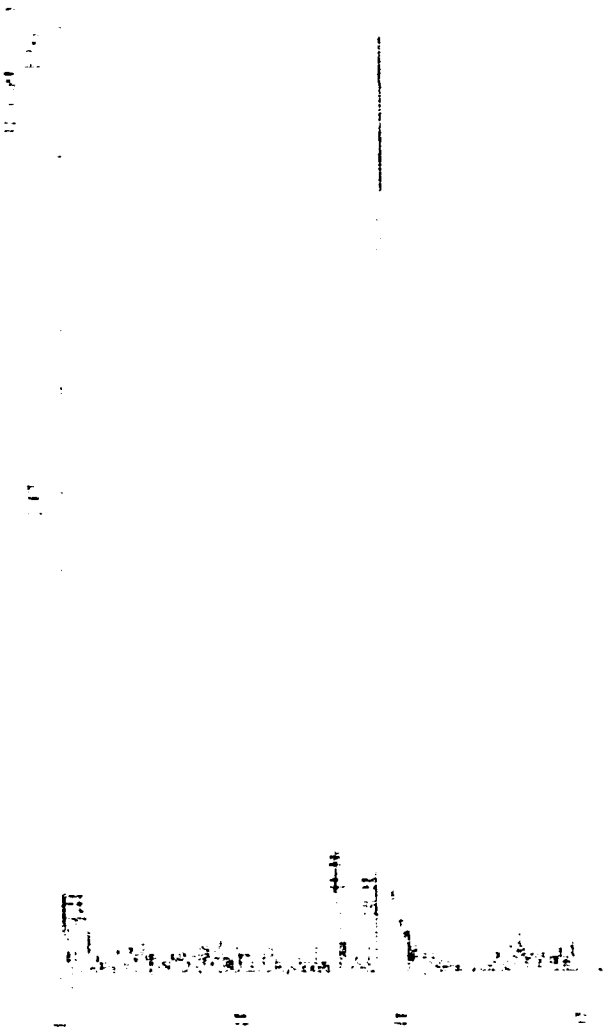

Figure 4.7A 2S,3S-TMP venous outflow

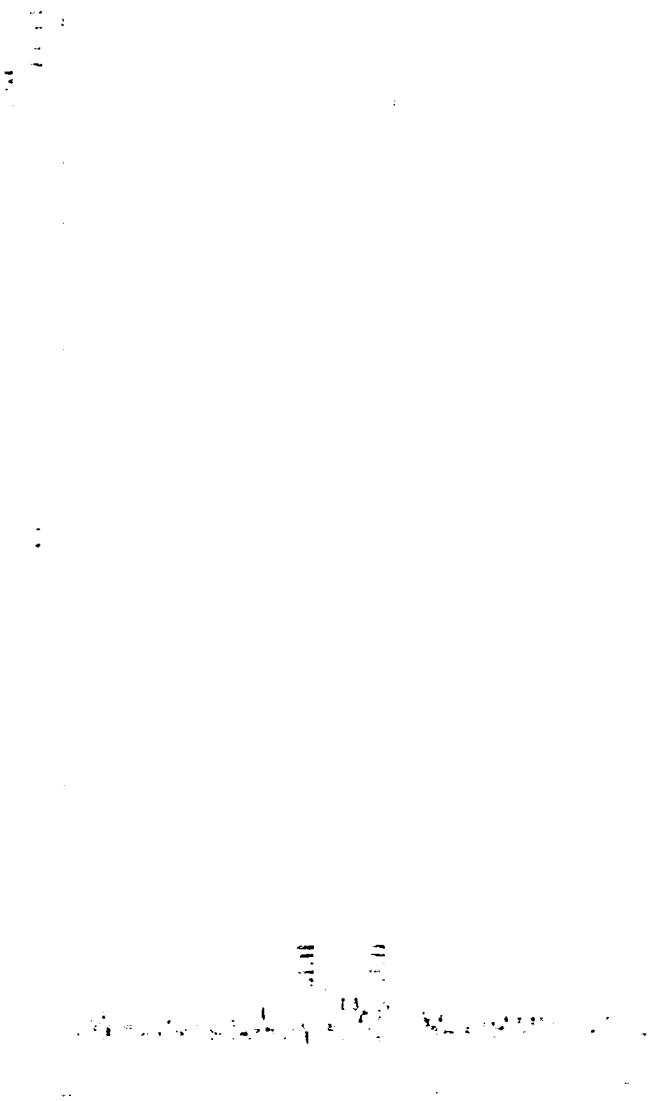

Figure 4.8A 2R,3S-TMP venous outflow

Figure 4.9A 2S,3R-TMP venous outflow

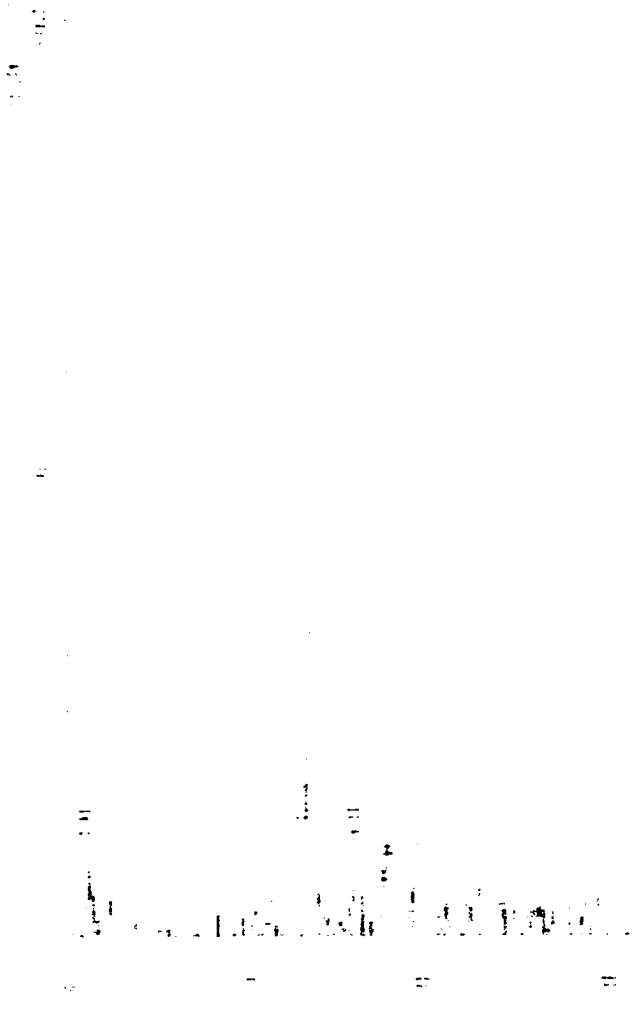

Figure 4.10A 2R,3R-TMP venous outflow

Chromatography analysis for the PEGstudy was carried out by RP-HPLC (Perkin-Elmer 250) with a Vydac™ analytical column (940415-21-1 #66). Samples were eluted at 37°C using a curvilinear gradient of 0.1% TFA in acetonitrile (10-60%) versus 0.1% aqueous TFA over 30 min at 1.5 $ml \cdot min^{-1}$.

Appendix B
(HPLC chromatographs for PEG study)

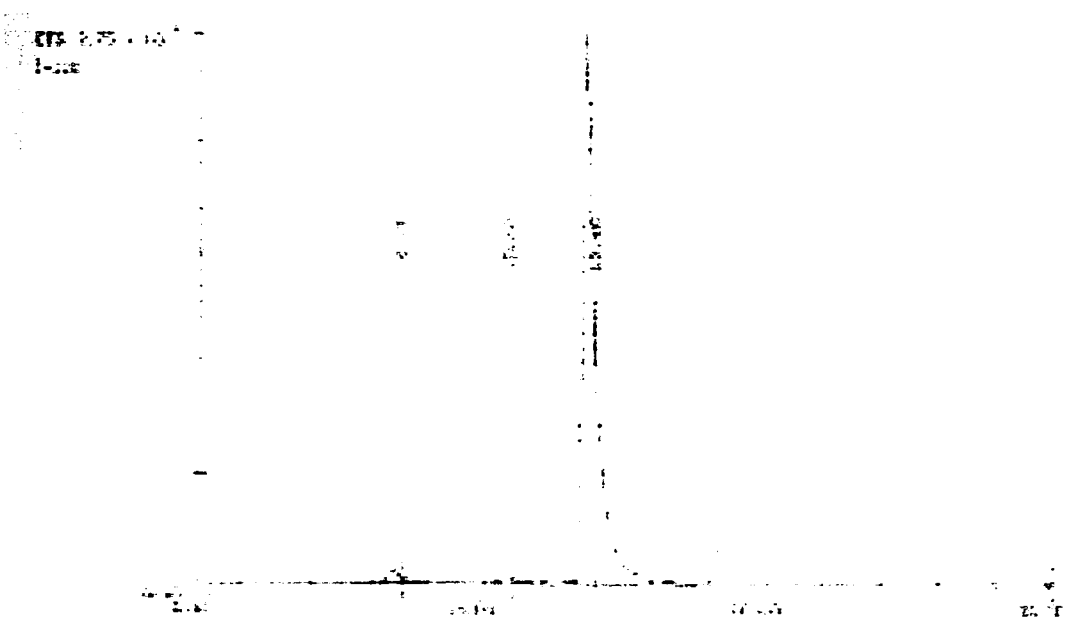

Figure 5.1B DPDPE control for PEG study

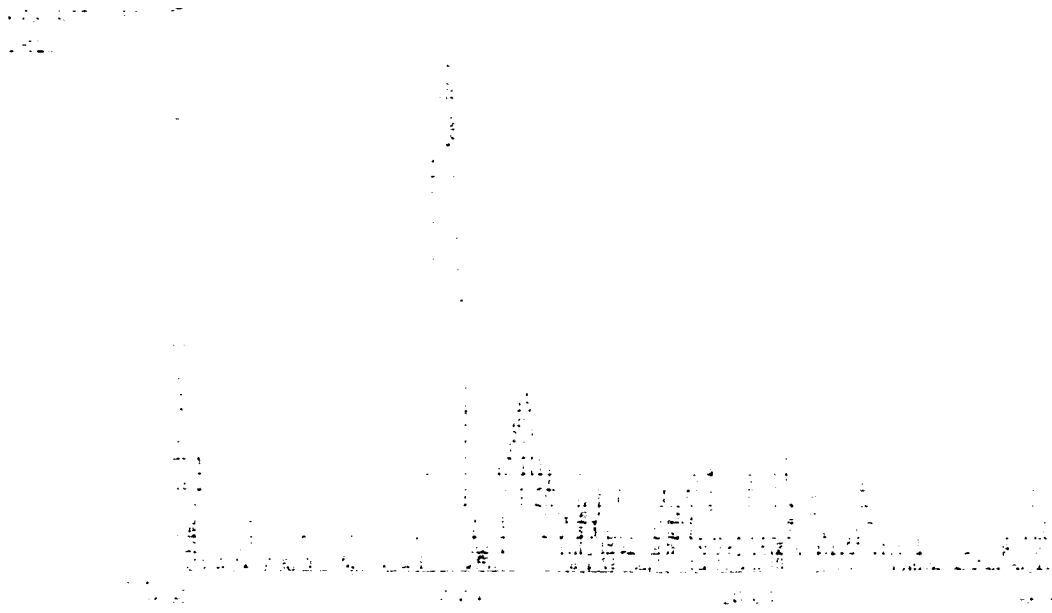

Figure 5.2B DPDPE in brain at 30 min

Figure 5.3B DPDPE in plasma at 30 min

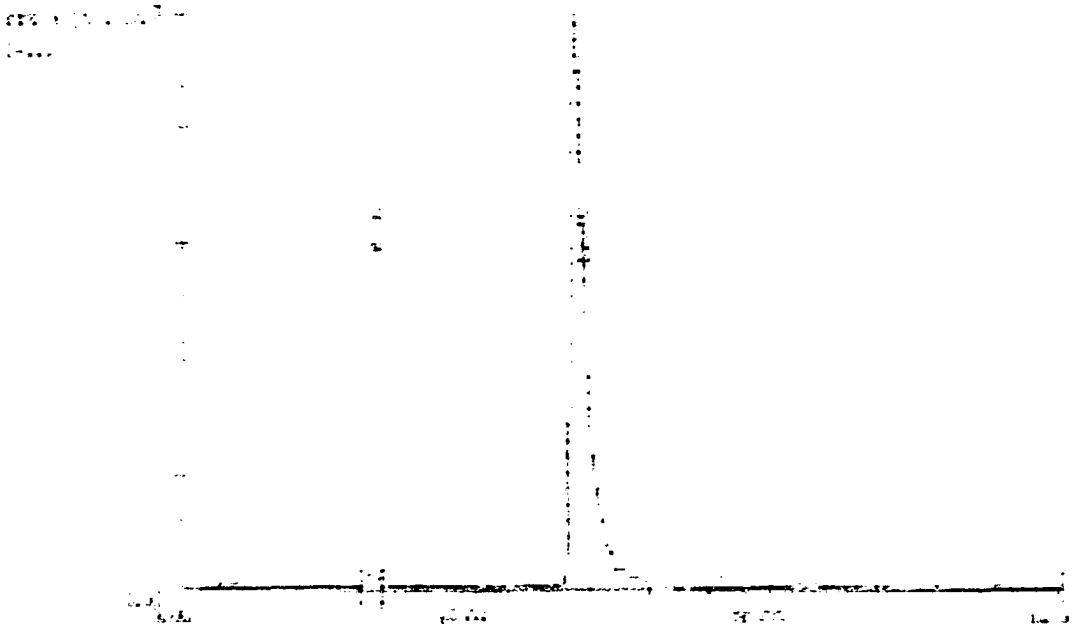

Figure 5.4B DPDPE in feces at 120 min

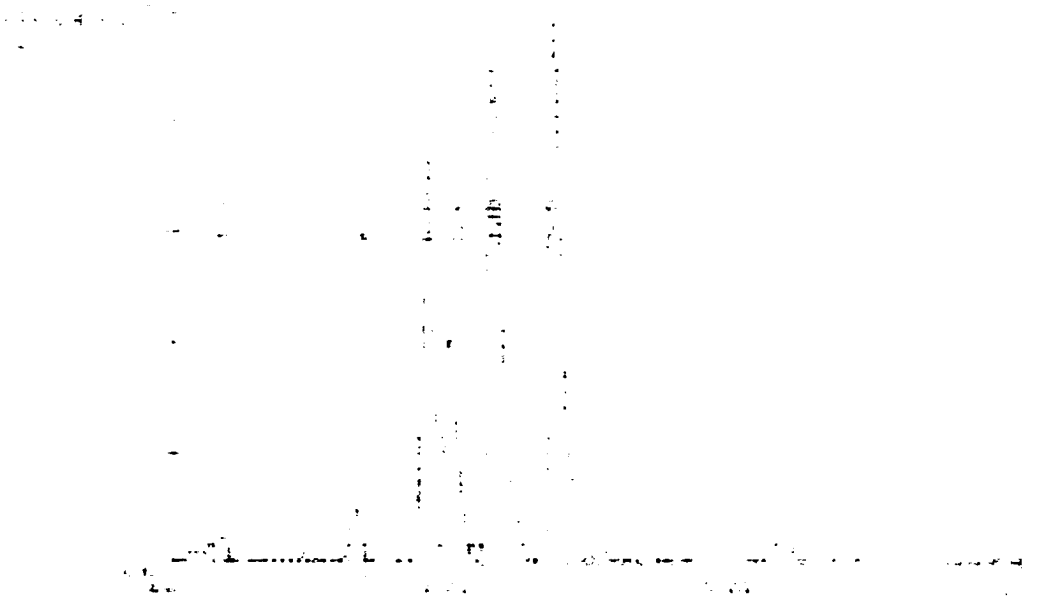

Figure 5.5B DPDPE in urine at 120 min

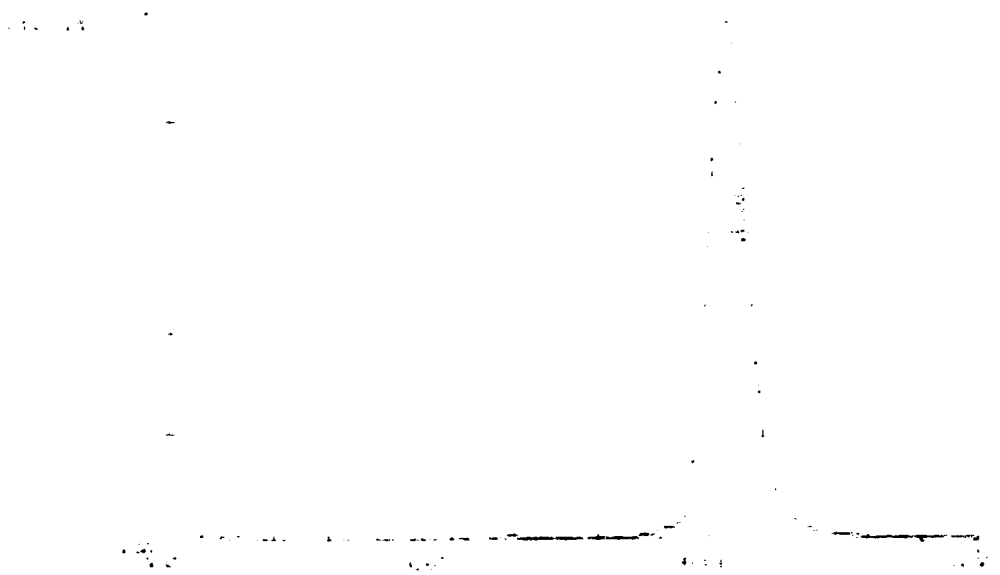

Figure 5.6B PEG-DPDPE control

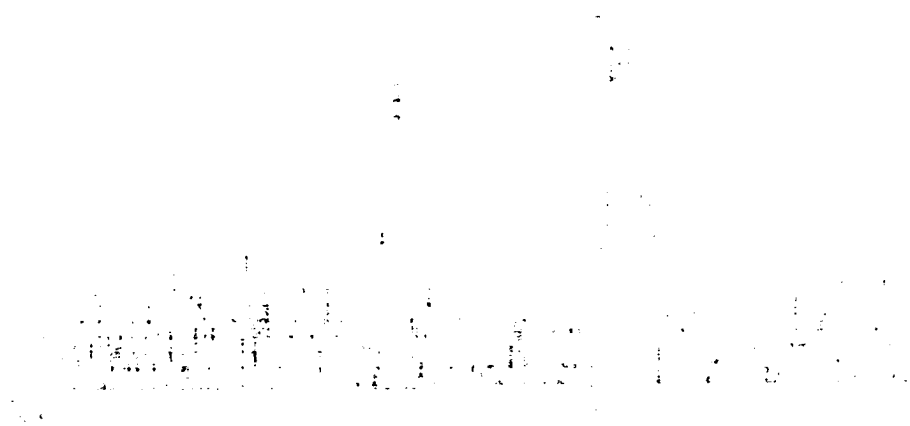

Figure 5.7B PEG-DPDPE in brain at 30 min

Figure 5.8B PEG-DPDPE in plasma at 30 min

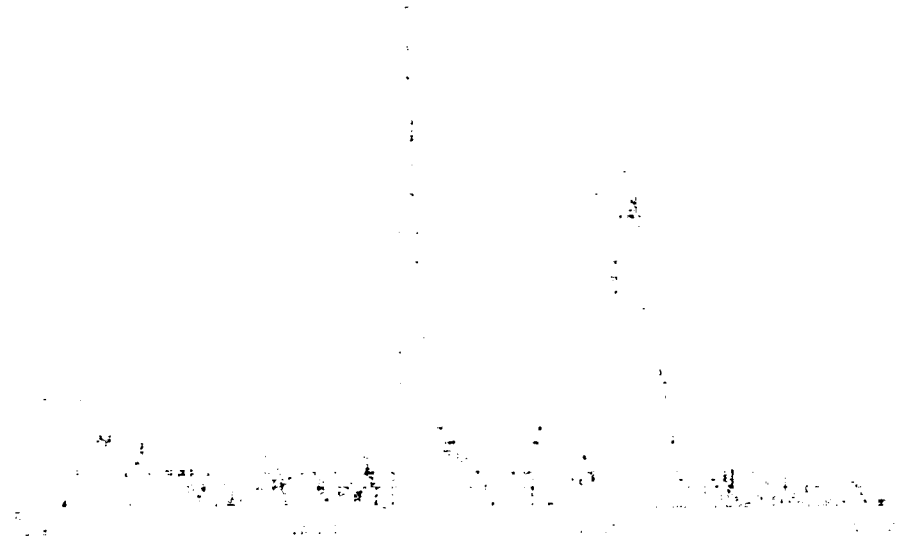

Figure 5.9B PEG-DPDPE in feces at 120 min

Figure 5.10B PEG-DPDPE in urine at 120 min

References

Abbott NJ (2000) Inflammatory mediators and modulation of blood-brain barrier permeability. *Cell Mol Neurobiol* **20**:131-147.

Abbruscato TJ, Williams SA, Misica A, Lipkowski AW, Hruby VJ and Davis TP (1996) Blood-to-central nervous system entry and stability of biphalin, a unique double-enkephalin analog, and its halogenated derivatives. *J. Pharmacol. Exp. Ther.* **276**:1049-1057.

Abbruscato TJ (1997) Opioid Peptide Permeation across the Blood-Brain Barrier and Blood-Cerebrospinal Fluid Barriers, in *Pharmacology and Toxicology*, University of Arizona, Tucson

Abbruscato TJ, Thomas SA, Hruby VJ and Davis TP (1997) Blood-brain barrier permeability and bioavailability of a highly potent and mu-selective opioid receptor antagonist, CTAP: comparison with morphine. *J Pharmacol Exp Ther* **280**:402-409.

Adriaensen H, Gybels J, Handwerker HO and Van Hees J (1983) Response properties of thin myelinated (A-delta) fibers in human skin nerves. *J Neurophysiol* **49**:111-122.

Abbruscato TJ and Davis TP (1999) Protein expression of brain endothelial cell E cadherin after hypoxia/aglycemia: influence of astrocyte contact. *Brain Res* **842**:277-286.

Alder SG, Wang H, Ward HJ, Cohen AH and Border WA (1983) Electrical charge. Its role in the pathogenesis and prevention of experimental membranous nephropathy in the rabbit. *J Clin Invest*:487-499.

Antonelli-Orlidge A, Smith SR and D'Amore PA (1989) Influence of pericytes on capillary endothelial cell growth. *Am Rev Respir Dis* **140**:1129-1131.

Arthur FE, Shivers RR and Bowman PD (1987) Astrocyte-mediated induction of tight junctions in brain capillary endothelium: an efficient in vitro model. *Brain Res* **433**:155-159.

Audus KL, Chikhale PJ, Miller DW, Thompson SE and Borchardt RT (1992) Brain Uptake of Drugs: The Influence of Chemical and Biological Factors. *Advances in Drug Research* **23**:1-64.

Audus KL and Borchardt RT (1986) Characterization of an in vitro blood-brain barrier model system for studying drug transport and metabolism. *Pharm. Res.* **3**:81-87.

Audus KL and Borchardt RT (1987) Bovine brain microvessel endothelial cell monolayers as a model system for the blood-brain barrier. *Ann. N. Y. Acad. Sci.* **507**:9-18.

Banks WA, Kastin AJ and Ehrensing CA (1993) Endogenous peptide Tyr-Pro-Trp-Gly-NH2 (Tyr-W-MIF-1) is transported from the brain to the blood by peptide transport system-1. *J Neurosci Res* **35**:690-695.

Banks WA, Kastin AJ, Huang W, Jaspan JB and Maness LM (1996) Leptin enters the brain by a saturable system independent of insulin. *Peptides* **17**:305-311.

Banks WA and Kastin AJ (1985) Peptides and the blood-brain barrier: lipophilicity as a predictor of permeability. *Brain Res. Bull.* **15**:287-292.

Banks WA and Kastin AJ (1996) Passage of peptides across the blood-brain barrier: pathophysiological perspectives. *Life Sci* **59**:1923-1943.

Banks WA, Schally AV, Barrera CM, Fasold MB, Durham DA, Csernus VJ, Groot K and Kastin AJ (1990) Permeability of the murine blood-brain barrier to some octapeptide analogs of somatostatin. Proc. *Natl. Acad. Sci.* USA **87**:6762-6766.

Basbaum AI. and Fields HL (1979) The origin of descending pathways in the dorsolateral funiculus of the spinal cord of the cat and rat: further studies on the anatomy of pain modulation. *J Comp Neurol* **187**:513-531.

Bartosz-Bechowski H, Davis P, Zalewska T, Slaninova J, Porreca F, Yamamura HI and Hruby VJ (1994) Cyclic enkephalin analogs with exceptional potency at peripheral delta opioid receptors. *J. Med. Chem.* **7**:146-150.

Batrakova EV, Miller DW, Li S, Alakhov VY, Kabanov AV and Elmquist WF (2001) Pluronic P85 enhances the delivery of digoxin to the brain: in vitro and in vivo studies. *J Pharmacol Exp Ther* **296**:551-557.

Bauer HC and Bauer H (2000) Neural induction of the blood-brain barrier: still an Enigma. *Cell Mol Neurobiol* **20**:13-28.

Bausback HH, Churchill L and Ward PE (1988) Angiotensin metabolism by cerebral microvascular aminopeptidase A. *Biochem Pharmacol* **37**:155-160.

Beck DW, Vinters HV, Hart MN and Cancilla PA (1984) Glial cells influence polarity of the blood-brain barrier. *J Neuropathol Exp Neurol* **43**:219-224.

Begley DJ (1996) The blood-brain barrier: principles for targeting peptides and drugs to the central nervous system. *J. Pharm. Pharmacol.* **48**:136-146.

Begley DJ (1999) Methods for determining CNS drug transport in animals, in *Brain Barrier Systems* (Pauson OB, Knudsen GM and Moos T eds) pp 91-113, Munksgaard, Copenhagen.

Benuck M, Berg MJ and Marks N (1981) A distinct peptidyl dipeptidase that degrades enkephalin: exceptionally high activity in rabbit kidney. *Life Sci* **28**:2643-2650.

Bertler A, Falck B, Owman C and Rosengrenn E (1966) The localization of monoaminergic blood-brain barrier mechanisms. *Pharmacol Rev* **18**:369-385.

Betz AL and Goldstein GW (1978) Polarity of the blood-brain barrier: neutral amino acid transport into isolated brain capillaries. *Science* **202**:225-227.

Betz AL, Firth JA and Goldstein GW (1980) Polarity of the blood-brain barrier: distribution of enzymes between the luminal and antiluminal membranes of brain capillary endothelial cells. *Brain Res* **192**:17-28.

Bewley TA and Li CH (1983) Evidence for tertiary structure in aqueous solutions of human beta- endorphin as shown by difference absorption spectroscopy. *Biochemistry* **22**:2671-2675.

Bickel U, Yoshikawa T and Pardridge WM (2001) Delivery of peptides and proteins through the blood-brain barrier. *Adv Drug Deliv Rev* **46**:247-279.

Bilsky EJ, Egleton RD, Mitchell SA, Palian MM, Davis P, Huber JD, Jones H, Yamamura HI, Janders J, Davis TP, Porreca F, Hruby VJ and Polt R (2000) Enkephalin glycopeptide analogues produce analgesia with reduced dependence liability. *J Med Chem* **43**:2586-2590.

Black KL, Baba T and Pardridge WM (1994) Enzymatic barrier protects brain capillaries from leukotriene C4. *J Neurosurg* **81**:745-751.

Blume AJ (1978) Interaction of ligands with the opiate receptors of brain membranes: regulation by ions and nucleotides. *Proc Natl Acad Sci U S A* **75**:1713-1717.

Blume G and Cevc G (1993) Molecular mechanism of the lipid vesicle longevity in vivo. *Biochim. Biophys. Acta* **1146:**157-168.

Bodor N and Buchwald P (1999) Recent advances in the brain targeting of neuropharmaceuticals by chemical delivery systems. *Adv Drug Deliv Rev* **36**:229-254.

Bodor N, Prokai L, Wu WM, Farag H, Jonalagadda S, Kawamura M and Simpkins J (1992) A strategy for delivering peptides into the central nervous system by sequential metabolism. *Science* **257**:1698-1700.

Bolton AE (1986) Comparative methods for the radiolabeling of peptides. *Meth. Enzymol.* **124**:18-29.

Bondi A (1964) Van der Waals volumes and radii. *J. Phys. Chem.* **68:**441-451.

Bourne A, Barnes K, Taylor BA, Turner AJ and Kenny AJ (1989) Membrane peptidases in the pig choroid plexus and on other cell surfaces in contact with the cerebrospinal fluid. *Biochem J* **259**:69-80.

Bradbury MW (1979) *The Concept of the Blood-Brain Barrier.* Wiley & Sons, New York.

Brecher P, Tercyak A, Gavras H and Chobanian AV (1978) Peptidyl dipeptidase in rabbit brain microvessels. *Biochim Biophys Acta* **526**:537-546.

Brem H, Mahaley MS, Jr., Vick NA, Black KL, Schold SC, Jr., Burger PC, Friedman AH, Ciric IS, Eller TW, Cozzens JW and et al. (1991) Interstitial chemotherapy with drug polymer implants for the treatment of recurrent gliomas. *J Neurosurg* **74**:441-446.

Brewster ME, Anderson WR, Webb AI, Pablo LM, Meinsma D, Moreno D, Derendorf H, Bodor N and Pop E (1997) Evaluation of a brain-targeting zidovudine chemical delivery system in dogs. *Antimicrob Agents Chemother* **41**:122-128.

Brewster ME, Estes KS and Bodor N (1988) Improved delivery through biological membranes. 32. Synthesis and biological activity of brain-targeted delivery systems for various estradiol derivatives. *J Med Chem* **31**:244-249.

Brewster ME, Raghavan K, Pop E and Bodor N (1994) Enhanced delivery of ganciclovir to the brain through the use of redox targeting. *Antimicrob Agents Chemother* **38**:817-823.

Brightman MW (1968) The intracerebral movement of proteins injected into blood and cerebrospinal fluid of mice. *Prog Brain Res* **29**:19-40.

Brightman MW and Reese TS (1969) Junctions between intimately apposed cell membranes in the vertebrate brain. *J Cell Biol* **40**:648-677.

Brightman MW, Klatzo I, Olsson Y and Reese TS (1970) The blood-brain barrier to proteins under normal and pathological conditions. *J Neurol Sci* **10**:215-239.

Brightman WM and Tao-Cheng JH (1993) Tight Junctions of Brain Endothelium and epithelium, in *The Blood-Brain Barrier Celular and Molecular Biology* (Pardridge WM ed) pp 107-126, Raven, New York.

Broadwell RD, Balin BJ and Salcman M (1988) Transcytotic pathway for blood-borne protein through the blood-brain barrier. *Proc Natl Acad Sci U S A* **85**:632-636.

Brocks D. R., and Fakhreddin J. (1995) Stereochemical aspects of pharmacotherapy. *Pharmacotherapy* **15,** 551-564.

Broman M (1941) The possibilities of the passage of substances from the blood to the central nervous system. *Acta. Psych. Neurol.*:1-25.

Brownson EA, Abbruscato TJ, Gillespie TJ, Hruby VJ and Davis TP (1994) Effect of peptidases at the blood brain barrier on the permeability of enkephalin. *J Pharmacol Exp Ther* **270**:675-680.

Brownlees J and Williams CH (1993) Peptidases, peptides, and the mammalian blood-brain barrier. *J Neurochem* **60**:793-803.

Brownson EA, Abbruscato TJ, Gillespie TJ, Hruby VJ and Davis TP (1994) Effect of peptidases at the blood brain barrier on the permeability of enkephalin. *J. Pharmacol. Exp. Ther.* **270**:675-680.

Buiatti E, Arniani S, Verdecchia A and Tomatis L (1999) Results from a historical survey of the survival of cancer patients given Di Bella multitherapy. *Cancer* **86**:2143-2149.

Bundgaard H and Moss J (1990) Prodrugs of peptides. 6. Bioreversible derivatives of thyrotropin- releasing hormone (TRH) with increased lipophilicity and resistance to cleavage by the TRH-specific serum enzyme. *Pharm Res* **7**:885-892.

Burton PS, Conradi RA, Ho NF, Hilgers AR and Borchardt RT (1996) How structural features influence the biomembrane permeability of peptides. *J. Pharm. Sci.* **85**:1336-1340.

Butt AM, Jones HC and Abbott NJ (1990) Electrical resistance across the blood-brain barrier in anaesthetized rats: a developmental study. *J Physiol* **429**:47-62.

Bylund DB and Yamamura HI (1990) Methods for Receptor Binding, in *Methods in Neurotransmitter Receptor analysis* (Yamamura HI ed), Raven, New York.

Cancilla PA and DeBault LE (1983) Neutral amino acid transport properties of cerebral endothelial cells in vitro. *J Neuropathol Exp Neurol* **42**:191-199.

Carvey PM, Maag TJ and Lin D (1994) Injection of biologically active substances into the brain. *Methods Neuroscience*:214-234.

Chen C and Pollack GM (1999) Enhanced antinociception of the model opioid peptide [D-penicillamine] enkephalin by P-glycoprotein modulation. *Pharm Res* **16:**296-230.

Chen C and Pollack GM (1997) Extensive biliary excretion of the model opioid peptide [D-Pen^{2,5}] enkephalin in rats. *Pharm. Res.* **14:**345-350.

Chen C and Pollack GM (1998) Altered disposition and antinociception of [D-penicillamine(2,5)] enkephalin in mdr1a-gene-deficient mice. *J. Pharmacol. Exp. Ther.* **287**:545-552.

Chen D and Lee KH (1993) Biodistribution of calcitonin encapsulated in liposomes in mice with particular reference to the central nervous system. *Biochim Biophys Acta* **1158**:244-250.

Chen ZR, Irvine RJ, Bochner F and Somogyi AA (1990) Morphine formation from codeine in rat brain: a possible mechanism of codeine analgesia. *Life Sci* **46**:1067-1074.

Clough G and Michel CC (1981) The role of vesicles in the transport of ferritin through frog endothelium. *J Physiol* **315**:127-142.

Collins JM and Dedrick RL (1983) Distributed model for drug delivery to CSF and brain tissue. *Am. J. Physiol.* **245,** R303-310.

Collins JM, Klecker RW, Jr., Kelley JA, Roth JS, McCully CL, Balis FM and Poplack DG (1988) Pyrimidine dideoxyribonucleosides: selectivity of penetration into cerebrospinal fluid. *J Pharmacol Exp Ther* **245**:466-470.

Conradi RA, Hilgers AR, Ho NF, and Burton PS (1992) The influence of peptide structure on transport across Caco-2 cells. II. Peptide bond modification which results in improved permeability. *Pharm. Res.* **9**:435-439.

Cool WM, Kurtz NM and Chu G (1990) Transnasal delivery of systemic drugs, in *Advances in Pain Research and Therapy* (Benedetti C, Chapamn CR and Giron G eds), Raven, New York.

Coomber BL and Stewart PA (1985) Morphometric analysis of CNS microvascular endothelium. *Microvasc Res* **30**:99-115.

Cordon-Cardo C, O'Brien JP, Casals D, Rittman-Grauer L, Biedler JL, Melamed MR and Bertino JR (1989) Multidrug-resistance gene (P-glycoprotein) is expressed by endothelial cells at blood-brain barrier sites. *Proc Natl Acad Sci U S A* **86**:695-698.

Cornford EM and Oldendorf WH (1975) Independent blood-brain barrier transport systems for nucleic acid precursors. *Biochim Biophys Acta* **394**:211-219.

Crone C (1963) The permeability of capillaries of various organs as determined by the use of the "indicator diffusiion" method. *Acta. Phys. Scand.*:292-305.

Crone C (1971) The blood-brain barrier-facts and questions., in *Ion Homeostasis of the Brain* (Siesjo BK and Sorensen SC eds) pp 52-62, Munksgaard, Copenhagen.

Crone C and Christensen O (1981) Electrical resistance of a capillary endothelium. *J Gen Physiol* **77**:349-371.

Dagenais C, Ducharme J and Pollack GM (2001) Uptake and efflux of the peptidic delta-opioid receptor agonist. *Neurosci Lett* **301**:155-158.

Davis TP, Abbruscato TJ, Brownson E and Hruby VJ (1995) Conformationally constrained peptide drugs targeted at the blood-brain barrier. *NIDA Res. Monogr.* **154**:47-60.

Davis TP, and Culling-Berglund (1985) High-performance liquid chromatographic analysis of in vitro central neuropeptide processing. *J. Chrom.* **327**:279-292.

Davson H and Danielli JF (1943) *The Permeability of Natural Membranes.* Cambridge University Press, Cambridge.

Davson H, Kleeman CR and Levin E (1961) Blood-brain barrier and extracellular space. *J. Physiol. (Lond.)* **159**:67P-68P.

Davson H and Segal MB (1996) Secretions of the cerebrospinal fluid., in *Physiology of the CSF and Blood-Brain Barriers* (Davson H and Segal MB eds) pp 193-255, CRC Press, New York.

de Boer AG and Sutanto W (1997) In Vitro and In Vivo Techniques, in *Drug Transport Across the Blood Brain Barrier*, Harwood Academic Publishers, Amsterdam.

de Lange EC, de Boer BA and Breimer DD (1999) Microdialysis for pharmacokinetic analysis of drug transport to the brain. *Adv Drug Deliv Rev* **36**:211-227.

Dehouck MP, Meresse S, Delorme P, Fruchart JC and Cecchelli R (1990) An easier, reproducible, and mass-production method to study the blood- brain barrier in vitro. *J Neurochem* **54**:1798-1801.

Delgado C, Francis GE and Fisher D (1992) The uses and properties of PEG-linked proteins. *Crit. Rev. Ther. Drug Carrier Sys.* **9**:249-304.

Devaux PF (1991) Static and dynamic lipid asymmetry in cell membranes. *Biochemistry* **30**:1163-1173.

Dietzmann K, Bossanyi PV and Franke DS (1994) [Expression of P-glycoprotein as a multidrug resistance gene product in human reactive astrocytes and astrocytoma]. *Zentralbl. Pathol.* **140**:149-153.

Dobbin PS, Hider RC, Hall AD, Taylor PD, Sarpong P, Porter JB, Xiao G and van der Helm D (1993) Synthesis, physicochemical properties, and biological evaluation of N-substituted 2-alkyl-3-hydroxy-4(1H)-pyridinones: orally active iron chelators with clinical potential. *J Med Chem* **36**:2448-2458.

Domb AJ, Rock M, Schwartz J, Perkin C, Yipchuk G, Broxup B and Villemure JG (1994) Metabolic disposition and elimination studies of a radiolabelled biodegradable polymeric implant in the rat brain. *Biomaterials* **15**:681-688.

Drewe J, Ball HA, Beglinger C, Peng B, Kemmler A, Schachinger H and Haefeli WE (2000) Effect of P-glycoprotein modulation on the clinical pharmacokinetics and adverse effects of morphine. *Br J Clin Pharmacol* **50**:237-246.

Drion N, Risede P, Cholet N, Chanez C and Scherrmann JM (1997) Role of P-170 glycoprotein in colchicine brain uptake. *J Neurosci Res* **49**:80-88.

Duffy KR and Pardridge WM (1987) Blood-brain barrier transcytosis of insulin in developing rabbits. *Brain Res* **420**:32-38.

Duffy KR, Pardridge WM and Rosenfeld RG (1988) Human blood-brain barrier insulin-like growth factor receptor. *Metabolism* **37**:136-140.

Duvernoy H, Delon S and Vannson JL (1983) The vascularization of the human cerebellar cortex. *Brain Res Bull* **11**:419-480.

Egleton RD, Abbruscato TJ, Thomas SA and Davis TP (1998) Transport of opioid peptides into the central nervous system. *J. Pharm. Sci.* **87**:1433-1439.

Egleton RD and Davis TP (1997) Bioavailability and transport of peptides and peptide drugs into the brain. *Peptides* **18**:1431-1439.

Egleton RD and Davis TP (1999) Transport of the δ-opioid receptor agonist [D-Penicillamine^{2,5}] enkephalin across the blood-brain barrier involves transcytosis. *J. Pharm. Sci.* **88**:392-397.

Egleton RD, Mitchell SA, Huber JD, Janders J, Stropova D, Polt R, Yamamura HI, Hruby VJ and Davis TP (2000) Improved bioavailability to the brain of glycosylated Met-enkephalin analogs. *Brain Res* **881**:37-46.

Ehrlich P (1885) Das Sauerstoff-Bedurfnis des Organismus: eine farbenanalytische Studie. *Hirschwald, Berlin.*

Ehrlich P (1906) *Uber die Beziehungen von chemischer Constitution, Verteilung, und pharmakologische Wirkung. In Collected Studies in Immunity.* John Wiley, New York.

Einstein A (1905) Uber die von der molekularkinetischen theorie der Earme geforderte bewegung von in ruhenden flussigkeiten suspendierten teilchen. *Ann. Phys.*:549-560.

Emerich DF, Dean RL, Osborn C and Bartus RT (2001) The development of the bradykinin agonist labradimil as a means to increase the permeability of the blood-brain barrier: from concept to clinical evaluation. *Clin Pharmacokinet* **40**:105-123.

Erchegyi J, Kastin AJ, Zadina JE and Qui XD (1991) Isolation of a heptapeptide Val-Val-Tyr-Pro-Trp-Thr-Gln (valorphin) and some opiate activity. *Int. J. Pept. Protein Res.* **39**:477-488.

Farquhar MG and Palade GE (1963) Junctional complexes in various epithelia. *J. Cell Bilology*:375-412.

Farrell CL and Pardridge WM (1991) Blood-brain barrier glucose transporter is asymmetrically distributed on brain capillary endothelial lumenal and ablumenal membranes: an electron microscopic immunogold study. *Proc Natl Acad Sci U S A* **88**:5779-5783.

Fischer E, Spatz H, Heller B and Reggiani H (1972) Phenethylamine content of human urine and rat brain, its alterations in pathological conditions and after drug administration. *Experientia* **28**:307-308.

Fisher JF, Harrison AW, Bundy GL, Wilkinson KF, Rush BD and Ruwart MJ (1991) Peptide to glycopeptide: glycosylated oligopeptide renin inhibitors with attenuated *in vivo* clearance properties. *J. Med. Chem.* **34**:3140-3143.

Fishman JB, Rubin JB, Handrahan JV, Connor JR and Fine RE (1987) Receptor-mediated transcytosis of transferrin across the blood-brain barrier. *J Neurosci Res* **18**:299-304.

Fontaine M, Elmquist WF and Miller DW (1996) Use of rhodamine 123 to examine the functional activity of P-glycoprotein in primary cultured brain microvessel endothelial cell monolayers. *Life Sci.* **59**:1521-1531.

Foxwell BM, Mackie A, Ling V and Ryffel B (1989) Identification of the multidrug resistance-related P-glycoprotein as a cyclosporine binding protein. *Mol. Pharmacol.* **36**:543-546.

Frank RN, Dutta S and Mancini MA (1987) Pericyte coverage is greater in the retinal than in the cerebral capillaries of the rat. *Invest Ophthalmol Vis Sci* **28**:1086-1091.

Frederickson RCA, Smithwick EL, Shuman R and Bemis KG (1981) Metkephamid, a systemically active analog of methionine enkephalin with potent delta-receptor activity. *Science* **211**:603-605.

Freiden PM, Walus LR, Watson P, Doctorow SR, Kozarich JW, Backman C, Bergman H, Hoffer B, Bloom F and Granholm A-C (1993) Blood-brain barrier conjugation and in vivo activity of an NGF conjugate. *Science*:373-377.

Friedemann U (1942) Blood-brain barrier. *Physiol. Rev.*:125-139.

Furuse M, Sasaki H and Tsukita S (1999) Manner of interaction of heterogeneous claudin species within and between tight junction strands. *J Cell Biol* **147**:891-903.

Gabizon A and Martin F (1997) Polyethylene glycol-coated (pegylated) liposomal doxorubicin. Rationale for use in solid tumours. *Drugs* **54**:15-21.

Gabizon A, Catane R, Uziely B, Kaufman B, Safra T, Cohen R, Martin F, Huang A and Barenholz Y (1994) Prolonged circulation time and enhanced accumulation in malignant exudates of doxorubicin encapsulated in polyethylene-glycol coated liposomes. *Cancer Res* **54**:987-992.

Gaillard PJ, van der Sandt IC, Voorwinden LH, Vu D, Nielsen JL, de Boer AG and Breimer DD (2000) Astrocytes increase the functional expression of P-glycoprotein in an in vitro model of the blood-brain barrier. *Pharm. Res.* **17**:1198-1205.

Galligan JJ, Mosberg HI, Hurst R, Hruby VJ and Burks TF (1984) Cerebral *delta* opioid receptors mediate analgesia but not intestinal motility effects of intracerebroventricularly administered opioids. *J. Pharmacol. Exp. Ther.* **229**:641-648.

Gao B, Hagenbuch B, Kullak-Ublick GA, Benke D, Aguzzi A and Meier PJ (2000) Organic anion-transporting polypeptides mediate transport of opioid peptides across blood-brain barrier. *J Pharmacol Exp Ther* **294**:73-79.

Gentry CL, Egelton RD, Gillespie TJ, Abbruscato TJ, Bechowski HB, Hruby VJ and Davis TP (1999) The effects of halogenation on blood-brain barrier permeability of a novel peptide drug. *Peptides* **20**:1229-1238.

Georgopoulous AP (1977) Stimulus-response relations in high treshold mechanothermal fibers innervating primate glaborous skin. *Brain Res*:547-551.

Gerhart DZ and Drewes LR (1987) Butyrylcholinesterase in pericytes associated with canine brain capillaries. *Cell Tissue Res* **247**:533-536.

Ghersi-Egea JF, Leninger-Muller B, Suleman G, Siest G and Minn A (1994) Localization of drug-metabolizing enzyme activities to blood-brain interfaces and circumventricular organs. *J Neurochem* **62**:1089-1096.

Ghersi-Egea JF, Minn A, Daval JL, Jayyosi Z, Arnould V, Souhaili-El Amri H and Siest G (1989) NADPH:cytochrome P-450(c) reductase: biochemical characterization in rat brain and cultured neurons and evolution of activity during development. *Neurochem Res* **14**:883-887.

Golden PL and Pardridge WM (1999) P-Glycoprotein on astrocyte foot processes of unfixed isolated human brain capillaries. *Brain. Res.* **20**:143-146.

Goldman E (1909) Die Aussere und innere Sekretion des gesunden und kranken Organismus im Lichte der 'vitalan Farbung'. *Beitr. Klin. Chi.*:192-265.

Goldman E (1913) Vitalfarbung am Zentralnervensystem. *Abh. Preuss. Akad. Wiss. Phys. Math.* **K1**:1-60.

Goldstein A, Tachibana S, Lowney LI, Hunkapiller M and Hood L (1979) Dynorphin-(1-13), an extraordinarily potent opioid peptide. *Proc Natl Acad Sci U S A* **76**:6666-6670.

Gonatas NK, Stieber A, Hickey WF, Herber SH and Gonatas JO (1984) Endosomes and Golgi vesicles in adsorptive and fluid phase endocytosis. *J. Cell Biol.*:1379-1390.

Greene DL, Hau VS, Abbruscato TJ, Bartosz H, Misicka A, Lipkowski AW, Hom S, Gillespie TJ, Hruby VJ and Davis TP (1996) Enkephalin analog prodrugs: assessment of in vitro conversion, enzyme cleavage characterization and blood-brain barrier permeability. *J Pharmacol Exp Ther* **277**:1366-1375.

Greenwald RB, Conover CD and Choe YH (2000) Poly(ethylene glycol) conjugated drugs and prodrugs: a comprehensive review. *Crit. Rev. Ther. Drug Carrier Sys.* **17**:101-161.

Greig NH, Daly EM, Sweeney DJ and Rapoport SI (1990) Pharmacokinetics of chlorambucil-tertiary butyl ester, a lipophilic chlorambucil derivative that achieves and maintains high concentrations in brain. *Cancer Chemother Pharmacol* **25**:320-325.

Gysin BF (1973) The preparation of merrifield-resins through total esterification with cesium salts. *Helv. Chem. Acta* **34**:595-598.

Habgood MD, Begley DJ and Abbott NJ (2000) Determinants of passive drug entry into the central nervous system. *Cell Mol Neurobiol* **20**:231-253.

Hambrook JM, Morgan BA, Rance MJ and Smith Cf (1976) Mode of deactivation of the enkephalins by rat and human plasma and rat brain homogenates. *Nature* **26**:782-3.

Hansch C, Bjorkroth JP and Leo A (1987) Hydrophobicity and central nervous system agents: on the principle of minimal hydrophobicity in drug design. *J Pharm Sci* **76**:663-687.

Hansen DW Jr, Stepelfeld A, Savage MA, Reichman M, Hammond DL, Haaseth RC and Mosberg HI (1992) Systemic analgesic activity and δ-opioid selectivity in [2,6-Dimethyl-Tyr^1,D-Pen^2,D-Pen^5] enkephalin. *J. Med. Chem.* **35**:684-687.

Hardebo JE and Nilsson B (1981) Opening of the blood-brain barrier by acute elevation of intracarotid pressure. *Acta Physiol Scand* **111**:43-49.

Harris JM and Zalipsky S (1997) Introduction to chemistry and biological applications of poly(ethylene glycol), in *Poly(ethylene glycol) chemistry and biological applications, ACS Symposium series 680* (Harris JM and Zalipsky S eds) pp 1-13, American Chemical Society, Washington DC.

Haskins J, Gu L, Wittchen ES, Hibbard J and Stevenson BR (1998) ZO-3, a novel member of the MAGUK protein family found at the tight junction, interacts with ZO-1 and occludin. *J Cell Biol* **141**:199-208.

Healy DP and Orlowski M (1992) Immunocytochemical localization of endopeptidase 24.15 in rat brain. *Brain Res* **571**:121-128.

Hellstrom M, Gerhardt H, Kalen M, Li X, Eriksson U, Wolburg H and Betsholtz C (2001) Lack of pericytes leads to endothelial hyperplasia and abnormal vascular morphogenesis. *J Cell Biol* **153**:543-553.

Heyman J. S., Mosberg H. I., and Porreca F. (1986) Evidence for delta receptor mediation of [D-Pen^2,D-Pen^5]-enkephalin (DPDPE) analgesia in mice. *NIDA Res. Monogr.* **75,** 442-445.

Higgins CF and Gottesman MM (1992) Is the multidrug transporter a flippase? *Trends Biochem Sci* **17**:18-21.

Holtzman SG and Sung Y-F (1998) Pain Control with Opioid Analgesics, in *Human Pharmacology Molecular to Clinical* (Brody TM, Larner J and Minneman KP eds) pp 395-408, Mosby, St. Louis.

Horn A, Kelly P and Westerink B (1979) A prodrug of ADTN: Selectivity of dopaminergic action and brain levels of ADTN. *European Journal of Pharmacology*:95-99.

Hostetler KY, Stuhmiller LM, Lenting HB, van den Bosch H and Richman DD (1990) Synthesis and antiretroviral activity of phospholipid analogs of azidothymidine and other antiviral nucleosides. *J Biol Chem* **265**:6112-6117.

Hruby VJ (1982) Conformational restrictions of biologically active peptides via side chain groups. *Life Sci.* **31**:189-199.

Hruby VJ, Barosz-Bechowski H, Davis P, Slaninova J, Zalewska T, Stropova D, Porreca F and Yamamura HI (1997) Cyclic enkephalin analogues with exceptional potency and selectivity for δ-opioid receptors. *J. Med. Chem.* **40**:3957-3962.

Hruby VJ, Kao L-F, Pettitt B M and Karplus M (1988) The conformational properties of the delta opioid peptide [D-Pen^2,D-Pen^5] enkephalin in aqueous soulution determined by NMR and energy minimization calculations. *J. Am. Chem. Soc.* **110**:3351-3359.

Hruby VJ, Kazmierski W, Kawasaki AM and Matsunaga TO (1991b) Peptide Pharmaceuticals: *Synthetic Chemistry and the Design of Peptide-Based Drugs.* (Ward D., ed.) pp. 135-184. Open University Press, Celtic Court, Buckingham.

Hruby VJ, Toth G, Gehrig CA, Kao L-F, Knapp R, Lui GK, Yamamura HI, Kramer TH, Davis P and Burks TF (1991a) Topographically designed analogs of [D-Pen^2,D-Pen^5] enkephalin. *J. Med. Chem.* **34**:1823-1830.

Hruby VJ, Yamamura HI and Porreca F (1995) Molecular organization of receptors. Efficacy, agonists, and antagonists. *Ann. N Y Acad. Sci.* **10**:7-22.

Hruby VJ and Mosberg HI (1982) Conformational and dynamic considerations in peptide structure-function studies. *Peptides* **3**:329-336.

Huang JT, Mannik M and Gleisner J (1984) In situ formation of immune complexes in the choroid plexus of rats by sequential injection of a cationized antigen and unaltered antibodies. *J Neuropathol Exp Neurol* **43**:489-499.

Huber JD, Witt KA, Hom S, Egleton RD, Mark KS and Davis TP (2001) Inflammatory pain alters blood-brain barrier permeability and tight junctional protein expression. *Am J Physiol Heart Circ Physiol* **280**:H1241-1248.

Hughes J, Smith TW, Kosterlitz HW, Fothergill LA, Morgan BA and Morris HR (1975) Identification of two related pentapeptides from the brain with potent opiate agonist activity. *Nature* **258**:577-580.

Hui KS, Wang YJ and Lajtha A (1983) Purification and characterization of an enkephalin aminopeptidase from rat brain membranes. *Biochemistry* **1**:1062-1067.

Hussain MA, Seetharam R, Wilk RR, Aungst BJ and Kettner CA (1995) Nasal mucosal metabolism and absorption of pentapeptide enkephalin analogs having varying N-terminal amino acids. *J Pharm Sci* **84**:62-64.

Huwyler J, Wu D and Pardridge WM (1996) Brain drug delivery of small molecules using immunoliposomes. *Proc Natl Acad Sci U S A* **93**:14164-14169.

Hynes RO (1992) Integrins: Versatility, modulation, and signaling in cell adhesion. *Cell*:379-416.

Joh T, Yamamoto K, Kagami Y, Kakuda H, Sato T, Yamamoto T, Takahashi T, Ueda R, Kaibuchi K and Seto M (1997) Chimeric MLL products with a Ras binding cytoplasmic protein AF6 involved in t(6;11) (q27;q23) leukemia localize in the nucleus. *Oncogene* **15**:1681-1687.

Johnson MD and Anderson BD (1996) Localization of purine metabolizing enzymes in bovine brain microvessel endothelial cells: an enzymatic blood-brain barrier for dideoxynucleosides? *Pharm Res* **13**:1881-1886.

Kaiser E, Colescott RL, Bossinger CD and Cook PI (1970) Color test for detection of free terminal amino groups in the solid-phase synthesis of peptides. *Anal. Biochem.* **34**:595-598.

Karp G (1999) *Cell and Molecular Biology*. John Wiley & Sons, Inc., New York.

Kazmierski W, Wire WS, Lui GK, Knapp RJ, Shook JE, Burks TF, Yamamura HI and Hruby VJ (1988) Design and synthesis of somatostatin analogues with topographical properties that lead to highly potent and specific mu opioid receptor antagonists with greatly reduced binding at somatostatin receptors. *J. Med. Chem.* **31**:2170-2177.

Keck PJ, Hauser SD, Krivi G, Sanzo K, Warren T, Feder J and Connolly DT (1989) Vascular permeability factor, an endothelial cell mitogen related to PDGF. *Science* **246**:1309-1312.

Khanvilkar K, Donovan MD and Flanagan DR (2001) Drug transfer through mucus. *Adv Drug Deliv Rev* **48**:173-193.

King M, Su W, Chang A, Zuckerman A and Pasternak GW (2001) Transport of opioids from the brain to the periphery by P-glycoprotein: peripheral actions of central drugs. *Nat Neurosci* **4**:268-274.

Kitagawa K, Mizobuchi N, Hama T, Hibi T, Konishi R and Futaki S (1997) Synthesis and antinociceptive activity of [D-Ala2]Leu-enkephalin derivatives conjugated with the adamantane moiety. *Chem Pharm Bull (Tokyo)* **45**:1782-1787.

Knapp RJ, Kazmierski W, Hruby VJ and Yamamura HI (1989) Structural characteristics of two highly selective opioid peptides. *Bioassays* **10**:58-61.

Knapp RJ, Sharma SD, Toth G, Duong MT, Fang L, Bogert CL, Weber SJ, Hunt M, Davis TP, Wamsley JK, Hruby VJ and Yamamura HI (1991) [D-Pen^{2},4'-^{125}I-Phe^{4}, D-Pen^{5}] enkephalin: a selective high affinity radioligand for delta opioid receptors with exceptional specific activity. *J. Pharmacol. Exp. Ther.* **258**:1077-1083.

Koski G and Klee WA (1981) Opiates inhibit adenylate cyclase by stimulating GTP hydrolysis. *Proc Natl Acad Sci U S A* **78**:4185-4189.

Kowaloff H, Gavras H and Brecher P (1980) Reninlike enzymatic activity in the cerebral microvessels of the rat. *Am J Physiol* **238**:H384-388.

Kreuter J (2001) Nanoparticulate systems for brain delivery of drugs. *Adv Drug Deliv Rev* **47**:65-81.

Kreuter J, Alyautdin RN, Kharkevich DA and Ivanov AA (1995) Passage of peptides through the blood-brain barrier with colloidal polymer particles (nanoparticles). *Brain Res* **674**:171-174.

Kumagai AK, Eisenberg JB and Pardridge WM (1987) Absorptive-mediated endocytosis of cationized albumin and a beta- endorphin-cationized albumin chimeric peptide by isolated brain capillaries. Model system of blood-brain barrier transport. *J Biol Chem* **262**:15214-15219.

Kusuhara H, Suzuki H, Naito M, Tsuruo T and Sugiyama Y (1998) Characterization of efflux transport of organic anions in a mouse brain capillary endothelial cell line. *J Pharmacol Exp Ther* **285**:1260-1265.

Larson DM, Carson MP and Haudenschild CC (1987) Junctional transfer of small molecules in cultured bovine brain microvascular endothelial cells and pericytes. *Microvasc Res* **34**:184-199.

Lasic DD, Martin FJ, Gabizon A, Huang SK, Paphadjopoulos D (1991) Sterically stabilitzed liposomes: a hypothesis on the molecular origin of the extended circulation times. *Biochim. Biophys. Acta* **1070**:187-192.

Laterra J and Goldstein GW (1993) Brain Microvessels and Microvascular Cells In Vitro, in *The Blood-Brain Barrier Cellular and Molecular Biology* (Pardridge WM ed) pp 1-24, Raven, New York.

Legrand O, Simonin G, Perrot JY, Zittoun R and Marie JP (1998) Pgp and MRP activities using calcein-AM are prognostic factors in adult acute myeloid leukemia patients. *Blood* **91**:4480-4488.

Letrent SP, Polli JW, Humphreys JE, Pollack GM, Brouwer KR and Brouwer KL (1999) P-glycoprotein-mediated transport of morphine in brain capillary endothelial cells. *Biochem. Pharmacol.* **15**:951-957.

Letrent SP, Pollack GM, Brouwer KR and Brouwer KL (1999) Effects of a potent and specific P-glycoprotein inhibitor on the blood- brain barrier distribution and antinociceptive effect of morphine in the rat. *Drug Metab Dispos* **27**:827-834.

Levin VA (1980) Relationship of octanol/water partition coefficient and molecular weight to rat brain capillary permeability. *J Med Chem* **23**:682-684.

Lewandowsky M (1900) Zur Lehre der Cerebrospinalflussigkeit. *Z. Klin. Med.*:480-494. Machen TE, Erlij D and Wooding FBP (1972) Permeable junctional complexes. *J.Cell Biol.*:302-312.

Liao S, Alfaro-Lopez J, Shenderovich MD, Hosohata K, Lin J, Li X, Stropova D, Davis P, Jernigan KA, Porreca F, Yamamura HI and Hruby VJ (1998) De novo design, synthesis, and biological activities of high-affinity and selective non-peptide agonist of the δ-opioid receptor. *J. Med. Chem.* **41**:4767-4776.

Lowry OH, Rosebrough NJ, Farr AL and Randall RJ (1951) Protein measurement with the Folin phenol reagent. *J. Biol. Chem.* **193**:265-275.

Lum BL and Gosland MP (1995) MDR expression in normal tissues. Pharmacologic implications for the clinical use of P-glycoprotein inhibitors. *Hematol. Oncol. Clin. North. Am.* **9**:319-336.

Maeda M, Kawasaki K, Takahashi M, Nakao K and Kaneto H (1994) Amino acids and peptides. XXIV. Preparation and antinociceptive effect of [D-Ala^2,(N-Me)Phe^4] enkephalin analog-poly(ethylene glycol) hybrids. *Chem Pharm. Bull.* **42**:1859-1863.

Mahaffey DT, Moore MS, Brodsky FM and Anderson RG (1989) Coat proteins isolated from clathrin coated vesicles can assemble into coated pits. *J Cell Biol* **108**:1615-1624.

Malingre MM, Beijnen JH, Rosing H, Koopman FJ, Jewell RC, Paul EM, Ten Bokkel Huinink WW and Schellens JH (2001) Co-administration of GF120918 significantly increases the systemic exposure to oral paclitaxel in cancer patients. *Br J Cancer* **84**:42-47.

Marshall D, Pedley RB, Boden JA, Boden R, Melton RG and Begent RHJ (1996) Polyethylene glycol modification of a galactosylated streptavidin clearing agent: effects on immunogenicity and clearance of a biotinylated anti-tumour antibody. *Br J. Cancer* **73**:565-572.

Martin WR and Sloan JW (1977) Neuropharmacology and neurochemistry of subjective effects, analgesia, tolerance and dependence produced by narcotic analgesics, in *Handbook of Experimental Pharmacology* (Martin WR ed).

Mathison S, Nagilla R and Kompella UB (1998) Nasal route for direct delivery of solutes to the central nervous system: fact or fiction? *J Drug Target* **5**:415-441.

Minakawa T, Bready J, Berliner J, Fisher M and Cancilla PA (1991) In vitro interaction of astrocytes and pericytes with capillary-like structures of brain microvessel endothelium. *Lab Invest* **65**:32-40.

Minn A, Ghersi-Egea JF, Perrin R, Leininger B and Siest G (1991) Drug metabolizing enzymes in the brain and cerebral microvessels. *Brain Res Brain Res Rev* **16**:65-82.

Misicka A and Hruby VJ (1994) Optimization of disulfide bond formation. *Polish J. Chem.* **68**:893-899.

Mogil JS, Chester EJ, Wilson SG, Juraska JM and Sternberg WF (2000) Sex differences in thermal nociception and morphine antinociception in rodents depend on phenotype. *Neurosci. Behav. Rev.* **24**:375-389.

Molineaux CJ and Ayala JM (1990) An inhibitor of endopeptidase-24.15 blocks the degradation of intraventricularly administered dynorphins. *J Neurochem* **55**:611-618.

Moore MS, Mahaffey DT, Brodsky FM and Anderson RG (1987) Assembly of clathrin-coated pits onto purified plasma membranes. *Science* **236**:558-563.

Mosberg HI, Hurst R, Hruby VJ, Gee K, Yamamura HI, Galligan JJ and Burks (1983) Bis-penicillamine enkephalins possess highly improved specificity toward delta opioid receptors. *Proc. Natl. Acad. Sci.* USA **80**:5871-5874.

Murakami H, Takanaga H, Matsuo H, Ohtani H and Sawada Y (2000) Comparison of blood-brain barrier permeability in mice and rats using in situ brain perfusion technique. *Am. J. Physiol. Heart Circ. Physiol.* **279**:H1022-H1028.

Muranishi S (1997) [Delivery system design for improvement of intestinal absorption of peptide drugs]. *Yakugaku Zasshi* **117**:394-414.

Muranishi S, Sakai A, Yamada K, Murakami M, Takada K and Kiso Y (1991) Lipophilic peptides: synthesis of lauroyl thyrotropin-releasing hormone and its biological activity. *Pharm Res* **8**:649-652.

Nabeshima S, Reese TS, Landis DM and Brightman MW (1975) Junctions in the meninges and marginal glia. *J Comp Neurol* **164**:127-169.

Nagy Z, Peters H and Huttner I (1983) Charge-related alterations of the cerebral endothelium. *Lab Invest* **49**:662-671.

Nehls V and Drenckhahn D (1991) Heterogeneity of microvascular pericytes for smooth muscle type alpha- actin. *J Cell Biol* **113**:147-154.

Neuwelt EA, Specht HD, Barnett PA, Dahlborg SA, Miley A, Larson SM, Brown P, Eckerman KF, Hellstrom KE and Hellstrom I (1987) Increased delivery of tumor-specific monoclonal antibodies to brain after osmotic blood-brain barrier modification in patients with melanoma metastatic to the central nervous system. *Neurosurgery* **20**:885-895.

Neuwelt EA, Weissleder R, Nilaver G, Kroll RA, Roman-Goldstein S, Szumowski J, Pagel MA, Jones RS, Remsen LG, McCormick CI and et al. (1994) Delivery of virus-sized iron oxide particles to rodent CNS neurons. *Neurosurgery* **34**:777-784.

Nikiforovich GV, Hruby VJ, Prakash O and Gehrig CA (1991) Topographical requirements for delta-selective opioid peptides. *Biopolymers* **31**:941-955.

Nomura T, Inamura T and Black KL (1994) Intracarotid infusion of bradykinin selectively increases blood-tumor permeability in 9L and C6 brain tumors. *Brain Res* **659**:62-66.

Nusrat A, Parkos CA, Verkade P, Foley CS, Liang TW, Innis-Whitehouse W, Eastburn KK and Madara JL (2000) Tight junctions are membrane microdomains. *J Cell Sci* **113**:1771-1781.

Ogihara T, Tamai I, Takanaga H, Sai Y and Tsuji A (1996) Stereoselective and carrier-mediated transport of monocarboxylic acids across Caco-2 cells. *Pharm. Res.* **13**:1828-1832.

Ohno K, Pettigrew KD and Rapoport SI (1978) Lower limits of cerebrovascular permeability to nonelectrolytes in the conscious rat. *Am J Physiol* **235**:H299-307.

Oldendorf WH (1970) Measurement of brain uptake of radiolabeled substances using a tritiated water internal standard. *Brain Res* **24**:372-376.

Oldendorf WH and Brown WJ (1975) Greater number of capillary endothelial cell mitochondria in brain than in muscle. *Proc Soc Exp Biol Med* **149**:736-738.

Oldendorf WH, Cornford ME and Brown WJ (1977) The large apparent work capability of the blood-brain barrier: a study of the mitochondrial content of capillary endothelial cells in brain and other tissues of the rat. *Ann Neurol* **1**:409-417.

Oldendorf WH, Hyman S, Braun L and Oldendorf SZ (1972) Blood-brain barrier: penetration of morphine, codeine, heroin, and methadone after carotid injection. *Science* **178**:984-986.

Otsuka M and Yanagisawa M (1988) Effect of a tachykinin antagonist on a nociceptive reflex in the isolated spinal cord-tail preparation of the newborn rat. *J Physiol* **395**:255-270.

Palade GE (1960) Transport in quanta across the endothelium of blood capillaries. *Anat. Rec*:254.

Pardridge WM (1995a) Blood -brain barrier peptide transport and peptide drug delivery to the brain., in *Peptide-Based Drug Design.* (Taylor MD and Amidon GL eds) pp 265-296, American Chemical Society.

Pardridge WM (1995b) *Peptide Drug Delivery to the Brain.* Raven, New York.

Pardridge WM, Buciak JL and Friden PM (1991) Selective transport of an anti-transferrin receptor antibody through the blood-brain barrier in vivo. *J. Pharmacol. Exp. Ther.* **259**:66-70.

Pardridge WM, Kang YS and Buciak JL (1994) Transport of human recombinant brain-derived neurotrophic factor (BDNF) through the rat blood-brain barrier in vivo using vector-mediated peptide drug delivery. *Pharm Res* **11**:738-746.

Pardridge WM, Kang YS, Yang J and Buciak JL (1995) Enhanced cellular uptake and in vivo biodistribution of a monoclonal antibody following cationization. *J. Pharm. Sci.* **84**:943-948.

Pardridge WM (1998) CNS drug design based on principles of blood-brain barrier transport. *J Neurochem* **70**:1781-1792.

Pardridge WM (1999) Vector-mediated drug delivery to the brain. *Adv Drug Deliv Rev* **36**:299-321.

Pardridge WM and Fierer G (1985) Blood-brain barrier transport of butanol and water relative to N- isopropyl-p-iodoamphetamine as the internal reference. *J Cereb Blood Flow Metab* **5**:275-281.

Pardridge WM, Boado RJ, Black KL and Cancilla PA (1992) Blood-brain barrier and new approaches to brain drug delivery. *West J Med* **156**:281-286.

Pardridge WM, Golden PL, Kang YS and Bickel U (1997) Brain microvascular and astrocyte localization of P-glycoprotein. *J Neurochem* **68**:1278-1285.

Pardridge WM, Triguero D, Buciak J and Yang J (1990a) Evaluation of cationized rat albumin as a potential blood-brain barrier drug transport vector. *J Pharmacol Exp Ther* **255**:893-899.

Pardridge WM, Triguero D, Yang J and Cancilla PA (1990b) Comparison of in vitro and in vivo models of drug transcytosis through the blood-brain barrier. *J Pharmacol Exp Ther* **253**:884-891.

Pasternak GW (1993) Pharmacological mechanisms of opioid analgesics. *Clin Neuropharmacol* **16**:1-18.

Patel A, Smith HJ and Sewell RD (1993) Inhibitors of enkephalin-degrading enzymes as potential therapeutic agents. *Prog. Med. Chem.* **30**:327-378.

Paulus H (1969) A rapid and sensitive method for measuring the binding of radioactive ligands to proteins. *Anal Biochem* **32**:91-100.

Perrin R, Minn A, Ghersi-Egea JF, Grassiot MC and Siest G (1990) Distribution of cytochrome P450 activities towards alkoxyresorufin derivatives in rat brain regions, subcellular fractions and isolated cerebral microvessels. *Biochem Pharmacol* **40**:2145-2151.

Polt R, Porreca F, Szabo LZ, Bilsky EJ, Davis P, Abbruscatto TJ, Davis TP, Hovath R, Yamamura HI and Hruby VJ (1994) Glycopeptide enkephalin analogues produce analgesia in mice: Evidence for penetration of the blood-brain barrier. *Proc. Natl. Acad. Sci.* **91**:7114-7118.

Porreca F, Mosberg HI, Hurst R, Hruby VJ, and Burks TF (1984) Roles of mu, delta and kappa opioid receptors in spinal and supraspinal mediation of gastrointestinal transit effects and hot-plate analgesia in the mouse. *J Pharmacol. Exp. Ther.* **230**:341-348.

Powell MF, Stewart T, Otvos L, Jr., Urge L, Gaeta FC, Sette A, Arrhenius T, Thomson D, Soda K and Colon SM (1993) Peptide stability in drug development. II. Effect of single amino acid substitution and glycosylation on peptide reactivity in human serum. *Pharm Res* **10**:1268-1273.

Preston JE, Al-Sarrif H and Segal MB (1995) Permeability of the developing blood-brain barrier to 14C-mannitol using the rat *in situ* brain perfusion technique. *Dev. Brain Res.* **87**:69-76.

Prokai L (1998) Peptide drug delivery into the central nervous system. *Progress in Drug Research* **51**:95-131.

Qian X, Liao S, Stropova D, Yamamura HI and Hruby VJ (1996a) Novel scaffolds for non-peptide mimetics of delta opioid receptor agonist based on peptide leads. *Regul. Pept.* **27**:79-82.

Qian X, Shenderovich MD, Kover KE, Davis P, Hovath R, Zalewska T, Yamamura HI, Porreca F and Hruby VJ (1996b) Probing the stereochemical requirements for receptor recognition of opioid agonists through topographical modifications in position 1. J. Am. Chem. Soc. **118**:7280-7290.

Quock RM, Burkey TH, Varga E, Hosohata Y, Hosohata K, Cowell SM, Slate CA, Ehlert FJ, Roeske W, Yamamura HI (1999) The delta-opioid receptor: molecular pharmacology, signal transduction, and the determination of drug efficacy. *Pharmacol. Rev.* **51**:503-32.

Rapoport SI (1970) Effect of concentrated solutions on blood-brain barrier. *Am J Physiol* **219**:270-274.

Raymond JJ, Robertson DM and Dinsdale HB (1986) Pharmacological modification of bradykinin induced breakdown of the blood-brain barrier. *Can J Neurol Sci* **13**:214-220.

Reddy KR (2000) Controlled-release, PEGylation, liposomal formulations: new mechanisms in the delivery of injectable drugs. *Ann. Pharm.* **34**:915-923.

Reese TS and Karnovsky MJ (1967) Fine structural localization of a blood-brain barrier to exogenous peroxidase. *J Cell Biol* **34**:207-217.

Saija A, Princi P, Lanza M, Scalese M, Aramnejad E and De Sarro A (1995) Systemic cytokine administration can affect blood-brain barrier permeability in the rat. *Life Sci* **56**:775-784.

Saito Y and Wright EM (1983) Bicarbonate transport across the frog choroid plexus and its control by cyclic nucleotides. *J Physiol* **336**:635-648.

Sar M and Stumpf WE (1983) Simultaneous localization of steroid hormones and neuropeptides in the brain by combined autoradiography and immunocytochemistry. *Methods Enzymol* **103**:631-638.

Satoh H, Zhong Y, Isomura H, Saitoh M, Enomoto K, Sawada N and Mori M (1996) Localization of 7H6 tight junction-associated antigen along the cell border of vascular endothelial cells correlates with paracellular barrier function against ions, large molecules, and cancer cells. *Exp Cell Res* **222**:269-274.

Segal MB (1999) Other barriers of the brain, in *Brain barrier Systems* (Pauson OB, Knudsen GM and Moos T eds) pp 165-181, Munksgaard, Copenhagen.

Schetz JA, Mayr CA, Taylor JE, Rosenblatt M, Chorev M, and Davis TP (1995) Distribution and pharmacokinetics of a potent peptide antagonist of parathyroid hormone and parathyroid hormone-related protein in the rat. *J. Pharmacol. Exp. Ther.* **274**:1456-1462.

Schinkel AH Wagenaar E, Mol CAand van Deemter L (1996) P-glycoprotein in the blood-brain barrier of mice influences the brain penetration and pharmacological activity of many drugs. *J. Clin. Invest.* 1:17-2524.

Schneeberger EE and Karnovsky MJ (1976) Substructure of intercellular junctions in freeze-fractured alveolar- capillary membranes of mouse lung. *Circ Res* **38**:404-411.

Shaffer CB, Critchfield FH, and Carpenter CP (1948) Renal excretion and volume distribution of some polyethylene glycols in the dog. *Am. J. Physiol.* **152**:93-99.

Shashoua VE, Jacob JN, Ridge R, Campbell A and Baldessarini RJ (1984) Gamma-aminobutyric acid esters. 1. Synthesis, brain uptake, and pharmacological studies of aliphatic and steroid esters of gamma- aminobutyric acid. *J Med Chem* **27**:659-664.

Sharom FJ, Lu P, Liu R and Yu X (1998) Linear and cyclic peptides as substrates and modulators of P- glycoprotein: peptide binding and effects on drug transport and accumulation. *Biochem J* **333**:621-630.

Shivers RR, Arthur FE and Bowman PD (1988) Induction of gap junctions and brain endothelium-like tight junctions in cultured bovine endothelial cells: local control of cell specialization. *J Submicrosc Cytol Pathol* **20**:1-14.

Shook JE, Pelton JT, Hruby VJ and Burks TF (1987) Peptide opioid antagonist separates peripheral and central opioid antitransit effects. *J Pharmacol Exp Ther* **243**:492-500.

Siakotos AN and Rouser G (1969) Isolation of highly purified human and bovine brain endothelial cells and nuclei and their phospholipid composition. *Lipids* **4**:234-239.

Simionescu M, Ghitescu L, Fixman A and Simionescu N (1987) How plasma macromolecules cross the endothelium. *News Physiol. Sci.*:97-100.

Simionescu M, Simionescu N and Palade GE (1975) Segmental differentiations of cell junctions in the vascular endothelium. The microvasculature. *J Cell Biol* **67**:863-885.

Simpkins JW, McCormack J, Estes KS, Brewster ME, Shek E and Bodor N (1986) Sustained brain-specific delivery of estradiol causes long-term suppression of luteinizing hormone secretion. *J Med Chem* **29**:1809-1812.

Singer SJ and Nicolson GL (1972) The fluid mosaic model of the structure of cell membranes. *Science* **175**:720-731.

Skarlatos S, Yoshikawa T and Pardridge WM (1995) Transport of [125I]transferrin through the rat blood-brain barrier. *Brain Res* **683**:164-171.

Smith QR and Rapoport SI (1986) Cerebrovascular permeability coefficients to sodium, potassium, and chloride. *J Neurochem* **46**:1732-1742.

Solhonne B, Gros C, Pollard H and Schwartz JC (1987) Major localization of aminopeptidase M in rat brain microvessels. *Neuroscience* **22**:225-232.

Song L, Wilk E, Wilk S and Healy DP (1993) Localization of immunoreactive glutamyl aminopeptidase in rat brain. I. Association with cerebral microvessels. *Brain Res* **606**:286-294.

Stahl P and Schwartz AL (1986) Receptor-mediated endocytosis. *J Clin Invest* **77**:657-662.

Stein WD (1967) *The Movement of Molecules Across Cell Membranes.* Academic Press, New York.

Stewart PA and Wiley MJ (1981) Developing nervous tissue induces formation of blood-brain barrier characteristics in invading endothelial cells: a study using quail-- chick transplantation chimeras. *Dev Biol* **84**:183-192.

Sutherland WA (1905) A Dynamic theory of diffusion for non-electrolytes and the molecular mass of albumin. *Phil. Mag.*:781-785.

Takasato Y, Rapoport SI and Smith QR (1984) An in situ brain perfusion technique to study cerebrovascular transport in the rat. *Am J Physiol* **247**:H484-493.

Tallarida RJ and Murry RB(1987) Manual of pharmacology calculations with computer programs. Springer-Verlag. N Y.

Tatsuta T, Naito M, Oh-hara T, Sugawara I and Tsuruo T (1992) Functional involvement of P-glycoprotein in blood-brain barrier. *J Biol Chem* **267**:20383-20391.

Terasaki T, Hirai K, Sato H, Kang YS and Tsuji A (1989) Absorptive-mediated endocytosis of a dynorphin-like analgesic peptide, E-2078 into the blood-brain barrier. *J Pharmacol Exp Ther* **251**:351-357.

Thomas SA Abbruscato TJ, Hruby VJ and Davis TP (1997) The entry of [D-Penicillamin^{2,5}] enkephalin into the central nervous system: saturation kinetics and specificity. *J. Pharm. Exp. Ther.* **280**:1235-1240.

Timpl R and Brown JC (1996) Supramolecular assembly of basement membranes. *BioEssays*:123-132.

Tomatis R, Marastoni M, Balboni G, Guerrini R, Capasso A, Sorrentino L, Santagada V, Caliendo G, Lazarus LH and Salvadori S (1997) Synthesis and pharmacological activity of deltorphin and dermorphin- related glycopeptides. *J Med Chem* **40**:2948-2952.

Tontsch U and Bauer HC (1991) Glial cells and neurons induce blood-brain barrier related enzymes in cultured cerebral endothelial cells. *Brain Res* **539**:247-253.

Torchilin VP, Omelyanenko VG, Papisov MI, Bogdanov AA, Trubetskoy VS, Herron JN, Gentry CA (1994) Poly(ethylene glycol) on the liposome surface: on the mechanism of polymer-coated liposome longevity. *Biochim. Biophys. Acta* **1195**:11-20.

Toth G, Russell KC, Landis G, Kramer TH, Fang L, Knapp R, Davis P, Burks TF, Yamamura HI and Hruby VJ (1992) Ring substituted and other conformationally constrained tyrosine analogues of [D-Pen^2,D-Pen^5] enkephalin with δ opioid receptor selectivity. *J. Med Chem.* **35**:2384-2391.

Torebjork HE (1974) Afferent C units responding to mechanical, thermal, and chemical stimuli in human, non-glaborous skin. *Acta. Phys. Scand.*:374-390.

Triguero D, Buciak J and Pardridge WM (1990) Capillary depletion method for quantification of blood-brain barrier transport of circulating peptides and plasma proteins. *J. Neurochem.* **54**:1882-1888.

Triguero D., Buciak J., and Pardridge W. M. (1990) Capillary depletion method for quantification of blood-brain barrier transport of circulating peptides and plasma proteins. *J. Neurochem.* **54**:1882-1888.

Tseng LF (1986) Stereoselective effect of beta-endorphin on the production of analgesia and the spinal release of met-enkephalin in rats. *J. Pharmacol. Exp. Ther.* **239**:160-165.

Tsuji A (2000) Specific Mechanisms for Transporting Drugs into Brain, in *The Blood-Brain Barrier and Drug Dleivery to the CNS* (Begley DJ, Bradbury MW and Kreuter J eds) pp 121-144, Marcel Dekker Inc., New York.

Tsuji A and Tamai II (1999) Carrier-mediated or specialized transport of drugs across the blood- brain barrier. *Adv Drug Deliv Rev* **36**:277-290.

Tsuzuki N, Hama T, Hibi T, Konishi R, Futaki S and Kitagawa K (1991) Adamantane as a brain-directed drug carrier for poorly absorbed drug: antinociceptive effects of [D-Ala2]Leu-enkephalin derivatives conjugated with the 1-adamantane moiety. *Biochem Pharmacol* **41**:R5-8.

Tsuzuki N, Hama T, Kawada M, Hasui A, Konishi R, Shiwa S, Ochi Y, Futaki S and Kitagawa K (1994) Adamantane as a brain-directed drug carrier for poorly absorbed drug. 2. AZT derivatives conjugated with the 1-adamantane moiety. *J Pharm Sci* **83**:481-484.

Unwin N and Henderson R (1984) The structure of proteins in biological membranes. *Sci Am* **250**:78-94.

van Bree JB, de Boer AG, Verhoef JC, Danhof M and Breimer DD (1989) Transport of vasopressin fragments across the blood-brain barrier: in vitro studies using monolayer cultures of bovine brain endothelial cells. *J Pharmacol Exp Ther* **249**:901-905.

Vanderah T, Takemori AE, Sultana M, Portoghese PS, Mosberg HI, Hruby VJ, Haaseth RC, Matsunaga TO and Porreca F (1994) Interaction of [D-Pen^2,D-Pen^5] enkephalin and [D-Ala^2,Glu^4] deltorphin with δ-opioid receptor subtypes in vivo. *Eur. J. Pharmacol.* **252**:133-137.

Veber DF and Freidlinger RM (1985) The design of metabolically-stable peptide analogs. *Trends in Neuroscience*:392-396.

Vehaskari VM, Chang CT, Stevens JK and Robson AM (1984) The effects of polycations on vascular permeability in the rat. A proposed role for charge sites. *J Clin Invest* **73**:1053-1061.

Veronese FM (2001) Peptide and protein PEGylation: a review of problems and solutions. *Biomaterials* **22**:405-417.

Vijayaraghavan J, Scicli AG, Carretero OA, Slaughter C, Moomaw C and Hersh LB (1990) The hydrolysis of endothelins by neutral endopeptidase 24.11 (enkephalinase). *J Biol Chem* **265**:14150-14155.

Wade LA and Katzman R (1975) Synthetic amino acids and the nature of L-DOPA transport at the blood- brain barrier. *J Neurochem* **25**:837-842.

Watson SJ, Barchas JD and Li CH (1977) beta-Lipotropin: localization of cells and axons in rat brain by immunocytochemistry. *Proc Natl Acad Sci U S A* **74**:5155-5158.

Weber SJ, Abbruscotto TJ, Brownson EA, Lipkowski AW, Poit R, Misicka A, Haaseth RC, Bartosz H, Hruby VJ and Davis TP (1993) Assessment of an *in vitro* blood-brain barrier model using several [Met^5] enkephalin opioid analogs. *J. Pharmacol. Exp. Ther.* **266**:1649-1655.

Weber SJ, Greene DL, Hruby VJ, Yamamura HI, Porreca F and Davis TP (1992) Whole body and brain distribution of [^{3}H] cyclic [D-Pen^2,Pen^5] enkephalin after intraperitoneal, intravenous, oral and subcutaneous administration. *J. Pharmacol. Exp. Ther.* **263**:1308-1316.

Weber SJ, Greene DL, Sharma SD, Yamamura HI, Kramer TH, Burks TF, Hruby VJ, Hersh LB and Davis TP (1991) Distribution and analgesia of [^{3}H] [D-Pen^2,D-Pen^5] enkephalin and two halogenated analogs after intravenous administration. *J. Pharmacol. Exp. Ther.* **259**:1308-1316.

Williams SA, Abbruscotto TJ, Hruby VJ and Davis TP (1996) Passage of a δ-opioid receptor selective enkephalin [D-Penicillamine^{2,5}] enkephalin, across the blood-brain and the blood-cerebrospinal fluid barriers. *J Neurochem.* **66**:1289-1299.

Witt KA, Slate CA, Egleton RD, Huber JD, Yamamura HI, Hruby VJ and Davis TP (2000) Assessment of stereoselectivity of trimethylphenylalanine analogues of δ-opioid [D-Pen^2,Pen^5]-enkephalin. *J. Neuro. Chem.* **75**:424-435.

Wolburg H and Rohlmann A (1995) Structure-function relationships in gap junctions. *Int Rev Cytol* **157**:315-373.

Woodcock DM, Linsenmeyer ME, Chojnowski G, Kriegler AB, Nink V, Webster LK and Sawyer WH (1992) Reversal of multidrug resistance by surfactants. *Br J Cancer* **66**:62-68.

Wu X, Yuan G, Brett CM, Hui AC and Giacomini KM (1992) Sodium-dependent nucleoside transport in choroid plexus from rabbit. Evidence for a single transporter for purine and pyrimidine nucleosides. *J Biol Chem* **267**:8813-8818.

Xiang L, Wu H and Hruby VJ (1995) Stereoselective synthesis of all individual isomers of β-methyl-2',6'-dimethylphenylalanine. *Tetrahedron Asym.* **6**:84-86.

Yamada Y, Furumichi T, Furui H, Yokoi T, Ito T, Yamauchi K, Yokota M, Hayashi H and Saito H (1990) Roles of calcium, cyclic nucleotides, and protein kinase C in regulation of endothelial permeability. *Arteriosclerosis* **10**:410-420.

Yoburn BC, Lufty K and Candido J (1991) Species differences in mu- and delta-opioid receptors. *Eur. J. Pharm.* **193**:105-108.

Yoshikawa T and Pardridge WM (1992) Biotin delivery to brain with a covalent conjugate of avidin and a monoclonal antibody to the transferrin receptor. *J Pharmacol Exp Ther* **263**:897-903.

Yu J, Butelman ER, Woods JH, Chait BT and Kreek MJ (1997) Dynorphin A (1-8) analog, E-2078, crosses the blood-brain barrier in rhesus monkeys. *J Pharmacol Exp Ther* **282**:633-638.

Zhang Y and Pardridge WM (2001) Conjugation of brain-derived neurotrophic factor to a blood-brain barrier drug targeting system enables neuroprotection in regional brain ischemia following intravenous injection of the neurotrophin. *Brain Res* **889**:49-56.

Zlokovic BV, Banks WA, Kadi HE, Erchegyi J, Mackic JB, McComb JG and Kastin AJ (1992) Transport, uptake and metabolism of blood-borne vasopressin by the blood-brain barrier. *Brain Res.* **590**:213-218.

Zlokovic BV, Banks WA, Kadi HE, Erchegyi J, Mackic JB, McComb JG and Kastin AJ (1992) Transport, uptake and metabolism of blood-borne vasopressin by the blood-brain barrier. *Brain Res.* **590**:213-218.

Zlokovic BV, Begley DJ, Djuricic BM and Mitrovic DM (1986) Measurement of solute transport across the blood-brain barrier in the perfused guinea pig brain: method and application to N-methyl-alpha- aminoisobutyric acid. *J Neurochem* **46**:1444-1451.